Control of biological phosphorus removal in an oxidation ditch using simple sensors

V.P.J. Bost
Civil Engineering
Delft University of Technology

Control of biological phosphorus removal in an oxidation ditch using simple sensors

Master of Science Thesis

by

V.P.J. (Vera) Bost

To obtain the degree of Master of Science at the Delft University of Technology.

Student number:	4165837	
Date:	Friday, 26 October 2018	
Thesis committee:	Prof. Dr. ir. M.K. (Merle) de Kreuk,	TU Delft, supervisor
	Dr. ir. H. (Henri) Spanjers,	TU Delft
	Prof. Dr. ir. B. (Bart) De Schutter,	TU Delft
	Ir. J.J.G. (Jasper) Wuister,	Royal HaskoningDHV

TU Delft Delft University of Technology

Royal HaskoningDHV
Enhancing Society Together

Acknowledgements

With this MSc thesis, I finalise my master programme Watermanagement at Delft University of Technology. I first came to Delft for my bachelor Mechanical Engineering. Although I was pleased with my bachelor programme, I missed a for me very important direct connection of the technology to people and environment. I decided to switch to Watermanagement with a specialisation in Water Treatment. This thesis topic on 'Control of biological phosphorus removal in an oxidation ditch using simple sensors' seemed like the perfect opportunity to combine two fields I encountered during my studies in Delft; system & control vs. water technology. I learned a lot from this thesis and found out that combining two different fields, brings challenges as well. I would like to take this opportunity to thank the many people that helped me through this process.

First, I would like to thank my thesis committee: Merle de Kreuk, Henri Spanjers, Bart de Schutter and Jasper Wuister. Thank you for being part of this thesis and for guiding me through this with all the help and advice I received. Many thanks to my supervisor Merle de Kreuk, who has been more than just a supervisor during the thesis. I really appreciate all the time you made for me this year and for listening and for the kind words and the nice meetings together with conversations on all kinds of topics. I would like to thank Jasper Wuister, for all the honest advice I received the past year from you. You have spent many hours and even evenings on helping me and on checking chapters of my report before deadlines. I am very thankful for that and it helped me a lot. Also, thanks for the always quick reply on my e-mails and messages and for being a bit strict when I was making too many hours. Thank you Henri Spanjers, for the detailed feedback I received from you. I learned a lot on writing an academic and technical report. I would also like to thank you for your help with looking into the existing models/ simulations and benchmarks and for presenting me the work of Abdallah Abusam and bringing me in contact with him. Thank you, Bart de Schutter, for your advice on useful literature concerning control, for making time to check my report and for your feedback.

Also, a special thanks to Abdallah Abusam, who gave me access to his benchmark and made time to help me and answer my questions on it.

Then I would like to thank the people at Royal HaskoningDHV and Waterschap Vallei & Veluwe who gave me this opportunity. And a special thanks to all the people who came to Hattem and helped me during my measurements; the the operational team at WWTP Hattem and all the people who helpt me with the measurements: Erik van den Berg, Tim van Erp, Koen Arends, Coen Leusink en Jelmer Sevenster. Thank you for the helping hands under the harsh conditions at the WWTP, I could not have completed these measurements without you. Also thanks to Colinda Blommenstijn and Aqualysis for helping me with setting up the sample analysis.

On a personal level, I would like to thank the people close to me who have supported me in many ways. My parents, for all their support and love during my time in Delft. And my brother and my sister, for always checking up on me and being concerned for me when I made long days.

I also want to thank my fellow students at Water Management and Environmental Engineering. Being on the fourth floor with you for the past 2.5 years and being part of the board, made it feel like home and made it fun to come every day. And a special thanks to Anna Waqué, for the many conversations we had about thesis life and for reading and checking my report.

Last but not least, I want to thank Zino. You have been by my side during this thesis. Every time it got a little though and I got stressed, you helped me through it. Thank you for your patience during the lasts weeks when I was working on my deadline and was less available. And thank you for making sure that even in the busiest times, there were fun moments together, where I could turn off the stress.

Vera Bost
Delft, October 2018

Abstract

Control of wastewater treatment plants has received more attention as a method to improve nutrient removal processes. An improved nutrient removal results in an increased effluent quality, whilst minimising the energy consumption. Aeration control of oxidation ditches often focuses on adjusting the aeration intensity based on the nitrogen removal process, using ammonium measurements. The control systems do not incorporate biological phosphorus removal. Biological phosphorus removal, on the one hand, needs sufficient aeration and on the other hand, can deteriorate when subjected to excessive aeration. The complex relation to aeration, makes control of biological phosphorus removal difficult.

This research investigates the control of biological phosphorus removal in an oxidation ditch using simple sensors. Control systems often require expensive instrumentation. To limit the costs, cheap sensors using alternative monitoring variables for biological phosphorus removal are desired. Literature research was done to investigate the principles of biological phosphorus removal, possible alternative monitoring variables, current control systems and existing mathematical models and benchmarks that could contribute to a renewed control strategy. Some important variables found in literature were potassium, pH, ORP, ortho-P, nitrate, ammonium, conductivity, and DO. A measurement campaign was set up and executed to measure the trend of these variables throughout the oxidation ditch and to obtain more information on the state of the variables in the (un)aerated zones. A full-scale operating wastewater treatment plant in Hattem was made available to execute the measurement campaign.

The results obtained from the measuring campaign did not point towards alternative monitoring variables for biological phosphorus removal. Relationships between the variables and phosphorus found in literature, could not be directly derived from the measurement results. However, nitrate and ammonium measurements, can give an insight into the biological phosphorus removal process. A change in ammonium and nitrate indicates an anaerobic, anoxic or anaerobic environment. Nitrate can in addition contribute to a control system by making sure that the zone before withdrawal from the oxidation ditch is anoxic, to inhibit P-release. However, it cannot on its own monitor the biological phosphorus removal fully as it cannot indicate the effect of the aeration intensity on biological phosphorus removal directly. The results from the measurements indicated a low biological phophorus removal activity. From literature, it is known that several factors can influence the biological phosphorus removal, such as insufficient anaerobic zone and aeration settings.

To investigate the repsonse of the WWTP to these factors, a BioWin model of the WWTP of Hattem was constructed. This BioWin model simulates the performance of the treatment plant and investigates the impact of several adjustments, such as altered aeration and an extended anaerobic zone.

The simulation results showed that the DO setpoints of the aerators influenced the process in several ways. Increasing the aeration improved the results to a certain extent, after which the biological phosphorus removal deteriorated due to over-aeration. An extended anaerobic tank improved the biological phosphorus removal.

Unfortunately, a control system for biological phosphorus removal, using alternative monitoring variables, was not obtained. Control strategies cannot straightforwardly be implemented and tested in BioWin. A benchmark of an oxidation ditch is suggested for further research. The implementation of biological phosphorus removal in a benchmark of an oxidation ditch was started. This benchmark could provide a method to investigate the complex process of biological phosphorus removal and test control strategies.

Contents

List of Figures

List of Tables

Abbreviations

AOB Ammonium Oxidizing Bacteria.

ASM1 Activated Sludge Model 1.

ASM2d Activated Sludge Model 2d.

ASM3 Activated Sludge Model 3.

BOD Biochemical Oxygen Demand.

BPR Biological Phosphorus Removal.

BSM1 Benchmark Simulation Model 1.

BSM2 Benchmark Simulation Model 2.

DO Dissolved Oxygen.

HRT Hydraulic Retention Time.

NOB Nitrite Oxidizing Bacteria.

ORP Oxidation-Reduction Potential.

PAO Polyphosphate Accumulating Organism.

PHB Poly-Hydroxy-Butyrate.

SBR Sequencing Batch Reactor.

SRT Solids Retention Time.

VFA Volitale Fatty Acids.

WWTP Wastewater Treatment Plant.

1 | Introduction

1.1 Background information

Biological processes are a cost-effective and environmentally sound alternative to the chemical treatment of wastewater (Mulkerrins et al., 2004). A commonly installed treatment system is an oxidation ditch, where activated sludge processes ensure biological nutrient removal. The oxidation ditch is popular, because of its reliability and simplicity. An oxidation ditch distinguishes from conventional activated sludge treatment by a long Solids Retention Time (SRT) and Hydraulic Retention Time (HRT), a simplified flowsheet lacking anaerobic digestion and by channel flow characteristics (Randall et al., 1998). A Carrousel® is an oxidation ditch patented by Royal HaskoningDHV. Over 1200 Carrousels are installed globally (RoyalHaskoningDHV, 2018). A Carrousel is equipped with an aeration system to provide sufficient Dissolved Oxygen (DO) for activated sludge processes, such as Biochemical Oxygen Demand (BOD) removal, nitrogen removal and Biological Phosphorus Removal (BPR). It also keeps the biomass in suspension. The aeration can be adjusted in two ways, by changing the aeration intensity or the aerated volume (Amand et al., 2013).

Aeration is the largest single energy consumer at treatment plants, amounting to 45-75% of plant power usage (Rosso et al., 2008). Control of aeration systems can optimise the process and limit excess aeration, resulting in better nutrient removal and in energy savings (Amand et al., 2013). Existing control systems mainly focus on the nitrogen- or BOD removal capacity (Åmand & Carlsson, 2012). A common aeration control system for activated sludge processes adjusts the DO concentration setpoint based on the nitrogen removal. This control is ammonium driven, where the aeration is increased or decreased based on the measured ammonium concentration (Rieger et al., 2014). Ammonium control can lead to energy savings of around 5-25% (Åmand & Carlsson, 2012).

One type of control is a feedback control system, where the ammonium value is measured downstream of the aerator and the aeration is altered from this value. An alternative type of control is feed-forward control, where the oxygen demand is based on the monitored inlet flow and concentrations instead of downstream measurements. These types of control do not take potential disturbances into account before they occur. However, air flow demand varies over time, due to the fluctuations in the influent wastewater flow rate, concentration and composition. These fluctuations are a result of drinking water consumption, industrial water usage and rain events. To take these disturbances into account, increased attention is given to predictive control where some kind of model predicts the incoming load (de Koning et al., n.d.); (Rieger et al., 2014); (El-Din & Smith, 2002).

Mathematical models and computer simulations can help to forecast and analyse plant performance and to develop and test control strategies (Jeppsson, 1996). Several mathematical models and benchmarks have been developed to analyse activated sludge processes and to test control strategies (Abusam, 2001); (Henze et al., 2000); (Henze et al., 1999); (Copp, 2002); (Alex et al., 2008).

Aeration control systems and benchmarks often do not incorporate biological phosphorus removal. The majority of treatment plants incorporating P-removal utilise chemical precipitation using alum or lime (Mulkerrins et al., 2004). BPR is a complex biological process, influenced by many environmental factors, like temperature, DO, pH, influent water composition and more (Janssen et al., 2002). It would be ideal to control the oxidation ditch on biological phosphorus removal, so that less or no chemicals are needed to obtain the desired phosphorus concentration. Aeration control incorporating BPR has been studied, but most research is done on Sequencing Batch Reactor (Luccarini et al., 2002) or via a benchmark (Solon et al., 2017). There is little research and development on BPR in an oxidation ditch and possible control of BPR at oxidation ditches. In an oxidation ditch, the aerobic/ anoxic/ anaerobic state of the water differs over the length of the ditch, but the state at each location is not specifically known. Another difficulty with oxidation ditches is that they have a large re-circulation factor. The influent entering the oxidation ditch

is therefore immediately diluted with the already present and aerated mixed liquor. In order to improve simultaneously the BPR and nitrogen removal, more information is needed on the state and the length of the (un)aerated zones.

The goal of this thesis is to investigate the optimisation of biological phosphorus removal in oxidation ditches using a control system. Such a control system is desired in order to improve the aeration control of oxidation ditches, to increase the biological nutrient removal, to save on chemicals for phosphorus removal and to minimise energy consumption. The control system could save costs at many treatment plants since oxidation ditches are a common practice. The control system should take nitrogen removal into account as well, such that good nitrogen removal is still obtained. The total costs of measuring equipment at WWTPs are often high. This research will therefore focus on using simple and cheap sensors. A Wastewater Treatment Plant in Hattem is made available for examination at an operating full-scale oxidation ditch. Measurements can be done and ideas can be tested at this Wastewater Treatment Plant.

1.2 Research questions

In this research, the following main research question was formulated:

Main question

Can the biological phosphorus removal be controlled and optimized in an oxidation ditch using simple and cheap sensors, whilst maintaining efficient nitrogen removal?

Sub-questions

To answer the main question, the following sub-research questions were formulated:

- Bio-P influencing factors
  - What variables are useful to monitor Bio-P?
  - How are the values of these useful variables distributed over the oxidation ditch?
  - How can these variables contribute to a control system for a stable operated oxidation ditch?
- Control system
  - What cheap sensors, measuring these useful variables, would be suitable to monitor biological phosphorus removal in an oxidation ditch?
  - How does the nitrogen removal efficiency respond to Bio-P driven control in an oxidation ditch?
  - What type of control is suitable for stable operation including biological phosphorus- and nitrogen removal in an oxidation ditch?
  - How can be determined if the aeration intensity should be increased or lowered when biological phosphorus removal is insufficient?

1.3 Thesis layout

The thesis is divided into 7 chapters as follows:

Chapter 1 - Introduction

Chapter 2 - Theoretical Background The literature is reviewed to study the available knowledge of interest for this research. This includes the basics of nitrogen removal, detailed information on biological phosphorus removal, current control systems at WWTPs, control variables interesting for biological phosphorus removal and existing models and benchmarks that describe activated sludge processes and WWTP performances.

Chapter 3 - Case study: WWTP Hattem In this chapter the characteristics of the Wastewater Treatment Plant in Hattem are described, explaining the used treatment steps and the current control strategy.

Chapter 4 - Materials and Methods The materials and methods chapter presents the used measuring set-ups, performed measurements and the simulations executed.

Chapter 5 - Results and Discussion The results of the measurement campaign and of the simulations are presented and discussed.

Chapter 6 - Conclusions The main conclusions are summarized in this chapter and the answers to the research questions are given.

Chapter 7 - Recommendations Recommendations for future research are given as well as some advice concerning the studied WWTP Hattem are presented.

2 | Theoretical background

In this chapter, the literature is discussed that is of value for this thesis. This includes research on nitrogen removal, the Biological Phosphorus Removal (BPR) process, current control systems in wastewater treatment plants, possible alternative monitoring variables for the control of biological phosphorus removal and finally on existing models and benchmarks that could be of benefit for the control of biological phosphorus removal in an oxidation ditch.

2.1 Nitrogen removal

Nitrogen removal is a a fundamental process in wastewater treatment and it is one of the basic principles on which design choices are made. The total N-removal process consists of multiple sub-processes. N-removal in an oxidation ditch is a result of the following three processes (den Engelse et al., 1992):

- Ammonification
- Nitrification
- Denitrification

Ammonification

Ammonification is the first step of the total nitrogen removal process. In this step, organic bound nitrogen is released in the form of ammonium. For Wastewater Treatment Plant (WWTP) design there is not much attention paid to this step as it takes place in the sewerage to a large extent (den Engelse et al., 1992).

Nitrification

Nitrification is the second step in biological nitrogen removal. This process requires oxygen and CO_2. Ammonium is converted in two steps. The first step is carried out by Ammonium Oxidizing Bacteria (AOB), which convert the ammonium into nitrite, see Equation 2.1. In the second step, the nitrite is converted to nitrate by Nitrite Oxidizing Bacteria (NOB), see Equation 2.2 (den Engelse et al., 1992). The combined conversion equation can be seen in Equation 2.3.

$$NH_4^+ + \frac{3}{2}O_2 \rightarrow NO_2^- + 2H^+ + H_2 + Energy \tag{2.1}$$

$$NO_2^- + \frac{1}{2}O_2 \rightarrow +NO_3^- + Energy \tag{2.2}$$

$$NH_4^+ + 2O_2 \rightarrow NO_3^- + 2H^+ + H_2O + Energy \tag{2.3}$$

Denitrification

Denitrification is the last step of the total N-removal process. Heterotrophic bacteria transform nitrate into nitrogen gas. The nitrogen gas can escape the wastewater into the atmosphere and nitrogen is thereby removed from the wastewater. There are many heterotrophic bacteria that can carry out the denitrification process (den Engelse et al., 1992).

$$C_{10}H_{19}O_3N + 10NO_3^- \rightarrow 5N_2 + 10CO_2 + 3H_2O + NH_3 + 10OH^- \tag{2.4}$$

2.2 Biological phosphorus removal

In this section, the principle of Biological Phosphorus Removal will be described and some important factors that influence the process will be explained.

2.2.1 Basics

The Biological Phosphorus Removal process is a complex process based on Polyphosphate Accumulating Organism (PAO)s that are present in activated sludge. By circulating the activated sludge through anaerobic and aerobic phases, the PAO growth is stimulated and BPR can be achieved.

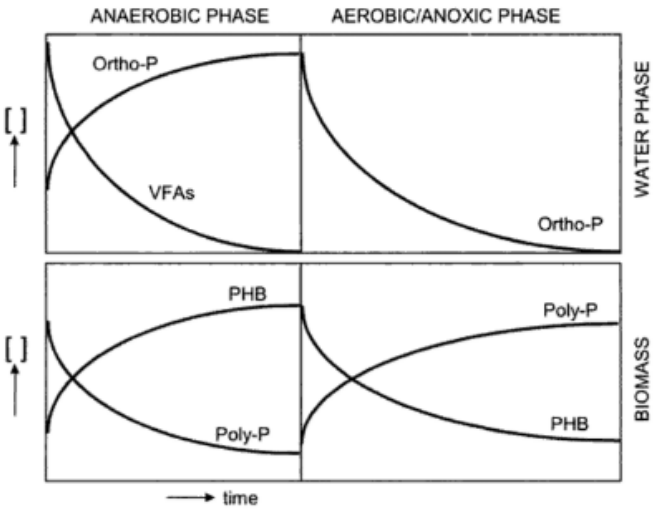

Figure 2.1: Metabolism of the bio-P process including glycogen and PHA cycles (Janssen et al., 2002)

Characteristic for the PAOs is that they can store large amounts of soluble ortho-phosphate intracellularly in the form of insoluble poly-phosphate (Janssen et al., 2002); (Smolders et al., 1994a). These poly-phosphate reserves function as an energy resource. In an anaerobic environment PAOs have an advantageous position towards other bacteria, because they can take up substrate (VFA) with the energy from the stored poly-phosphate. A sufficiently long anaerobic phase can result in a dominant position for PAOs with respect to other bacteria, since other bacteria have no or a lower availability to substrate. The substrate that is taken up by the PAOs is converted and stored as Poly-Hydroxy-Butyrate (PHB). This process utilises energy coming from both the degradation of the poly-phosphate as well as from the conversion of glycogen. The degradation of poly-phosphate results in phosphate release and thus an increase of phosphate in the water matrix. A schematic overview of these processes can be seen in Figure 2.1 and Figure 2.2a.

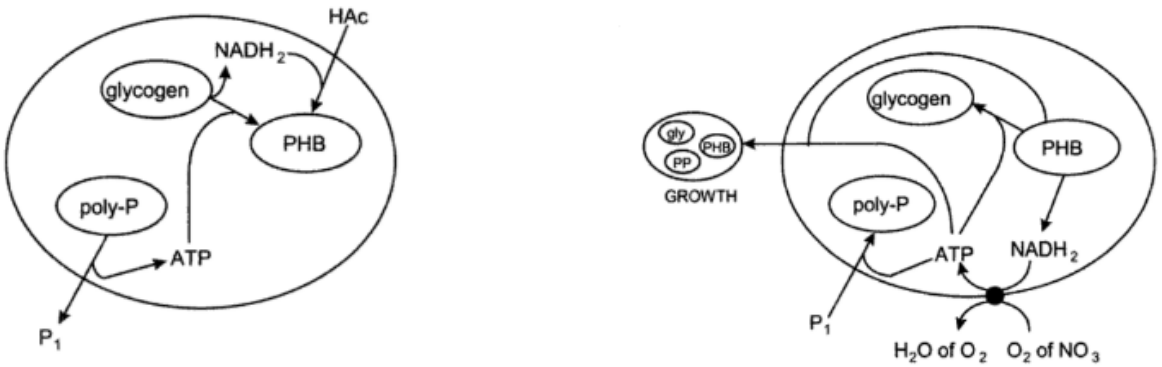

(a) Anaerobic phase

(b) Anoxic/ Aerobic phase

Figure 2.2: Schematic overview of the biochemical processes in the bio-P metabolism

Under aerobic or anoxic conditions, the PHB is then used as energy to grow and for the uptake of

ortho-phosphate resulting in storage of poly-phosphate in the cell (Smolders et al., 1994b); (Janssen et al., 2002). Figure 2.1 and Figure 2.2b show these processes schematically. The metabolism of the PAOs under aerobic and anoxic conditions is almost identical. Under aerobic conditions oxygen is used for the formation of ATP, whereas nitrate is used under anoxic conditions (Janssen et al., 2002).

For bio-P removal it is necessary that the influent is mixed with activated sludge in a strictly anaerobic zone, no nitrate, with sufficient retention time. As explained, this anaerobic environment is advantageous for PAOs with respect to other bacteria. Since the BPR capacity is directly linked to the amount of PAOs in the sludge, the increase of PAOs in this environment can increase the phosphate removal capacity. The phosphate can be removed from the water, by removing sludge from the treatment system carrying the intracellularly stored phosphate (Janssen et al., 2002).

2.2.2 PAO organisms

Biological phosphorus removal is a complex process, involving different organisms. Biological phosphorus removal is still not completely understood and new insights into the existing knowledge are still emerging. Candadidatus Accumilibactor phosphateis (Accumulibacter) was the organism thought to be largely responsible for biological phosphorus removal in laboratory and full-scale plants. New research suggests that the organism Tetrasphaera is mainly responsible for biological phosphorus removal. The Tetrasphaera has somewhat different features compared to the Accumilibactor. Under anaerobic conditions the Tetraspahera PAOs take up glucose and ferment this to succinate and other components. They synthesise glycogen as a storage polymer, using energy generated from the degradation of stored poly-phosphate and substrate fermentation. During the aerobic phase, the stored glycogen is needed for subsequent anaerobic metabolism (Kristiansen et al., 2013). A metabolic model of both the anaerobic and anoxic/aerobic phase can be seen in, Figure 2.3 and Figure 2.4 respectively.

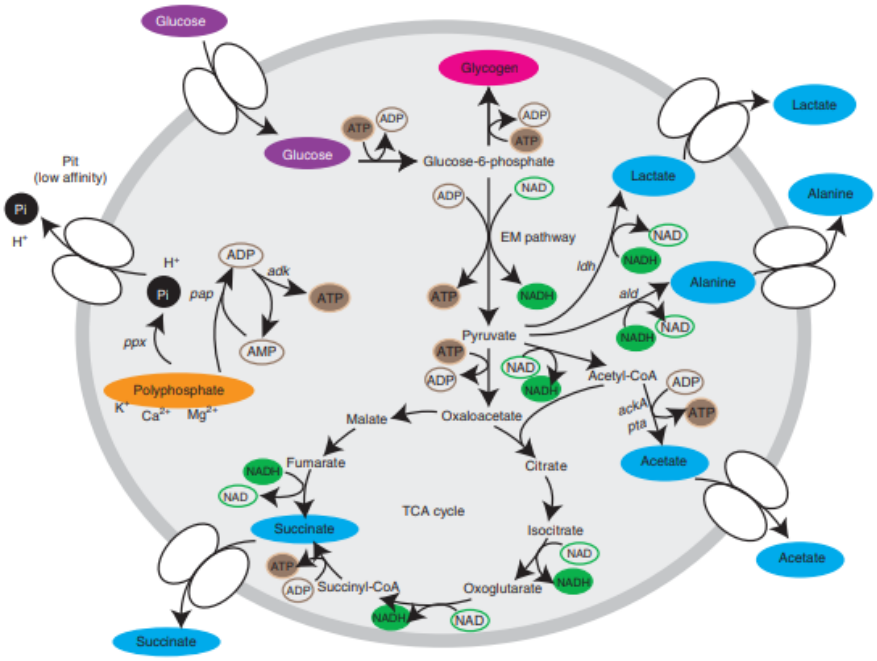

Figure 2.3: A metabolic model for Tetrasphaera: Anaerobic phase (Kristiansen et al., 2013)

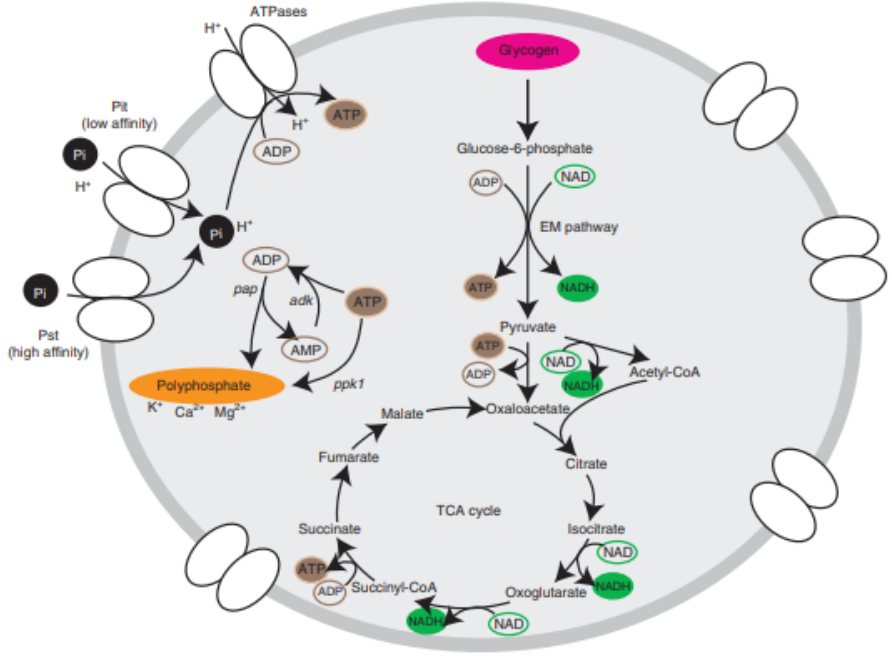

Figure 2.4: A metabolic model for Tetrasphaera: Anoxic/ Aerobic phase (Kristiansen et al., 2013)

2.2.3 Environmental factors influencing the biological phosphorus removal

Temperature

Biological phosphorus removal is influenced by temperature in multiple ways. The effect of a temperature change is therefore not always clear. The biological reaction rates are temperature dependent. Temperature not only influences the metabolic activities of the bacteria, but it also has an effect on other factors like gas-transfer rates and settling characteristics of biological solids (Crites & Tschobanoglous, 1998). Generally, an increase in temperature results in higher P-release and P-uptake rates of PAOs (Janssen et al., 2002). Brdjanovic, Logemann, et al. (1998) investigated the effect of long-term temperature change on both stoichiometry and kinetics of the anaerobic and aerobic phases of the bio-P removal process. Results from their study indicate that the temperature impact on the stoichiometry of BPR is marginal, while it has a rather strong influence on anaerobic kinetics. Temperature also has a strong effect on most aerobic processes. The study, (Brdjanovic, Logemann, et al., 1998), also indicates a significant change in required SRT to maintain sufficient bio-P removal; at 20 degrees Celsius the minimum SRT to maintain PAO is about two days, which increased to 16 days at 10 degrees Celsius and 32 days at 5 degrees Celsius.

pH

The pH affects the biological phosphorus removal process. An important influence of pH on the process is that the transport of acetate into the cell is sensitive to pH. A low pH has a negative effect on both the acetate uptake and the P-release (Mulkerrins et al., 2004). This means that at a low pH, more acetate is needed per amount of released phosphate. A relatively high pH value (>7.5) can be beneficial as it contributes to an increased phosphate uptake as well as increased chemical precipitation. The last of the two is only beneficial if chemical dosing for enhanced P removal is applied (Janssen et al., 2002).

The process of biological phosphorus removal affects the pH. Certain phases in the BPR process can be recognised in pH patterns. This will be further explained in subsection 2.3.1.

Cations

For the transport of the phosphorus, from the water environment into the cell, cations are needed. Potassium and magnesium play an important role with the uptake of phosphate, (Rickard & McClintock, 1992); (Mulkerrins et al., 2004). For each milligram of phosphorus, 0.33 mg potassium and 0.26 mg of magnesium are taken up (Janssen et al., 2002). Potassium influences the membrane permeability. Potassium is also an

essential ion for poly-phosphate in the cell (Machnicka et al., 2004). In the metabolic models in Figure 2.3 and Figure 2.4 the use of these cations for the metabolism is displayed. Brdjanovic et al. (1996) studied the effects of potassium limitation on phosphorus uptake. It was concluded that when there is a potassium shortage in the influent, phosphorus removal cannot be achieved. The poly-phosphate concentration in the biomass decreases and anaerobic P-release and acetate uptake is negatively affected.

Nitrate and Oxygen

Both nitrate and oxygen can influence the BPR process negatively and positively. Nitrate and oxygen are both essential for the phosphate uptake in the aerobic or anoxic phase. However, it is necessary to maintain an anaerobic zone. In this anaerobic zone, the introduction of oxygen or nitrate (via influent or return streams) should be strictly prohibited.

Shehab et al. (1996) studied the effect of the DO concentration on activated sludge processes in aeration tanks. It was concluded that in the aerobic tank a DO concentration of 3.0-4.0 mg/L is required when both nitrification and phosphorus uptake are desired. When only nitrification is required, this can be lowered to 2.0 mg/L DO. Brdjanovic, Slamet, et al. (1998) showed that excessive aeration of activated sludge can lead to deterioration in the BPR efficiency. Over-aerations leads to depletion of PHB. Phosphorus uptake stops, when subjected to excess aeration, because this process needs PHB.

Volitale Fatty Acids and glucose

Volitale Fatty Acids (VFA) and glucose are substrate for the PAOs, namely the Accumulibacter and Tetrasphaera respectively (Kristiansen et al., 2013). VFA is present in the influent and is partially formed in the sewage system, especially in the case of a pressured sewage system. The concentration of VFA in the wastewater can be increased by fermentation of COD and fermentation of primary sludge (Janssen et al., 2002).

Sludge Retention Time

The sludge retention time can affect the biological phosphorus removal in multiple ways. A higher SRT increases the storage capacity of poly-phosphate, due to decreased nitrification which minimises the inhibition of the BPR process by nitrate. A very high SRT can lead to an increased chance of over-aeration, as a result the growth of the PAOs and consequently the bio-P process is inhibited (Janssen et al., 2002). Very long SRT and HRT can also lead to deterioration of the biological phosphorus removal due to the proliferation of glycogen accumulating organisms (GAOs) (Mino et al., 1998).

2.3 Monitoring variables for control

In this section, several variables are presented that have been studied in literature as a possible monitoring variable for the control of biological phosphorus removal.

2.3.1 pH

pH is a commonly used variable for on-line monitoring and control of activated sludge processes, because of the reliability of the instruments and the low costs. In batch reactors, the relationship between pH and activated sludge processes has been studied. Maurer & Gujer (1995) found that the pH increases during the anoxic phase, due to the production of hydroxyl ions. Afterwards pH decreases until P-release has ended. Under aerobic conditions, if P uptake finishes before ammonia oxidation does, pH can be used to assess P uptake. Tanwar et al. (2008) showed that phosphate release during anaerobic conditions coincided with a sharp decrease in pH. After a continuous increase, the pH stabilises at a constant value with the end of phosphate uptake. Spagni et al. (2001) found a good correlation between P-release and pH. However, it is difficult to assess whether the pH relation is related to bio P removal or to carbon dioxide stripping if P uptake ends later than ammonia oxidation.

pH profiles and ORP profiles

Chang & Hao (1996) studied Oxidation-Reduction Potential (ORP) profiles and pH profiles in SBRs. They found that pH and ORP could be useful for monitoring and real-time control purposes. Several significant points associated with the activated sludge processes are identified in pH profiles, see Figure 2.5 and Table 2.1. Slope changes in pH profiles are found to represent the corresponding biological reactions better, see Figure 2.6 and Table 2.1.

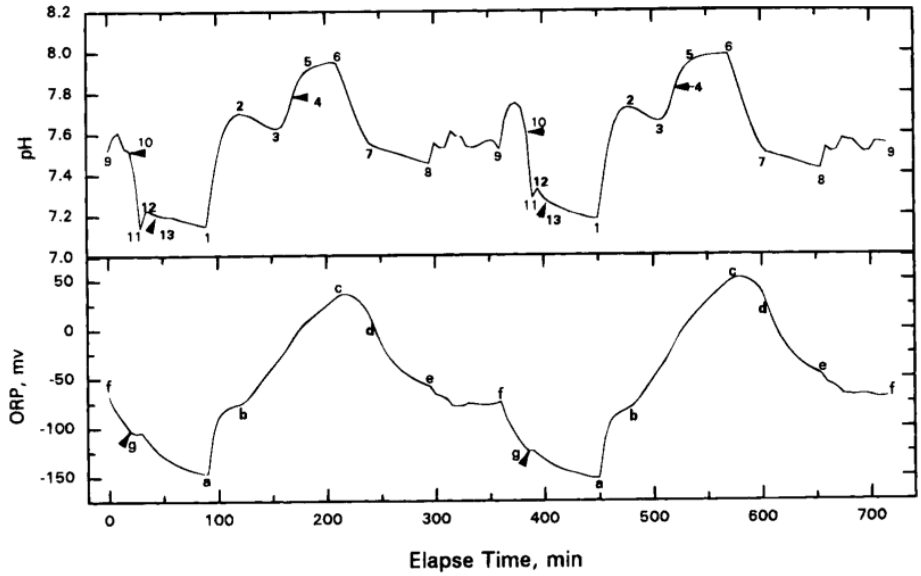

Figure 2.5: pH and ORP profiles from Chang & Hao (1996) indicating breakpoints in nutrient removal, see Table 2.1 for legend

Table 2.1: Legend for points in pH and ORP profiles(Chang & Hao, 1996)

pH Profiles		*ORP Profiles*	
1	beginning of aerobic cycle	a	beginning of aerobic cycle
2	**beginning of initial nitrification**	**b**	**beginning of initial nitrification**
3	**ammonia valley** (end of initial nitrification)		
4	**phosphate uptake end point**		
5	**end of ammonification**		
6	end of air-on period	c	end of air-on period
7	**beginning of endogenous denitrification**	**d**	**beginning of endogenous denitrification**
8	end of IDLE stage	e	end of IDLE stage
9	beginning of FEED stage	f	beginning of FEED stage
10	beginning of MIXED-REACT stage	g	beginning of MIXED-REACT stage
11	beginning of well-mixed system		
12	**nitrate apex** (end of denitrification)		
13	**phosphate release end point**		

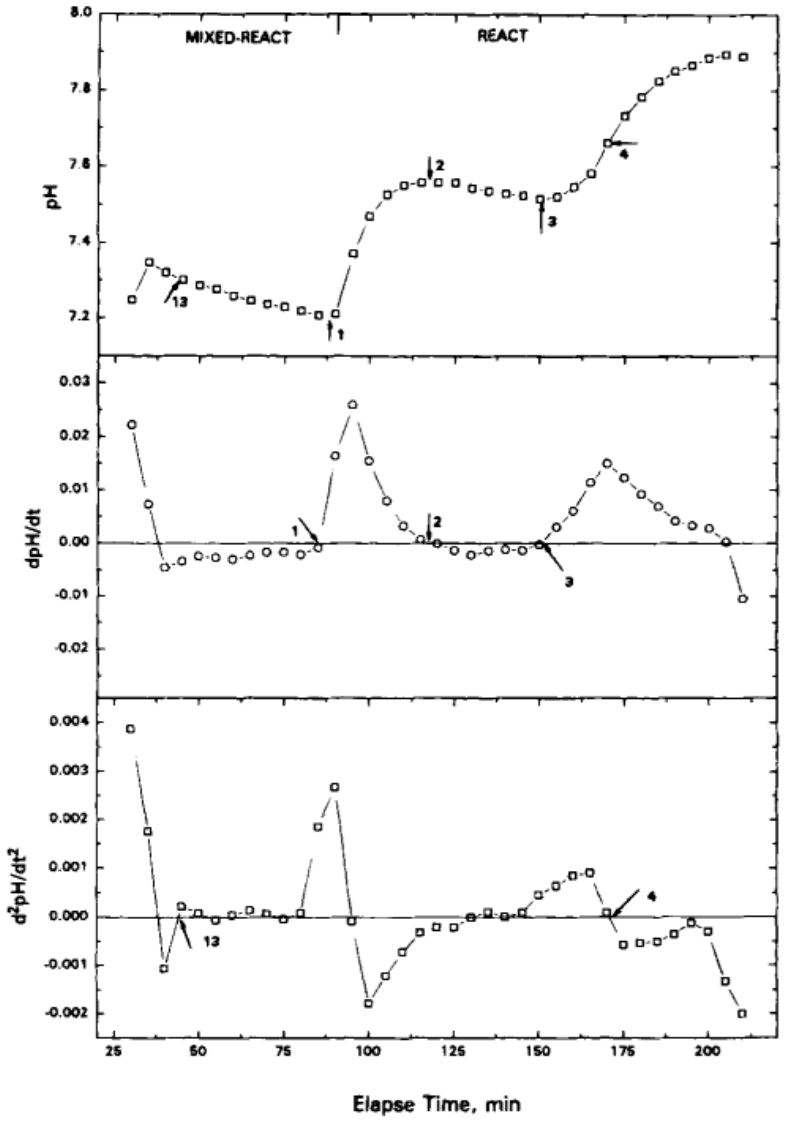

Figure 2.6: First and second derivative profiles of pH and the corresponding breakpoints in nutrient removal, see Table 2.1 for legend (Chang & Hao, 1996)

2.3.2 ORP

Spagni et al. (2001) found that during the aerobic phase ORP can monitor the nitrification successfully. Nitrate depletion can be correlated with a sudden change in the signal slope, while the end of the P release phase is not related to any evident effect on the ORP trend. In the anaerobic phase, ORP is not reliable in monitoring simultaneous denitrification and P-release. Spagni et al. (2001) concluded that pH shows better performance.

As already mentioned in subsection 2.3.1, Chang & Hao (1996) studied the pH and ORP profiles with respect to nutrient removal in an SBR. Although some points of N removal can be identified from the ORP profile, Chang & Hao (1996) concluded that the ORP profile does not provide clear evidence corresponding to different biological reactions. Tanwar et al. (2008) showed that the ORP profile can detect the end of various processes, such as denitrification and the end of the anaerobic phase. Biological phosphorus removal processes are more difficult to detect by ORP.

2.3.3 Conductivity

Conductivity increases when denitrification is over and reaches a plateau when P-release is ended. It can be used as a variable for monitoring and control of denitrification and P-release (Spagni et al., 2001). Maurer & Gujer (1995) also showed that for an SBR, conductivity can be a valuable control variable for biological phosphorus removal. Conductivity decreases during denitrification and increases under anaerobic

conditions proportionally to the phosphate concentration. Potassium, magnesium, calcium and phosphate show a positive correlation to the conductivity, whereas acetate and pH show a negative correlation.

2.3.4 Potassium

Phosphate release and uptake in enhanced biological phosphorus removal from wastewater are dependent on the presence of Potassium (Brdjanovic et al., 1996). As explained in section 2.2.3, for each milligram of phosphorus, 0.33 mg potassium is taken up (Janssen et al., 2002). The relationship between potassium and phosphorus can be of interest to monitor potassium for the control of biological phosphorus removal.

2.3.5 DO

The DO concentration indicates whether the activated sludge is in an aerobic phase at the location or not. Tanwar et al. (2008) showed that during the aerobic phase, the DO could also be an effective control variable in an Intermittent Cyclic Process Bio-reactor (ICPBR) to describe nutrient removal. The DO profile over time in the aerobic phase could be linked to nutrient removal processes. DO is important in the control of nutrient removal as it directly influences the process and can be easily adjusted by increasing or decreasing the aeration. DO based control systems are common, however these control systems are not designed for BPR (Jeppsson et al., 2002).

2.3.6 Nitrate/ Ammonium

Online nitrate and ammonium measurements indicate the state of the nitrification/ denitrification. It can also give some indication on the state of the BPR process as it is known that when nitrate is present, P-release will not occur and the change in ammonium and nitrate can indicate an aerobic, anoxic or anaerobic environment (Janssen et al., 2002).

2.3.7 Soft sensors

Soft sensors are used to predict response variables, which are difficult to measure, using the data of predictors that can be obtained relatively easier. Soft sensors can be useful when a certain process variable cannot be measured by a sensor, or when the sensor is expensive, unreliable or has other disadvantages. To predict a certain response variable, other process variables which are easily measured in the plant and mathematical model of the process are used. Therefore, the main task in soft sensor development is the process model building which approximates unknown relationship between easy-to-measure variables and difficult-to-measure variable (Grbic et al., 2012). One example of a soft sensor is a neural network based soft sensor, which uses artificial Neural Networks (NNs). Artificial Neural Networks (NNs) are computing procedures used to model complex systems through a process of learning from examples.

As explained, in subsection 2.3.1, subsection 2.3.2 and subsection 2.3.3, Spagni et al. (2001) studied the possibility to use ORP, pH and conductivity to monitor nitrogen and phosphorus removal in an SBR. The study shows some promising results, however from this study it was concluded that for reliable and effective control of nutrient removal a more sophisticated control system seems to be necessary, such as a fuzzy logic and neural network control system. A study by Luccarini et al. (2002) shows that Neural Networks (NN) can be used as soft on-line sensors for controlling biological processes in SBRs. Elmans NNs are used to predict the N and P concentrations during different SBR phases by measuring ORP and pH. Therefore, the end of the biological nutrient removal processes can be identified. As there are currently no cheap and reliable N and P sensors, the NNs could be an effective tool to solve that gap by only using only ORP and pH sensors. This can be used to design control strategies for biological nutrient removal. Belchior et al. (2012) studied the use of an adaptive fuzzy control for DO control of activated sludge processes and the results of the study show that this controller can learn and improve control rules resulting in accurate DO control.

2.4 Control systems for WWTPs

Much research has been done on control systems for WWTPs. However often these do not include biological phosphorus removal, or are not applied to oxidation ditches. Already some examples of control have been

discussed, but in this section, a short overview of some examples is given. These examples could bring ideas for a solution to control an oxidation ditch with respect to biological phosphorus removal.

Olsson et al. (2005) studied 36 WWTPs, with in total 83 controllers, of which 61% are on/off controllers, 37% are PID controllers, 1.8% are advanced controllers, and 0.34% is unknown. The type of aeration control differed from constant aeration rate, to applied manual control of aeration, to control of aeration by DO sensor, to DO profile control and lastly ammonium sensor based aeration control, see Figure 2.7.

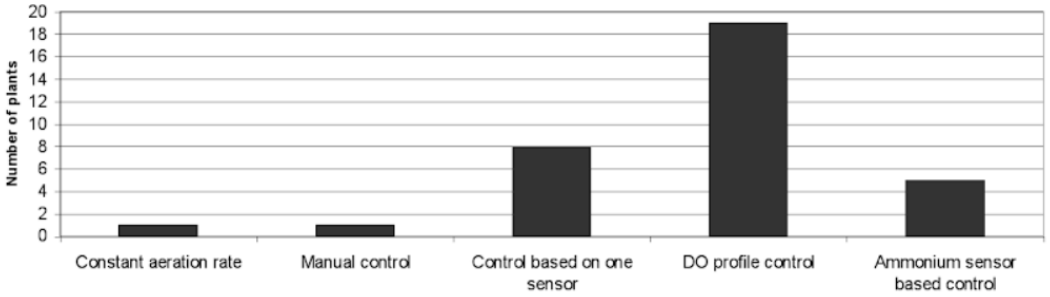

Figure 2.7: Choice of control strategy for aeration at different WWTPs Olsson et al. (2005)

Jeppsson et al. (2002) surveyed thirteen European countries regarding instrumentation, control and automation (ICA) in wastewater treatment. A summary of the most common types of control applied in WWTPs can be seen in Table 2.2.

Table 2.2: Most common types of real-time control applied in large European WWTPs. Where: +++ = normally used, i.e. standard, ++ = frequently used, + = seldom used; used for B = feedback control, F = feed-forward control. Jeppsson et al. (2002)

Aeration by measuring	Control handle	Comment and (usage, type of control)
Dissolved oxygen (one or more sensors)	Air flow and/or pressure	Constant set point (+++, B)
Air pressure in common rail	Air flow and/or pressure	General air demand set point (+++, B)
Dissolved oxygen (multiple sensors)	Air flow and/or pressure	DO profile control (++, B)
Redox potential	Air flow and/or pressure	Primarily in SBR plants (++, B)
Respiration	Air flow and/or pressure	Standard in Austria (+, B)
Nitrification by measuring		
Ammonia at end of aerobic part	Dissolved oxygen set point	Also intermittent aeration, on/off (+, B)
Ammonia at head of aerobic part	Dissolved oxygen profile	Adjust to ammonia load (+, F)
Denitrification by measuring		
Influent flow rate	Internal recirculation flow	(++, F)
Nitrate at end of reactor	Internal recirculation flow	Use denitrification capacity (++, B)
Nitrate in anoxic part	Internal recirculation flow	Use denitrification capacity (+, B or F)
Nitrate in anoxic part	External carbon flow	Enhance denitrification (+, B or F)
Sludge inventory by measuring		
Influent flow rate	Return sludge flow	Ratio control (+++, F)
Suspended solids in reactor	Return sludge flow	Often constant MLSS (++, B)
Suspended solids in reactor	Waste sludge flow	Often constant MLSS (++, B)
Sludge blanket level	Return sludge flow	Standard in Finland (+, B)
Sludge age (indirectly)	Waste sludge flow	Normally manually (+, B)
Chemical additions by measuring		
Flow rate	Coagulants, polymers, P-precipitants	(++, F)
Phosphate	P-precipitants	Based on load (+, B or F)
Suspended solids	P-precipitants	(+, F)
pH	Lime addition	Mainly anaerobic digestion (++, B or F)
Others by measuring		
Influent flow rate	Internal flow distribution	Step-feed approaches (+, F)
Flow, levels, rain measurements	Influent buffering, storm tanks etc.	Including sewers, equalise influent (+, F)
Phosphate	Flow rates, acetate addition etc.	In bio-P processes (+, B or F)

One of the control systems used in WWTP's is real-time control on DO measurements. This feedback type of control aims at maintaining a set DO concentration, which is set by the operator. The DO concentration is set to a level at which low residual effluent ammonia is achieved. The DO profile in the oxidation ditch and the DO demand variate constantly. Now the DO is usually set at a safe setpoint, ensuring sufficient aeration, which often results in over-aeration during low loading periods. Optimising this, can result in saving energy and costs on aeration. An improved control system can be found in ammonia-based control, where ammonia measurements are used for feedback control of the aeration capacity. Another improvement for a control system can be found in predicting disturbances in the process, like rain weather events or changes in the wastewater load. A solution is found by using feed-forward control, predicting the inflow and concentrations before they occur and adjusting the control to these predictions (Rieger et al., 2014); (de Koning et al., n.d.); (El-Din & Smith, 2002). de Koning et al. (n.d.) comes with a control scheme that includes feed-forward control as well as feedback control. This control system is based on a

load forecast and self-learned relationship between load and required oxygenation. The influent prediction uses the principle that consumption of drinking water and thus production of wastewater is very regular. The prediction takes different types of days into account and deals with special days such as holidays. The control system collects data and control actions are analysed in relation to the measured values. A self-learning mechanism will then regularly update the relationship between load and required oxygenation. El-Din & Smith (2002) came up with a neural model that uses rainfall data, observed in the collection system discharging to the plants, as inputs to predict the wastewater inflow at a WWTP. Rieger et al. (2014) discusses the benefits from the feed-forward control based on load predictions as often the ammonia peaks result from a kinetic constraint and increasing the DO likely will not help. Though feed-forward control can in some cases offer benefits to reduce the effluent peak in ammonia, careful case analysis should be applied to determine whether it does as implementing feed-forward control can also bring additional costs. As discussed in subsection 2.3.7, Luccarini et al. (2002) showed that neural networks can be used to control biological processes in an SBR, and that it can be used to predict N and P concentrations.

2.5 Modeling and Benchmarks

In this section, some important models and benchmarks are explained.

2.5.1 Activated Sludge Models

The Activated Sludge Models are mathematical models describing the kinetics and stoichiometry of activated sludge processes. The models are used for several purposes, like design, control and research. The first activated sludge model ASM1 was developed to create a tool to model nitrogen-removal processes. After the first model, more have come, where later also phosphorus removal was incorporated (ASM2d and ASM3) (Henze et al., 2000). The models consist of components that are soluble $S_?$ and components that are particulate $X_?$. The soluble components will only be transported with the water, while the particulate components can change due to settling/ thickening. The soluble components can carry ionic charge, whilst the particulate components must be electrically neutral (Henze et al., 2000).

ASM1

The ASM1 model contains thirteen differential equations to describe the concentrations of:

1. S_I: Soluble inert organic matter
2. S_S: Readily biodegradable soluble substrate
3. X_I: Particulate inert organic matter
4. X_S: Readily biodegradable particulate substrate
5. X_{BH}: Active heterotrophic particulate biomass
6. X_{BA}: Active autotrophic particulate biomass
7. X_P: Particulate from biomass decay
8. S_O: Soluble oxygen
9. S_{NO}: Soluble nitrate and nitrite nitrogen
10. S_{NH}: soluble ammonium nitrogen
11. S_{ND}: soluble biodegradable organic nitrogen
12. X_{ND}: particulate biodegradable organic nitrogen
13. S_{ALK}: Alkalinity

These variables are described using eight processes, namely:

1. Aerobic growth of heterotrophs
2. Anoxic growth of heterotrophs
3. Aerobic growth of autotrophs
4. Decay of X_{BH}
5. Decay of X_{BA}
6. Ammonification of S_{ND}
7. Hydrolysis of entrapped organics
8. Hydrolysis of X_{ND}

With the corresponding eight process rates:

$$\rho = \begin{pmatrix} \mu_H \left(\frac{S_S}{K_S + S_S}\right)\left(\frac{S_O}{K_{OH} + S_O}\right) X_{BH} \\ \mu_H \eta_g \left(\frac{S_S}{K_S + S_S}\right)\left(\frac{K_{OH}}{K_{OH} + S_O}\right)\left(\frac{S_{NO}}{K_{NO} + S_{NO}}\right) X_{BH} \\ \mu_A \left(\frac{S_{NH}}{K_{NH} + S_{NH}}\right)\left(\frac{S_O}{K_{OA} + S_O}\right) X_{BA} \\ b_H X_{BH} \\ b_A X_{BA} \\ k_a S_{ND} X_{BH} \\ k_h \frac{X_S}{K_X X_{BH} + X_S}\left(\frac{S_O}{K_{OH} + S_O} + \eta_h \frac{K_{OH}}{K_{OH} + S_O}\frac{S_{NO}}{K_{NO} + S_{NO}}\right) X_{BH} \\ k_h \frac{X_{ND}}{K_X X_{BH} + X_S}\left(\frac{S_O}{K_{OH} + S_O} + \eta_h \frac{K_{OH}}{K_{OH} + S_O}\frac{S_{NO}}{K_{NO} + S_{NO}}\right) X_{BH} \end{pmatrix}$$

Figure 2.8: Process rates rates ASM1. Benhalla et al. (2010)

To obtain the ordinary differential equation representing a specific component, the conversion rates need to be coupled with the appropriate mass balance equations. This is compactly presented in matrix form, see Table 2.3 (Henze et al., 2000):

Table 2.3: ASM1 in matrix form (Henze et al., 2000)

Component → i	1	2	3	4	5	6	7	8	9	10	11	12	13	
j Process ↓	S_I	S_S	X_I	X_S	X_{BH}	X_{BA}	X_P	S_O	S_{NO}	S_{NH}	S_{ND}	X_{ND}	S_{ALK}	Process rate ρ_j [ML^{-3}T^{-1}]
1 Aerobic growth of heterotrophs		$-\frac{1}{Y_H}$			1			$-\frac{1-Y_H}{Y_H}$		$-i_{XB}$			$-\frac{i_{XB}}{14}$	$\hat{\mu}_H \frac{S_S}{K_S+S_S}\frac{S_O}{K_{O,H}+S_O} X_{BH}$
2 Anoxic growth of heterotrophs		$-\frac{1}{Y_H}$			1				$-\frac{1-Y_H}{2.86Y_H}$	$-i_{XB}$			$\frac{1-Y_H}{14\cdot 2.86\cdot Y_H}-\frac{i_{XB}}{14}$	$\hat{\mu}_H \frac{S_S}{K_S+S_S}\frac{K_{O,H}}{K_{O,H}+S_O}\frac{K_{O,N}}{K_{O,N}+S_O}\eta_g X_{BH}$
3 Aerobic growth of autotrophs						1		$-\frac{4.57-Y_A}{Y_A}$	$\frac{1}{Y_A}$	$-i_{XB}-\frac{1}{Y_A}$			$-\frac{i_{XB}}{14}-\frac{1}{7Y_A}$	$\hat{\mu}_A \frac{S_{NH}}{K_{NH}+S_{NH}}\frac{S_O}{K_{O,A}+S_O} X_{BA}$
4 Decay of X_{BH}				$1-f_P$	-1		f_P					$i_{XB}-f_P\cdot i_{XP}$		$b_H X_{BH}$
5 Decay of X_{BA}				$1-f_P$		-1	f_P					$i_{XB}-f_P\cdot i_{XP}$		$b_A X_{BA}$
6 Amonif. of S_{ND}										1	-1		1/14	$k_a S_{ND} X_{BH}$
7 Hydrolysis of entrapped organics		1		-1										$k_H \frac{X_S/X_{BH}}{K_X+X_S/X_{BH}}\left(\frac{S_O}{K_{O,H}+S_O}+\eta_h\frac{K_{O,H}}{K_{O,H}+S_O}\frac{S_{NO}}{K_{NO}+S_{NO}}\right)X_{BH}$
8 Hydrolysis of X_{ND}											1	-1		$\rho_7 \frac{X_{ND}/X_S}{}$
Stoichiom. param.: Heterotrop. yield Y_H Autotrop. yield Y_A Biomass fraction to particulates f_P Biomass N/COD i_{XB} N/COD in products from biomass i_{XP}	Sol. inert org. matter [M(COD)L^{-3}]	Readily biod. substrate [M(COD)L^{-3}]	Partic. inert org. matter [M(COD)L^{-3}]	Slowly biod. substrate [M(COD)L^{-3}]	Active heterotrophs [M(COD)L^{-3}]	Active autotrophs [M(COD)L^{-3}]	Partic. from biomass decay [M(COD)L^{-3}]	Oxygen (negative COD) [M(-COD)L^{-3}]	Nitrate and nitrite nitrogen [M(N)L^{-3}]	NH_4^++NH_3 N N [M(N)L^{-3}]	Sol. biod. org. N[M(N)L^{-3}]	Particulate biod. org. N[M(N)L^{-3}]	Alkalinity [Mol L^{-3}]	*Kinetics param.:* Heterotrophic growth and decay: $\hat{\mu}_H, K_S, K_{OH}, K_{NO}, b_H$ Autotrophic growth and decay: $\hat{\mu}_A, K_{NH}, K_{OA}, b_A$ Factor of anox. growth of X_{BH}: η_g Ammonification: k_a Hydrolysis: k_H, K_X Factor for anoxic hydrolysis: η_h

Observed conversion rates [ML^{-3}T^{-1}]: $r_i = \sum_j v_{ij}\rho_j$

As an example to show how this matrix can be interpreted, the ordinary differential equation (ODE) for component 5, X_{BH}, is shown. The processes involved can be found by looking which processes (j) are addressed in the column of component 5. This is the case for j=1,2,4. Then the component reaction rate can be calculated by:

$$r_i = \sum_j v_{i,j}\rho_{i,j} \tag{2.5}$$

$$r_5 = 1 * \rho_1 + 1 * \rho_2 + (-1) * \rho_4 \tag{2.6}$$

ASM2d

ASM2d is an extension of the activated sludge model number 1. There are more components added to include additional biological processes to deal with biological phosphorus removal. To incorporate biological phosphorus removal, the concentration of biomass cannot be described by the variable X_{BM}, as it now has to contain internal cell structure. In ASM2d it is taken into account that PAOs can use intracellularly stored organics for their growth. In ASM2d also Total Suspended Solids (TSS) are taken into account, which was not the case in ASM1, there all particulate organic material was based on COD. Henze et al. (1999). The matrix form of ASM2d can be seen in Appendix L (Meijer, 2004). The matrix can be used the same way the ASM1 matrix can be used, as explained previously.

2.5.2 Benchmark

Activated sludge processes explained before, benefit from being controlled, as this can achieve more effective and more efficient treatment. A true comparison and review of control strategies from literature are difficult because of the many variables that impact the process. Therefore, a standardised procedure, the Benchmark Simulation Model BSM1, to evaluate control strategies by computer simulations is introduced (Copp, 2002). In the simulation benchmark a plant design is comprised of five reactors in series with a 10-layer settling tank. The biological processes are represented by the ASM1 model, described in subsection 2.5.1. The settling processes of the settling tank are represented by the double-exponential settling velocity

function of Takacs (1991). The influent files consist of three files, each to represent a different weather event, namely dry weather, rain weather and storm weather. Each file contains 14-day influent data at fifteen minute intervals, in the following order: time, S_S, X_{BH}, X_S, X_I, S_{NH}, S_I, S_{ND}, X_{ND}, Q, S_O, X_{BA}, X_P, S_{NO}, S_{ALK}. The simulation benchmark describes a two-step simulation procedure involving simulation to steady-state followed by dynamic simulations using the three influent data files. Initially, the system needs to be simulated under steady-state using constant flow and composition influent dry weather data. The data is defined using steady state solver software, simulating 100 days using a constant influent. With this steady state starting data, a consisted starting point is ensured. After the steady state simulation, dynamic simulations, using the three influent files described, should be performed. Since BSM1, more platforms arose, modified to other plant configurations Gernaey & Jørgensen (2004), longer evaluation periods Rosén et al. (2004), different mathematical model assumptions Menniti et al. (2012) and novel treatment technologies. Solon et al. (2017) presented a modified BSM2, that incorporates biological phosphorus removal into the benchmark. One benchmark using ASM1 and BSM1 is of particular interest for this research as it simulates an oxidation ditch (Abusam, 2001), see subsection 2.5.3 and Appendix K.

2.5.3 Benchmark for oxidation ditch

The IWA benchmark, subsection 2.5.2, is used by Abusam (2001) to come up with a benchmark specialised for an oxidation ditch. In this benchmark, instead of the plant presented in Copp (2002) consisting of five bioreactors and a settling tank, a representation of an oxidation ditch is researched and used. The benchmark uses Simulink, Matlab, the ASM1 model and the ten-layer settling model by Takacs (1991). The oxidation ditch is modelled by a loop of 10 CSTR's, see Figure 2.9. In Appendix K more detailed information on this benchmark is given and a start has been made to incorporate biological phosphorus removal into the benchmark, which could be of interest for future research.

The Simulink lay-out, using 10 CSTRs in a loop to model an oxidation ditch, of the oxidation ditch benchmark by Abusam (2001) can be seen in Figure 2.9.

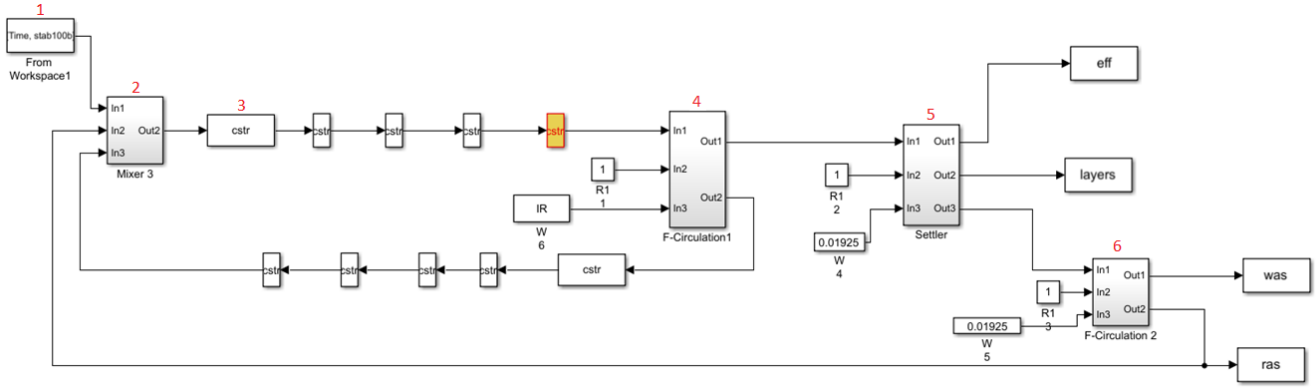

Figure 2.9: Simulink lay-out of the benchmark of an oxidation ditch from Abusam (2001)

2.6 Summery Theoretical Background

Nitrogen removal is a fundamental process in wastewater treatment and it is one of the basic principles on which design choices are made. N-removal in an oxidation ditch is a result of the following three processes: ammonification, nitrification and denitrification. During these processes organic bound nitrogen is released in the form of ammonium first, after which ammonium is transformed into nitrite and nitrate and lastly nitrate is then transformed into nitrogen gas.

Biological phosphorus removal is a complex process based on Polyphosphate Accumulating Organisms that are present in activated sludge. By circulating the activated sludge through anaerobic and aerobic phases, the PAO growth is stimulated and biological phosphorus removal can be achieved. Characteristic for the PAOs is that they can store large amounts of soluble ortho-phosphate intracellularly in the form of insoluble poly-phosphate. In an anaerobic environment PAOs can take up substrate with the energy from the stored poly-phosphate. The degradation of poly-phosphate results in phosphate release and thus an increase of soluble ortho-phosphate in the water matrix. Under aerobic conditions the PAOs grow and take

up ortho-phosphate resulting in a storage of poly-phosphate in the cell. There are many environmental factors influencing the biological phosphorus removal, such as temperature, pH, cations, nitrate and oxygen, substrate availability and the sludge retention time.

Multiple studies have been done on finding alternative monitoring variables for nutrient removal processes. The studied alternative monitoring variables interesting for control of biological phosphorus removal and nitrogen removal are pH, ORP, Conductivity, Potassium, DO and nitrate. Also, the use of soft sensors to monitor biological phosphorus removal has been studied, resulting in for example neural network based soft sensors. It should be noted that most studies, investigating alternative monitoring variables and soft sensors to monitor biological phosphorus removal, are on other treatment systems than oxidation ditches.

Current control systems at WWTPs consist use feedback, feedforward or predictive control. The control strategy often focusses on control of aeration by DO sensors, DO profile control or ammonium sensor based control of aeration.

Mathematical models and computer simulations can help to forecast and analyse WWTP performance and to develop and test control strategies. Several mathematical models and benchmarks have been developed to analyse activated sludge processes and to test control strategies. Aeration control systems and benchmarks often do not incorporate Biological Phosphorus Removal. A benchmark by Abusam (2001) specialises on an oxidation ditch, but phosphorus removal is not included in the benchmark.

3 | Case study: WWTP Hattem

The Wastewater Treatment Plant in Hattem is designed to treat the wastewater coming from the residents and some industries of the municipalities Hattem and Oldebroek, including Hattemerbroek, Broekdijk, 't Loo, Oldebroek, Oosterwolde and Wezep. The water is transported partly with pressurised pipes and partly gravitational pipes. The treatment plant has a biological loading capacity of 71,000 population equivalent or 136 g TOD. The hydraulic capacity is 1500 m^3/h.

The treatment plant was built in 1962 and is a conventional treatment plant using an oxidation ditch. The details of the treatment scheme are explained in this chapter. The layout of treatment plant can be seen in Figure A.1 in Appendix A. The effluent of the wastewater treatment plant is discharged into the IJssel.

Figure 3.1: WWTP Hattem

3.1 Wastewater treatment train

The wastewater is treated during several treatment steps in the WWTP Hattem. A simplified representation is given in Figure 3.2 for a quick overview.

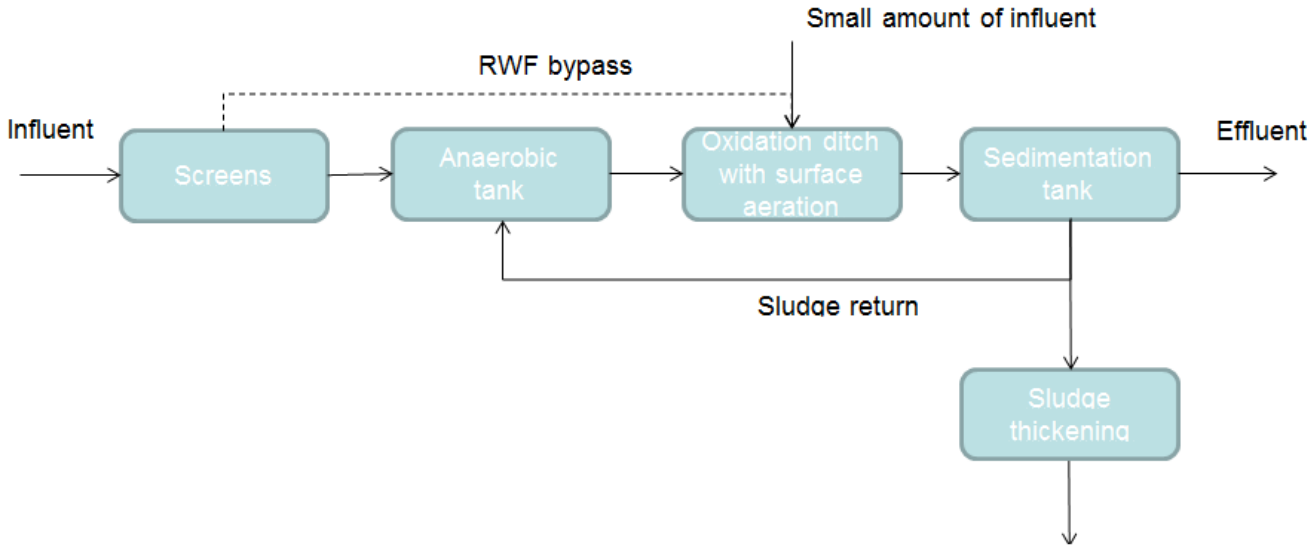

Figure 3.2: Simplified treatment scheme of WWTP Hattem

As mentioned the wastewater enters the treatment plant partially via gravitational pipes and partially via pressurised pipes. The pre-treatment of the arrived wastewater consists of screens which capture the coarse material from to water to prevent clogging in the subsequent treatment steps. After the screens, it used to be transported to a primary sedimentation tank as can be seen in Figure A.1, but not in Figure 3.2 since this sedimentation tank has been out of use for a long time. From the screens, the wastewater now goes directly to an anaerobic tank after which it enters the oxidation ditch. The anaerobic tank is constructed as a plug flow gutter, where at the beginning of the gutter, activated sludge is partially returned. The oxidation ditch has two surface aerators. The current inlet location of the oxidation ditch is located near aerator 2 at location 3, see Figure C.1, however it used to be located at the other aerator, aerator 1 at location 14. It should be noted that the oxidation ditch also has a secondary inlet point, see 'In2' in Figure C.1, where occasionally a small amount of wastewater from several surrounding houses enters the oxidation ditch without primary treatment. After the oxidation ditch it enters the secondary sedimentation tank, where sludge is captured and cleaned water is discharged into the river IJssel. The sludge is partly returned to the treatment scheme in the anaerobic tank and is partly captured for further processing externally.

3.2 Design parameters

A table, Table B.1, with detailed information on the design parameters, dimensions and loading rates can be found in Appendix B.

For the design of the treatment plant an inventory was made to estimate the wastewater produced by current residents, industries, recreation and the barracks in the neighbourhood and to incorporate estimated growth in the future. As it is a combined sewer system, also rain weather prediction was incorporated in the design. This lead to a design load of $676m^3/h$ for dry weather flow and $1384m^3/h$ for rain weather flow. The total pump capacity at RWF is $1500m^3/h$, because of the pumping capacities of the pumping stations. The dimensions of the oxidation ditch were mainly chosen based on hydraulical data, to ensure a sufficient flow rate to keep the activated sludge suspended. The oxidation ditch is equipped with two aerators and all channels are $3.75m$ deep and $8.5m$ wide, with a total volume of $13,566m^3$. The anaerobic tank prior to the oxidation ditch is relatively small, with a volume of $300m^3$. The sedimentation tank was designed based on the settling properties of the sludge, but it was designed before the STORA guideline of 1981 and the STOWA guideline of 2002 and therefore sludge buffering was not incorporated in the design. The sedimentation tank has a volume of 3000 m^3, more details can be found in Table B.1 in Appendix B.

3.3 Wonderware

Wonderware is the platform used by Waterschap Vallei & Veluwe to monitor and operate the Wastewater Treatment Plant. The WWTP Hattem is equipped with several online analysers, namely:

- ORP
- DO
- Dry matter
- Phosphate
- Ammonium
- Nitrate

The values measured are logged and stored in Wonderware. Historical data can be viewed and trend lines of variables over time can be studied. An example of such a representation of variables can be seen in Figure 3.4. The variables and time frame can be chosen as desired to obtain figures of any measured variable at any chosen period of time.

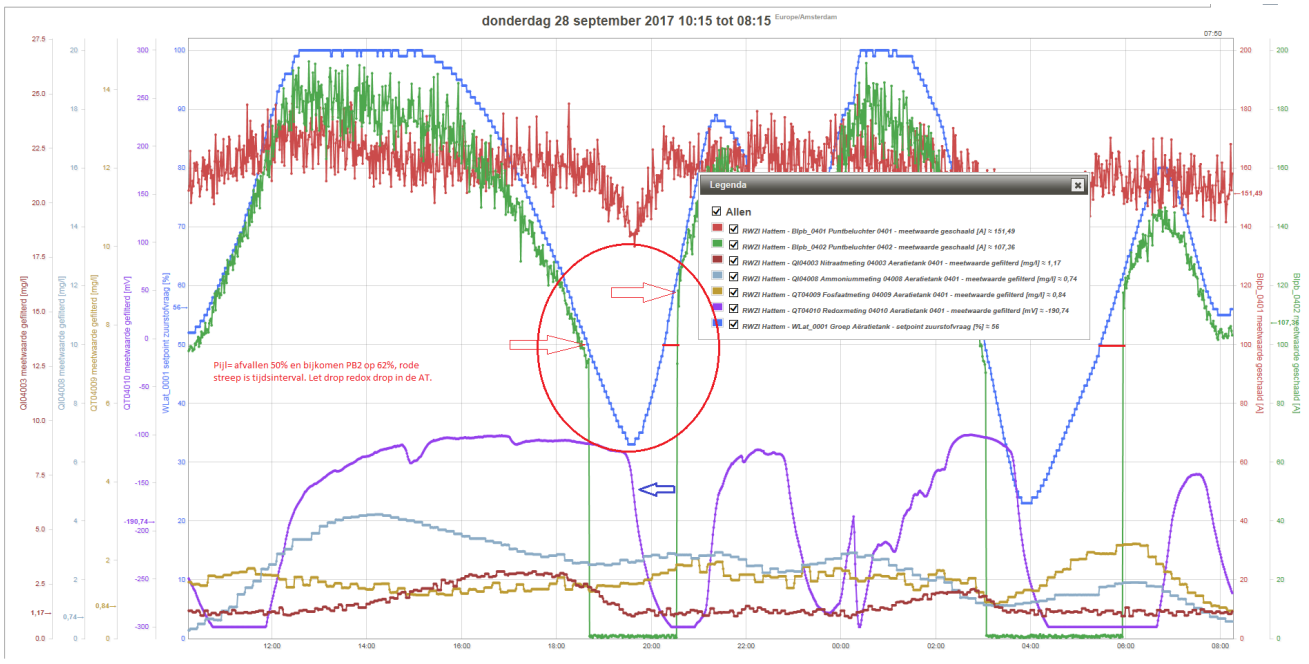

Figure 3.3: Wonderware interface - trendlines

Besides historical and current data and graphs, also the operation and control of the WWTP are done via Wonderware. The treatment scheme is schematically presented in Wonderware, including the equipment, the current operation and live updates. As an example, the schematic overview of the oxidation ditch in Wonderware can be seen in Figure 3.4.

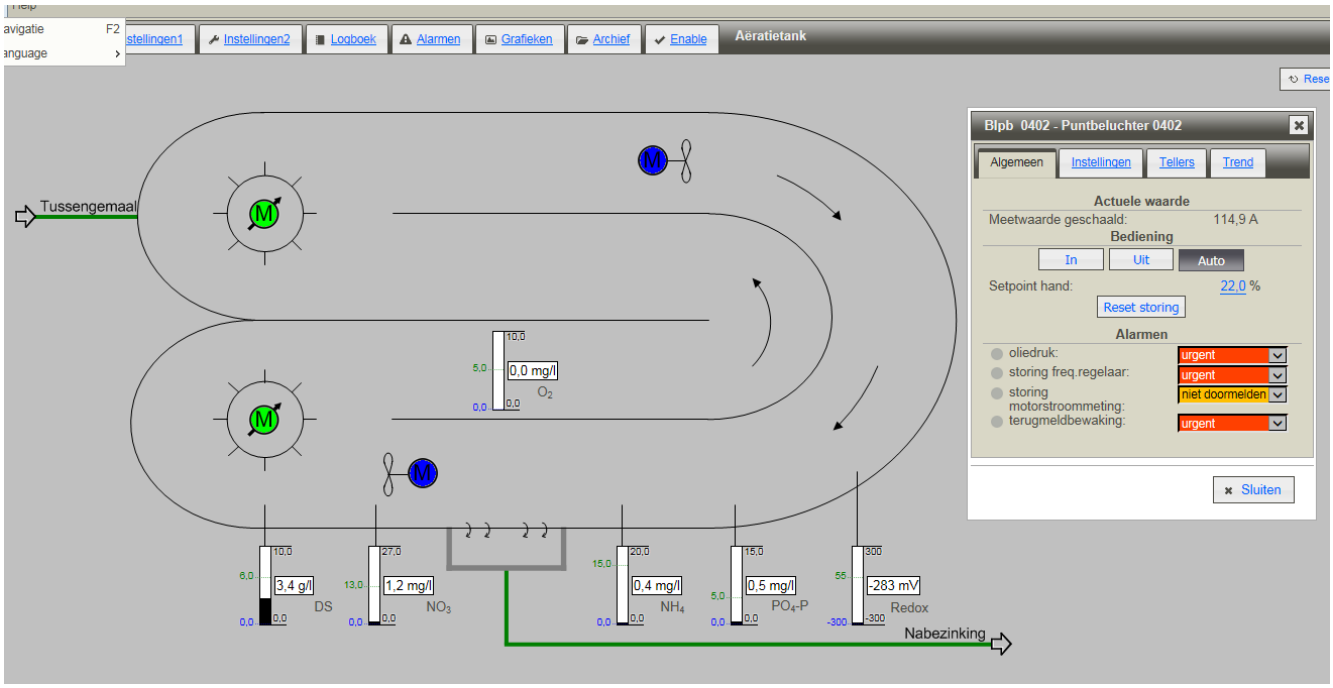

Figure 3.4: Wonderware interface - oxidation ditch

3.4 Current control strategy

The aeration preferences and control preferences can be adjusted in Wonderware, a preview of the Wonderware display can be seen in Figure 3.5 (in Dutch). The current control strategy of the oxidation ditch in Hattem is based on total N removal in the aeration circuit. The aerator is manipulated using combined oxygen or ORP and ammonium monitoring. At a sufficiently low ammonium concentration (current set-point is 1.5 mgN/L, see Figure 3.6) the aeration is switched off. At an ammonium concentration higher than the set-point, aerator 1 is switched on. When the measured ammonium concentration is higher than 1.5 mgN/L, the DO set-point is increased corresponding to the linear relationship shown in Figure 3.6. Phosphorus removal is not incorporated in the control strategy, only when the phosphorus concentrations cross certain limits, the DO setpoints are manually altered. In Hattem, aerator 1 is the main aerator, meaning that if the aeration capacity needs to be increased, it will first be done by increasing aerator 1. If aerator 1 is at full capacity and more aeration is required, aerator 2 jumps in to increase the aeration capacity further. Aerator 1 is the so-called 'main aerator' and aerator 2 is the so-called 'slave aerator'.

The limiting effluent quality standards for nitrogen and phosphorus removal that WWTP Hattem has to ensure are the following:

- Nitrogen: 10 mg/L
- Phosphorus: 3.5 mg/L

The limiting effluent quality values have to be met by the treatment plant and are checked by the municipality.

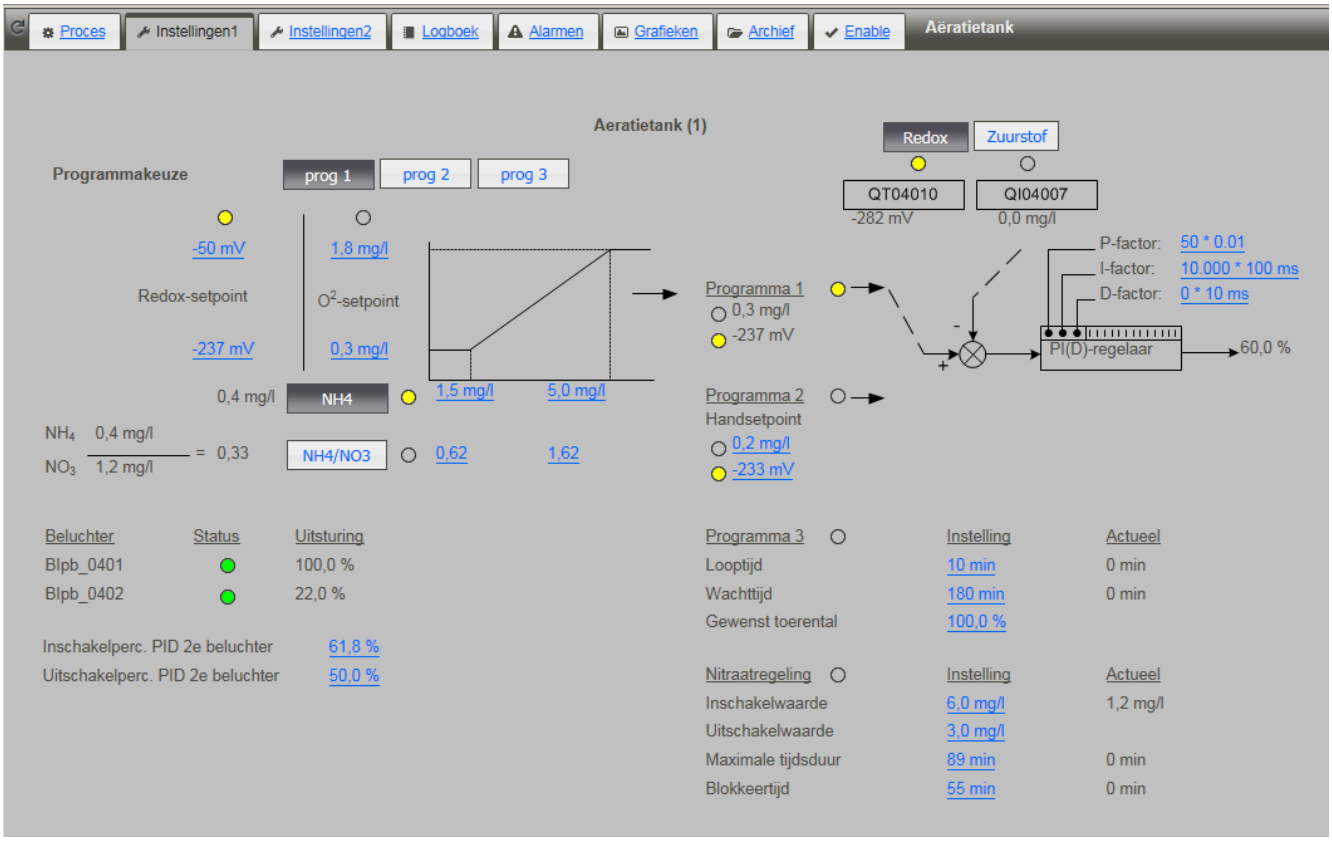

Figure 3.5: Wonderware interface - control

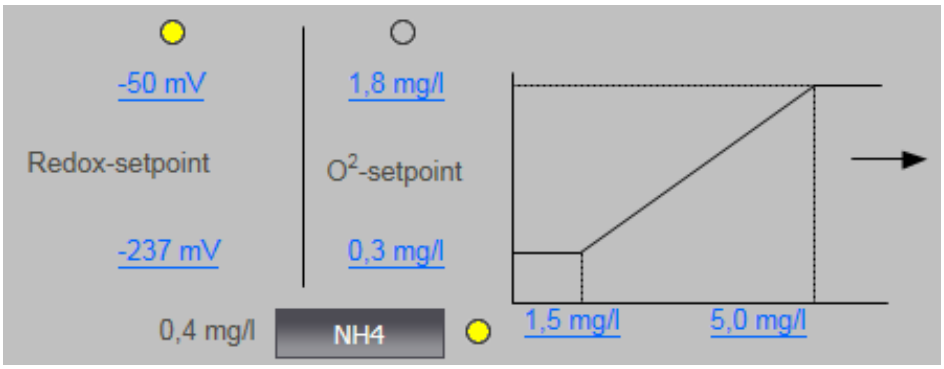

Figure 3.6: Wonderware interface - Control relation Ammonium - ORP

3.5 Summary Hattem

The WWTP of Hattem treats the wastewater coming from the residents and some industries of the municipalities of Hattem and Oldebroek. The treatment plant consists of screens, an anaerobic contact tank, an oxidation ditch, a sedimentation tank and sludge thickening. Sludge extracted in the sedimentation tank is partly returned to the anaerobic tank. The oxidation ditch has a total volume of 13,566 m^3. Currently the WWTP is monitored and controlled using the platform Wonderware. In Wonderware the values measured by the online analysers are logged and can be studied, including measurements of ORP, DO, Dry Matter, Phosphate, Ammonium and Nitrate. The current aeration control of the oxidation ditch is focused on nitrogen removal, using the online DO, ORP and ammonium measurements.

4 | Materials and methods

For the design of the control system, first the current situation needs to be known. To investigate the situation several methods were used. First of all a literature study has been done, chapter 2, to gain knowledge of the relevant processes and systems. Then a measuring campaign on a full-scale treatment plant was executed to gain extensive real-life knowledge of the situation. Lastly a BioWin model and a Benchmark system were described. BioWin was used to simulate and test several scenarios, where the response of the oxidation ditch to several (operational) adjustments was tested, such as other aeration settings and an extended anaerobic tank. The Benchmark in Matlab/ Simulink was proposed for further investigation as it is possible to incorporate control strategies in this platform, whereas this is not possible in BioWin. A beginning to incorporate BPR in the oxidation ditch benchmark was made and can be seen in Appendix K.

4.1 Measuring campaign

The measuring campaign was designed to gain more knowledge on the oxidation ditch in practice and on the distribution of interesting variables found in literature throughout the oxidation ditch. The variables were measured at multiple locations throughout a full-scale oxidation ditch. In this section the measuring campaign materials and methods are explained. Details behind specific choices for the materials, methods and set-up can be found in the internship report Bost (2018), during which it was designed. Due to practical reasons, some alterations were made on the measurement campaign proposed in Bost (2018). These alterations are explained in the relevant sections in this chapter.

4.1.1 Variables to measure

From literature, several variables were selected for the measuring campaign which showed interesting relations with biological phosphorus removal. The measured variables are given in Table 4.1. Detailed theory behind the chosen variables can be found in chapter 2.

Table 4.1: Measured variables

Sample analysis				Sensors	
Water matrix (filtered)		Sludge matrix (unfiltered)			
Variable	Unit	Variable	Unit	Variable	Unit
COD	mg/L	Phosphate release rate	mg/ g.h	Conductivity	μS/cm
sum N	mgN/L	tKN	g/ kg ds	DO	mg/L
NH4	mgN/L	FOS/TAC ratio		pH	
NO2	mgN/L	TSS	g/L	ORP	mV
NO2 + NO3	mgN/L	Dry matter	%	Temperature	degree celsius
NO3	mgN/L	Total P	g/ kg ds		
Ortho-P	mgP/L	Potassium	mg/ kg ds		
Potassium	mg/L	Magnesium	mg/ kg ds		
Magnesium	mg/L	Calcium	mg/ kg ds		
Calcium	mg/L	Sodium	mg/ kg ds		
Sodium	mg/L	Nitrification capacity	mg N/ g.ds.h		

4.1.2 Measuring locations and set-up

In Appendix C an image, C.1, with the chosen measuring locations for the several measurements can be seen. At these locations, the measurement was done at 1 [m] below the surface. The oxidation ditch is huge with many inaccessible locations that are difficult to reach. To make sure every location could be measured, a set-up was constructed to reach all locations. A simplified view of this set-up can be seen in Figure 4.1.

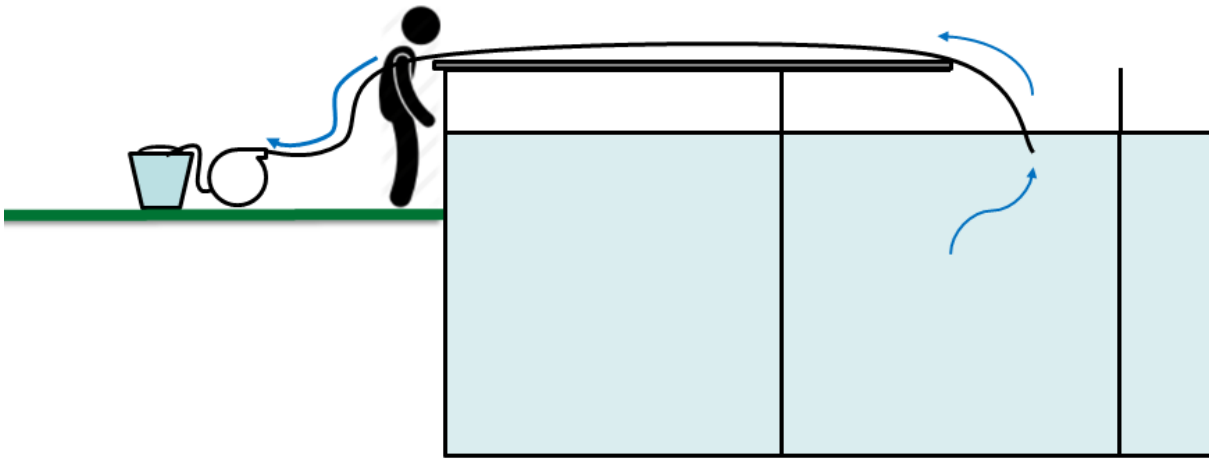

Figure 4.1: Schematic representation of the used measuring set-up

The measuring set-up consisted of a large telescopic pole of around 2 meters, that can be elongated to around 11 meters. A hose was attached to the pole, using tie wraps, and one end of the hose was connected to a peristaltic pump. The other end of the hose was attached to the end of the telescopic pole and could then be placed at any desired location that stretches around 11 meters from the pump. With one end of the hose placed around 1 meter below the water surface of the oxidation ditch and the other via the peristaltic pump to a bucket, water could be pumped from any spot of the oxidation ditch into a bucket. The pole was placed on the edge of the oxidation ditch or on the bridge over the aerators, to place the hose at the desired locations, an example can be seen in Figure 4.2. Here the pole lays on the bridge over the aerators, to reach measurement location 14.

Figure 4.2: The used mearuing set-up in action from the top of the oxidation ditch at WWTP Hattem

4.1.3 Type of measurement

Some of the variables were measured using sensors, while other variables needed to be measured in the laboratory, for which samples were taken. The prepared samples were analysed by Aqualysis, a laboratory specialized in water analysis. In Table 4.1 it can be seen what method was used to measure a certain parameter. In Appendix D an overview is given of the needed measurement at each measuring location. It

can be seen that not all the locations mentioned in C.1 are in there. The locations that are not mentioned in Appendix D were only supposed to be measured with sensors. Eventually some of these locations had to be skipped, to make sure all measurements could be done during one day. The feasibility of the number of measurements for one day and the number of samples to prepare was misjudged and therefore the locations with samples were prioritized. Aqualysis performed the sample analysis by NEN standards, an overview of this is given in Appendix F Table F.1. The method number in Table F.1 is a given number by Aqualysis, that they use for their registration.

4.1.4 Required materials

To perform the measurements, quite some equipment was needed, for personal protection, the set-up, the sensors, storing and preserving samples and more. A whole list of all materials required is given in Appendix E. For the samples, many pots were needed to store them, and specific preservatives, filters and syringes were required. As the samples were analysed at Aqualysis, the material was provided by them. In Table 4.2 a list is presented with the required type of sample pot (FGH001, FGH004, FGH011, FGH013, FGH014, FGH015) for each variable to measure, including the required sample volume, the need for filtration and the preservative used. In Appendix E an overview is given of the amount and type of sample pots needed at any measurement location, see Table E.1.

Table 4.2: The sample pots from Aqualysis used for the measurements

Sample pot	Variables to measure	Volume [mL]	Preservative	Filtered/ unfiltered
FGH001	Ammonium	100	0,15mL 50% sulphuric acid	Filtered
FGH004	Nitrate, Nitrite, Ortho-P	100	no	Filtered
FGH011	Sludge measurements	720	no	Unfiltered
FGH013	COD, TKN, Total-P, Sum N	500	2.0 mL 50% sulphuric acid	Unfiltered
FGH014	Suspended Solids	1000	no	Unfiltered
FGH015	Metals	125	1.25 mL 35% nitric acid	Filtered

4.1.5 Operational settings

The measuring campaign was executed in two variants. These two versions had mostly identical operational settings, except for the DO setpoint of the aerators.

During version 1, aerator 1 was turned on at a fixed rate, whilst aerator 2 was turned off. The flow was regulated at one rate, namely around 450 m^3/h. During version 2, similar settings were used, but the aerator settings were switched, so aerator 2 was turned on at a fixed rate, whilst aerator 1 was turned off.

The reason to execute the measurements twice with two different operational settings is because the aerators are located at different spots. One is located where the influent enters the oxidation ditch, whilst the other is located just after the location where the mixed liquor is withdrawn from the oxidation ditch and before the influent enters it. Keeping the eventual goal in mind of obtaining a control system that benefits the BPR and N removal, the influence of the location of 'main'- and 'slave'-aerator could be important. By measuring the two variants, the effect of the location of the main aerator on the effluent quality can be compared, as all other conditions were kept the same during the two versions.

A third measurement day was executed in which only the outer arm of the oxidation ditch was measured using sensors, now instead of using the measurement set-up explained in subsection 4.1.2 the wastewater was measured by holding the sensors directly in the wastewater. This was done to compare the measured values from the sensors of the two measuring methods: directly, by holding the sensors in the water and indirectly, by first collecting the water in the bucket and then holding the sensors in the captured water.

4.1.6 Measuring method

A step wise measuring plan is presented to follow during the measurement campaign in Appendix G. Some important steps are highlighted in this subsection. To prepare the measurements, a miniature laboratory with all the essentials was set-up next to the oxidation ditch, see Figure 4.3. Everything necessary for the measurements was easily accessible, which was necessary to perform the measurements at pace and to make the amount of measurements during one day achievable. Also, the pole, with attached hose was

prepared and ready beforehand. The set-up was tested with buckets of tap water. Also, a test was done using warm water and cold water, to test how long it takes for the water to go through the hose at a certain pump capacity. This was used during the measurements, to make sure the previous sample still present in the hose was pumped out, before capturing the new sample.

Figure 4.3: Small laboratory set up at Hattem

It is important to make sure the operational settings chosen for the execution of the measurements are already implemented some time before executing the measurements, as the treatment system has a response time. Therefore, the water flow was already set to a constant flow of 450 m^3/h beforehand and the aerator settings were adjusted the day before.

On the day of the measurements everything was ready in place and the measurements could be started. To do all measurements, the pole was placed at the right location, making sure the hose was 1 [m] below water surface (using a weighted tip of the hose). Then the pump was turned on and the water was pumped through the hose. The first part was not captured in the bucket as it still contains previous sample. Then the bucket was filled with the wastewater from the current location. The sensors, using WTW multimeter (3420) and WTW sensors (IDS SenTix pH electrode 940, IDS SenTix ORP-T 900, IDS TetraCon 325, IDS FDO 925), were hold in the bucket and the values were noted, see Figure 4.5. Then the necessary sample pots were filled with the captured wastewater and filtered, using 0,45 μm syringe filters, and preserved when necessary, see Figure 4.4. To ensure the right sample pots were filled Table E.1 was used together with Table 4.2 to make sure the sample was properly prepared.

Figure 4.4: Filtering the samples next to the oxidation ditch

Figure 4.5: Reading the sensors

4.1.7 Practicalities

There were some practicalities that needed to be considered. Firstly, the government needed to be notified of the measuring campaign. The usual operation of the WWTP is disrupted by altering the operational settings and performing the measurements and this can affect the results of the treatment plant. When the municipality is informed and approves, the WWTP will not be fined when it under performs. Secondly, it was important that the measurements were performed during dry weather flow.

4.2 BioWin

A model in BioWin was made to simulate the WWTP of Hattem. The model was made following the set-up and design variables of the WWTP in Hattem. Then existing data of the influent and effluent of Hattem, obtained from the waterboard, was used to design the base case. Having the influent data, the effluent data and the design variables, there was one unkown variable left, which was the exact DO set-point at the time of operation during the obtained influent and effluent data. As this was the main unknown, the influent data can be used as the input in BioWin and then the DO setpoint could be iterated until the effluent data from the simulation approached the effluent data from Hattem. After the base case was simulated, some scenarios were modelled to test the responses of the treatment system to these changes.

In chapter 5 the results are presented of all simulations:

- Base case
- Temperature change
- Switch of main aerator
- Different aeration modes
- Extended anaerobic tank
- Different aeration modes with extended anaerobic tank

4.3 Matlab/ Simulink

The benchmark presented by Abusam (2001) incorporates the ASM1 in a benchmark for an oxidation ditch, implemented in Matlab and Simulink. This model has shown to be reliable and applicable, but it does not take phosphorus removal into account. As it would be interesting to design and test control strategies incorporating biological phosphorus removal for oxidation ditches, it would be desirable to incorporate phosphorus removal into the benchmark, as it is not possible to implement control systems in BioWin. A

start was made to expand the model to incorporate phosphorus removal for future simulations and control strategy design. This was done by executing the following steps:

1. Investigate current model
   (a) Understanding the Simulink lay-out
   (b) Tracking down meaning and origin of the variables in the Matlab and C^{++} code
   (c) Tracking down the origin and meaning of the calculations in the C-MEX files
2. Explain necessary changes for renewed model
   (a) Presenting an adjusted Simulink lay-out
   (b) Explain the necessary changes/ expansion in the variables of the Matlab and C^{++} code
   (c) Explain the necessary changes/ expension in the calculations in the C-MEX files

The results are presented in Appendix K. The existing model was described and the necessary changes are indicated.

4.4 Summery Materials and Methods

A measurement campaign was set-up to obtain more information on multiple variables interesting for biological phosphorus removal in an oxidation ditch, including measurements of DO, ORP, pH, conductivity, nitrate, ammonium, phosphorus, potassium and more. These variables were measured at several locations in the oxidation ditch, to obtain a profile of these variables over the length of the oxidation. To access each location a measuring set-up was constructed using a telescopic pole, a hose and a peristaltic pump. Using this set-up, the mixed liquor could be pumped out of the oxidation ditch from any location into a bucket. The collected mixed liquor in the bucket could be measured using sensors and laboratory analysis, for which samples were taken and prepared. The measurement campaign was executed twice, version 1 and version 2, under different operational settings. Both times the flow was set at 450 m^3/h. During version 1, aerator 1 was turned on at a fixed rate and aerator 2 was switched off. During version 2, aerator 1 was turned off and aerator 1 was turned on at a fixed rate. Additionally, a third day of measurements was executed to only measure the outer arm of the oxidation ditch with sensors, holding the sensors directly in the oxidation ditch instead of using the measuring set-up.

Besides the measurement campaign, a BioWin model was made to simulate the WWTP of Hattem. The model was made following the set-up and design variables of the WWTP in Hattem. Then existing data of the influent and effluent of Hattem, obtained from the waterboard, was used to design the base case. Several scenarios were simulated to test the response of the WWTP to these changes, namely: temperature change, switching the 'main' and 'slave' aerators, using different aeration modes and extending the anaerobic tank.

Lastly, as control strategies cannot straightforwardly be implemented and tested in BioWin, a benchmark of an oxidation ditch is suggested for further research. As the existing benchmark of an oxidation ditch does not incorporate biological phosphorus removal, a method to implement biological phosphorus removal in the benchmark was presented in Appendix K for future research.

5 | Results and Discussion

In this chapter, the results of the measurement campaign and BioWin simulations will be displayed and discussed. More details about the set-up of the measurement campaign can be found in chapter 4. Some slight changes to the measurement campaign were made during the measuring days due to practicalities, these will be explained, and some important factors from chapter 4 will be repeated to help understand the results.

5.1 Measuring campaign

A measurement campaign at an oxidation ditch in Hattem was executed to obtain more information on multiple variables interesting for biological phosphorus removal in an oxidation ditch. In this section of the chapter, the results from these measurements will be presented, discussed and compared to the literature presented in chapter 2.

5.1.1 Recap measurement campaign

Measured locations

During the measuring campaign, multiple variables were measured as explained in chapter 4. These variables were measured at several location points in the oxidation ditch, to obtain a profile of these variables over the length of the oxidation ditch, see Figure C.1 for these locations. Measuring location 1 and 2 are not displayed in the figure since these are in the anaerobic contact tank at the beginning and end of the tank respectively. Every location would be measured with sensors and some would be sampled additionally, as explained in chapter 4. Eventually, due to tight time planning, some locations that would only be measured with sensors were skipped to make sure that all the planned sample locations were fully measured using sensors and sample analysis.

Measured variables

During the measurement campaign many variables were measured, they are listed in Table 4.1. The reason for choosing these variables is explained in chapter 2. In Appendix H the complete results of the measurement campaign can be found. Some important measured variables for this research are plotted and discussed in this chapter, such as potassium, pH, ORP, NH_4^+, NO_2, NO_3^- and Ortho-P. In the plots, also some important locations are indicated by vertical lines. The green 'In' line indicates the location where the influent enters the oxidation ditch. At the same location a red line indicates 'A2' when the second aerator was turned on, namely in variant 2. Another green line 'In2' indicates the second inlet location, where occasionally some wastewater from surrounding houses enters the oxidation ditch. The blue line indicates the location where the mixed liquor is withdrawn from the oxidation ditch. The red 'A1' afterwards represents aerator 1 when it is turned on, namely in variant 1. Location 1 and 2 are in at the beginning and ending of the anaerobic contact tank respectively. As the oxidation ditch recirculates, it should be noted that from location 22 the mixed liquor is returned to location 3.

Several operational settings

The whole measurement campaign is executed twice, namely variant 1 and variant 2, with a difference in the operational settings. In variant 1 the first aerator is on, while the second is off, see Figure C.1. Aerator 1 is the main aerator of the oxidation ditch, which is under normal operations of the oxidation ditch always

on. Aerator 2 is the slave aerator which is only switched on if the first aerator is operating at full power, but more aeration is needed, as explained in section 3.4. The influent wastewater enters the oxidation ditch at the location of aerator 2, location 3, see Figure C.1. In variant 2 the slave aerator, aerator 2, is turned on, whilst the main aerator, aerator 1, is turned off. In the original measurement campaign, a third variant was proposed, to execute the measurements with both aerators on. However, it was chosen to use the third measuring day to measure the outer arm of the oxidation ditch by holding the sensors directly in the oxidation ditch. The reason for this is that the used measuring set-up, pumping water from the oxidation ditch in a bucket as explained in chapter 4, could alter the results for some variables, such as DO and ORP. By measuring the outer arm another time by holding the sensors directly in the mixed liquor of the oxidation ditch, with the operational settings of Variant 2, these results can be compared to the indirect measurements using the set-up and a DO profile from the aerator onwards could be achieved.

5.1.2 Interpretation results

General observations

First, differences between the results from the measurements in the anaerobic tank (location 1 and 2) and the moment the water enters the aeration tank (location 3 and onwards) are compared, see Figure 5.1 and Figure 5.2.

The ortho-P, potassium and ammonium were higher in the anaerobic tank. The decreased concentrations of ortho-P, potassium and ammonium when entering the oxidation ditch make sense, since the wastewater is mixed with already aerated wastewater present in the oxidation ditch. The recirculation factor of the oxidation ditch could be calculated using the measured concentrations. It is necessary to use the results from variant 1 for this calculation, as then the aerator located at the influent inlet, aerator 2, is turned off and does not influence the concentrations near the inlet. Taking the ammonium concentrations in variant 1, see Table H.3, the recirculation factor could be calculated as follows:

$$(NH_4)_j = NH_4 \textit{ at location } j:$$
$$(NH_4)_2 = 14.7 mgN/L$$
$$(NH_4)_3 = 3.8\ mgN/L$$
$$(NH_4)_{22} = 3.1 mgN/L$$

$$R = \frac{(NH_4)_2}{(NH_4)_3 - (NH_4)_{22}} = \frac{14.7}{3.8 - 3.1} = 21 \tag{5.1}$$

The influent is thus diluted by a factor 1/21 when it enters the oxidation ditch. At the aerator, the concentrations decreased due to the subjection to oxygen, where the P-uptake and nitrification processes can be recognized.

The Ortho-P is increased at the end of the anaerobic contact tank with respect to the beginning of that tank. This indicates P-release, as expected in an anaerobic tank. There is no P-release in the oxidation ditch, this can be explained by the anoxic environment after the aerobic environment. It can also be seen that the BPR activity is low, this could be (partly) due to low temperatures or the anaerobic contact time could be short.

A decrease in the concentration of ammonium, ORP, Ortho-P and Potassium was found for variant 2 at location 14, where aerator 1 is located. However, during these measurements of variant 2, aerator 1 was not in operation. From these graphs, it would almost seem as if this aerator was in operation, whereas this has not been the case. A possible explanation could be that influent is also partly bypassed to aerator 1, as in the past the influent inlet location was located at aerator 1 instead of the current location at aerator 2. This construction still exists, but was later diverted to the current location. It might be that this diversion is not fully closed and some wastewater can bypass. This is however not proved and should be looked into.

Further, it is observed that the mixed liquor is withdrawn from the oxidation ditch around location 11. Looking at the results, this is not the optimal location to withdraw the mixed liquor from the oxidation ditch, since the newly entered wastewater (at location 3) is then withdrawn (at location 11) before arriving at the main aerator (at location 14). This means that in the cases that only the main aerator, aerator 1, is in operation the newly entered wastewater can be withdrawn from the oxidation ditch without being

subjected to aeration. Using the second aerator as the main aerator would make sure all wastewater is aerated before being withdrawn from the oxidation ditch.

Ortho-P in relation to Potassium, pH and ORP

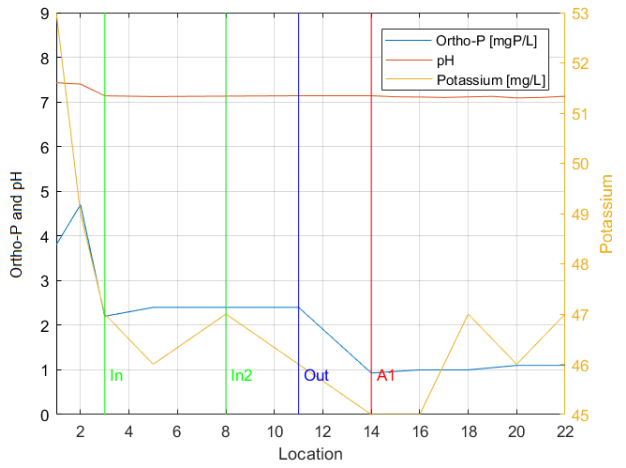

(a) Variant 1 - Ortho-P, pH and potassium

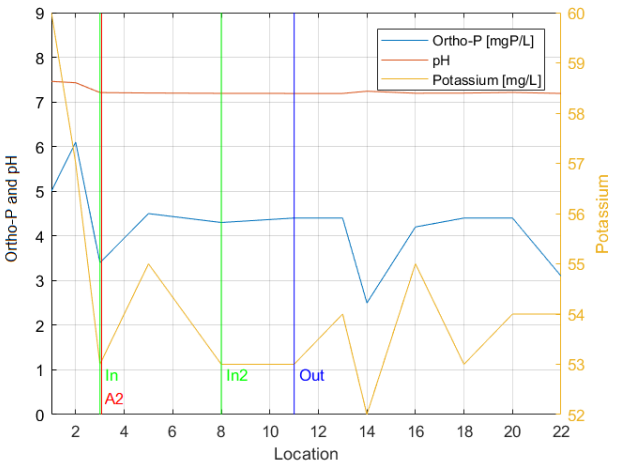

(b) Variant 2 - Ortho-P, pH and potassium

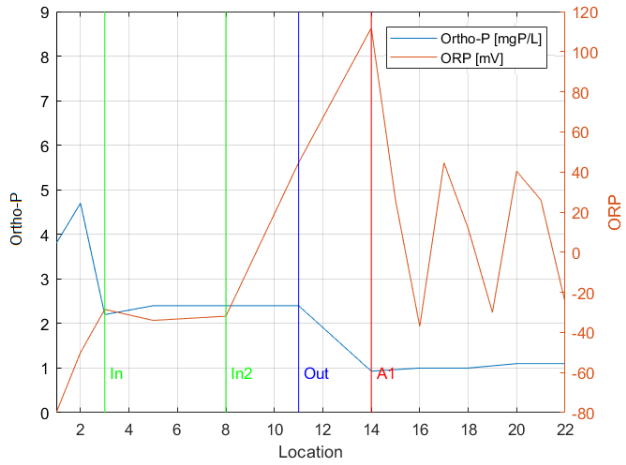

(c) Variant 1 - Ortho-P and ORP

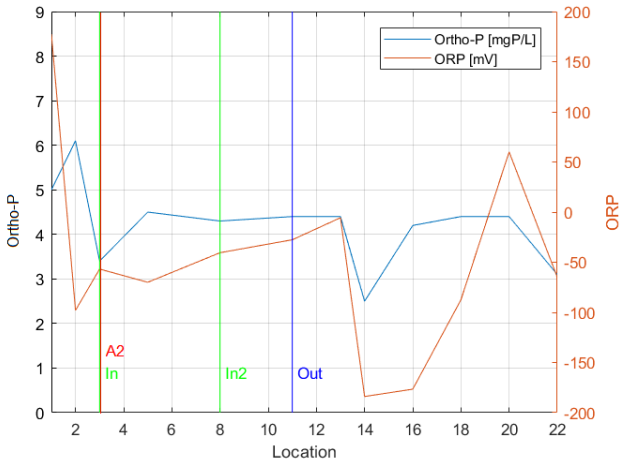

(d) Variant 2 - ortho-P and ORP

Figure 5.1: Measurement results: Potassium, ORP, pH and Ortho-P over the anaerobic tank and oxidation ditch. Location = measurement location

It was expected that the profiles of potassium, pH and/or ORP would show a relationship with the Ortho-P such that one of them could be used as a surrogate variable to control Ortho-P. Although from literature this would seem an interesting possibility, as discussed in section 2.3, this did not seem to be the case for this full-scale oxidation ditch based on these results. A reason for this could have to do with the high recirculation rate, by which the new wastewater that arrives the oxidation ditch is mixed with the already present, aerated mixed liquor by a factor 1 to 21. This impacts the conditions of the mixed liquor and could distinguish the pH and ORP patterns that are found in literature. In literature, these findings are not based on tests at an oxidation ditch, but on for example SBRs. These treatment systems provide a more shielded and more predictable environment.

Also, the patterns of ORP do not seem logical. This might be the result of the indirect way of measuring, using a pump to collect the water from the oxidation ditch into a bucket. This way of measuring turned out to be inappropriate to obtain reliable ORP (and DO) results. However, the measurement locations could not be reached otherwise. A comparison between direct and indirect measurements is made later on in this section.

The relationship between potassium and bio-P removal found in literature, see subsection 2.2.3, cannot be found in the results. The profiles, see Figure 5.1, did not show a relationship. From the measurement

results, see Table H.3 and Table H.4, the ΔK and ΔP were calculated. The results of these calculations can be seen in Table H.7 and Table H.7. The results show that the ΔK is sometimes only 1 mg/L. At these locations, the calculated $\frac{\Delta K}{\Delta P}$ relationship could be affected by measuring errors, due to the precision of the measurements. To make sure the precision of the measurements does not affect the interpretation of the calculated relationship, the first two locations are used. At these locations $\Delta K > 1$. The $\frac{\Delta K}{\Delta P}$ was calculated for both variant 1 and variant 2. The results can be seen in Table 5.1. From literature, it was expected that $\frac{\Delta K}{\Delta P} = \frac{0.33}{1}$ however as can be seen in the results, this is not the case and all kinds of different values were obtained, including negative and positive ratios, indicating no relationship.

Table 5.1: $\frac{\Delta K}{\Delta P}$ for Variant 1 and Variant 2

	Variant 1	Variant 2
$\frac{K_2-K_1}{P_2-P_1}$	-4.4	-2.7
$\frac{K_3-K_2}{P_3-P_2}$	0.8	1.5

N-profiles

The first variant shows an N-profile that can be expected. The ammonium concentration dropped when the mixed liquor was aerated, due to nitrification, and is transformed into nitrite and nitrate. After the aerobic zone, the anoxic zone follows. In the anoxic zone denitrification can take place, which removes nitrate and nitrite from the water by the transformation of nitrate into nitrogen gas. It is striking that the ammonium concentration rises again. The reason for this is not known, however a possibility is that the influent is partly bypassed due to the old construction that used to lead the influent to the old inlet location of the oxidation, near aerator 1. Ammonification could also lead to a rising ammonium concentration, but it is unlikely that ammonification occurs here.

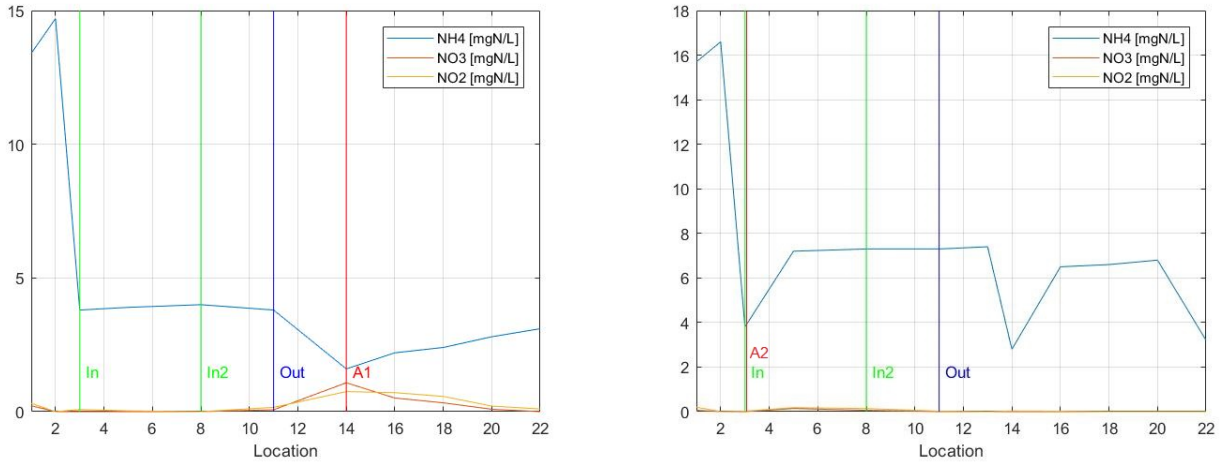

(a) Variant 1

(b) Variant 2

Figure 5.2: Measurement results: N-profiles over the anaerobic tank and oxidation ditch. Location = measurement location

Comparing direct and indirect sensor measurements

At all comparison plots, Figure 5.3, Figure 5.6, Figure 5.4, Figure 5.5, it can be seen that the indirect measurements show a more smooth line compared to the direct measurements. A reason for this could be that for the indirect measurements the sensors were placed in a bucket and had some time to stabilize (the ORP sensor for example has a very slow response time) and there were fewer influences from for example the current, bringing chunks of waste that got attached to the sensors. However, this does not mean that the indirect measured pattern is more reliable.

It should be noted that the direct measurements were measured a day later, so this could also bring some differences between the two results, though the operational conditions were the same.

For pH, Figure 5.3, it can be seen that the two measurements give corresponding results.

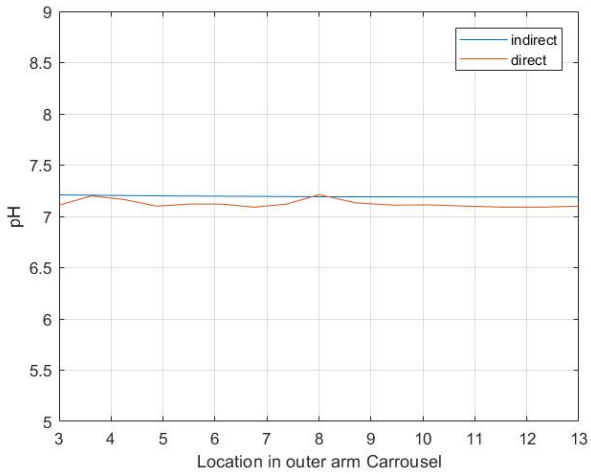

Figure 5.3: Measurement results: Comparison direct vs. indirect measurements - pH variant 2

For DO, Figure 5.4, the indirect pattern seems unlikely, since the oxygen concentration increases the further away from the aerator. An increasing DO concentration could partly be explained by a combination of the used measuring method, the residence time and the respiration rate. The measuring method using a pump and a long hose, introduces some residence time before the DO is measured. During this time, the oxygen can be taken up by the organisms. When the activated sludge has just been introduced to the DO the respiration rate is higher, then later in the oxidation ditch, when they have already been subjected to some oxygen and they are more saturated. If the measuring set-up somehow adds oxygen to the mixed liquor and therefore induces additional aeration, this could together with the previously mentioned reason, explain an increasing DO trend. Although it should be noted that the DO even with this explanation is astounding at the end of the aeration tank. This DO is not representative for the real conditions in the oxidation ditch. The trend of the direct measurement shows a decline in oxygen, when the peaks are ignored. The wastewater in the oxidation ditch in Hattem contains a lot of course material, such as lumps of toilet paper, hair and more, as the screens do not function optimally and occasionally some wastewater enters the oxidation ditch unscreened via the second inlet, see section 3.1. This means that the sensors were clogged repeatedly, and the waste had to be removed.

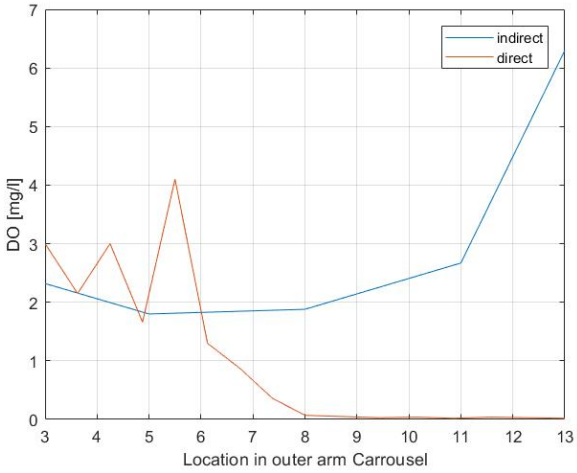

Figure 5.4: Measurement results: Comparison direct vs. indirect measurements - Dissolved Oxygen variant 2

Figure 5.5 shows that the direct and indirect method give completely different results for ORP. Here the indirect method indicates that at the aerated location (location 3) the wastewater is anaerobic. Also, the ORP rises further away from the aerated zone, which seems odd, but could partly be explained by the increasing DO concentration measured by the indirect measurements. The direct measurements seem more logical, although more of a decline in ORP would have been expected. It should be noted that the

ORP sensors caused some difficulties for the measurements as the response time of the sensors was quite long. The ORP sensor used during the measurements were also tested in the TU Delft laboratory after the measurements, to assess the reliability of the used sensor and the response rate of the sensor. The used ORP sensor during the measurements was tested in tap water, calibration liquid and a pH4 buffer, together with two other ORP sensors of the same type (WTW, IDS SenTix ORP-T 900). The results of the final ORP values measured from all sensors can be found in. Although the ORP sensors gave similar results and therefore seem reliable it should be noted that the response of the sensors was extremely slow.

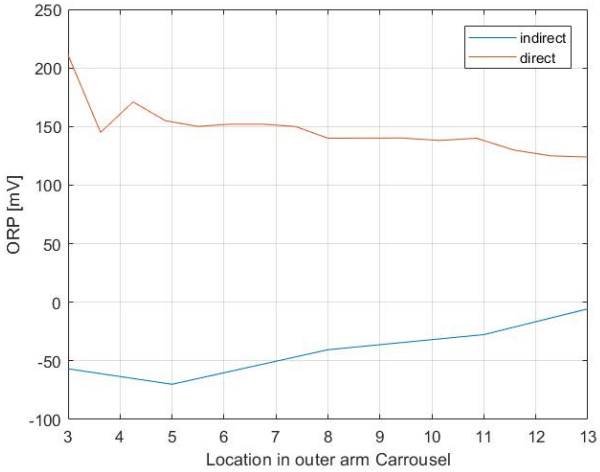

Figure 5.5: Measurement results: Comparison direct vs. indirect measurements - ORP variant 2

And lastly the conductivity results, Figure 5.6, are close to each other, but the indirect measurements show a bit of a lower conductivity.

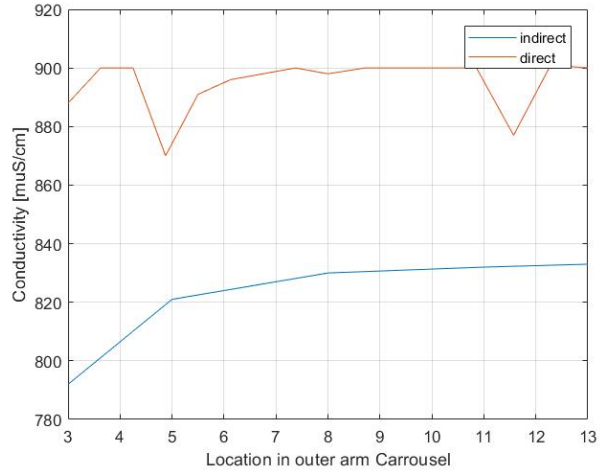

Figure 5.6: Measurement results: Comparison direct vs. indirect measurements - conductivity variant 2

Results versus data from Waterschap

Waterschap Vallei & Veluwe monitor some values at fixed locations to control the oxidation ditch. These are monitored continuously at that location and could therefore be compared with data obtained in this research. The time at which each measurement was taken during this campaign was noted, so the time and place could be matched. In Table 5.2 these values are displayed.

Table 5.2: Comparing data waterboard and data from measurement results

Variable	Variant	Waterschap data	Data from this study
ORP [mV]	Variant 1	-219.15	-37.00
	Variant 2	-300.00	-176.60
NH4 [mgN/L]	Variant 1	3.82	3.80
	Variant 2	7.49	7.3
NO3 [mgN/L]	Variant 1	0.82	0.07
	Variant 2	0.96	0

The ORP measured by the waterboard differs completely from the results obtained during the measuring campaign. This was already expected as explained before. Unfortunately, there are no direct measurements at that location, because this location is in the inner arm and is unreachable for direct measurement. The NH_4^+ concentrations measured by the waterboard are very close to the results obtained, which indicates the results from these measurements are trustworthy. The NO_3^- results are not completely similar. The reason for this slight difference cannot be pointed out with certainty. The way of testing by the water board differs from the way of testing from the measuring campaign; the waterboard uses the Hach Amtax sc Ammonium analyser, whilst the lab analysis was done using Hach cuvette tests. Also, field conditions could play a part here, like fouling in the Amtax, but a conclusion on this cannot be made.

5.1.3 Limitations measurement campaign

The measuring set-up brings some measuring errors with respect to DO and ORP measurements. It would be better to directly measure and sample the wastewater in the oxidation ditch, however as explained that was not possible, so this was the best method to make the measurements possible and most variables could be measured using this method. Also, time management is very important when executing these measurements. If there is too much time between sampling and filtration and preservation, the results can already be influenced. Therefore, the sample preparation was immediately done after obtaining the sample, however it takes some time and effort to filter the amount of water to fill all sample pots at each location. Therefore, it would be strongly advised to execute this measuring campaign with more than two people.

5.1.4 Summary measurement results

The measurement results did not give comparable results to the relationships found in literature. As was stated in the introduction, a difficulty is that most research on biological phosphorus removal is focused on other types of wastewater treatment systems than oxidation ditches. Therefore, many literature was found on other treatment systems, but the applicability of this literature towards an oxidation ditch was not known. Based on the results from the measurements it can be concluded that the relationships found in other treatment systems are not straightforwardly translatable to an oxidation ditch. The pH-profile throughout the oxidation ditch was rather constant and the pH profile seen in literature was not recognized. The ORP measurements gave unreliable results and showed a slow response rate. The potassium concentration did not show the relationship that was expected, even though this relationship follows from the stoichiometry. The obtained $\frac{\Delta K}{\Delta P}$ ratios varied from negative values to positive values, instead of the expected $\frac{\Delta K}{\Delta P} = \frac{0.33}{1}$. Conductivity had no clear relation with biological phosphorus removal. DO cannot be used as a monitoring variable on itself for a cheap alternative sensor for biological phosphorus removal in an oxidation ditch. The DO profiles from the results were unreliable. Combined nitrate and ammonium concentrations, can give an insight into the biological phosphorus removal process, as the change in ammonium and nitrate indicates the state of the nitrification and denitrification processes. Measuring the nitrate can in addition contribute to a control system, by making sure that the zone before withdrawal of the mixed liquor from the oxidation ditch is anoxic, to inhibit P-release. However, it cannot on its own monitor the biological phosphorus removal fully as it does not provide information on the state of the biological phosphorus removal process and the desired aeration intensity for the PAOs.

5.2 BioWin

A model of the WWTP in Hattem was constructed using BioWin. Influent and effluent data obtained from the waterboard was used to simulate the wastewater treatment steps and some scenarios were modelled to test the responses of the treatment system to these changes. The results from the measurement campaign showed low BPR activity and from literature it is known that several factors can influence this, such as a low temperature, insufficient anaerobic zone and aeration settings. Simulations of multiple scenarios in BioWin can contribute to show the impact of these changes to the WWTP and suggestions could be made based on the findings.

5.2.1 Design variables

The design variables used in the BioWin model are based on the known variables of the wastewater treatment plant in Hattem, as described in chapter 3. The used variables for the BioWin model can be seen in Table 5.3.

Table 5.3: Used variables BioWin model

Oxidation Ditch		
Volume	14000	m^3
Width	8.5	m
Depth	3.75	m
Nr. of CSTRS	10	
Volume CSTR	1400	m^3
Anaerobic Tank		
Volume	300	m^3
Width	4	m
Depth	6	m
Settler		
Volume	3000	m^3
Underflow	590	m^3/day
Depth	2	m
Percent removal	99.8	%
Fraction of settler height	0.05	
Return sludge		
Return sludge rate	562	m^3/day

The influent and effluent data was obtained from the waterboard itself, and is listed in Table 5.4.

Table 5.4: Used wastewater influent/effluent data for BioWin from WWTP Hattem in January, T=11 degrees Celsius

Element	Total COD [mg/L]	TKN [mgN/L]	Nitrate + Nitrite [mgN/L]	Total P [mgP/L]
Influent	600	52.9		8.2
Effluent	18	3.7	0.63	0.83

The variables left are temperature and DO setpoint. The data from the waterboard was obtained in January and the wastewater temperature was around 11 degrees Celsius. The DO setpoint is not known, but it is known that aerator 1 was functioning as the main aerator and aerator 2 as the slave aerator, which means that aerator 1 was operating at full capacity. As explained in section 4.2, the DO concentrations were found by iterating the DO settings until the effluent values of the TKN and the total P obtained from the simulations matched the data obtained from the waterboard. The resulting DO setpoints were:

- DO setpoint Aerator 1 = 7 mg/L (aerator 1 is the main aerator)
- DO setpoint Aerator 2 = 2.7 mg/L (aerator 2 is the slave aerator)

5.2.2 Lay-out

The anaerobic tank is modelled as one CSTR. The oxidation ditch is modelled as 10 equally sized CSTRs in a loop. The influent enters the oxidation ditch at the second aerator, as it does in the WWTP in Hattem. The water is partly withdrawn from the oxidation ditch after the fifth tank, which is in agreement the location of the spillway in the WWTP in Hattem. The resulting BioWin layout can be seen in Figure 5.7. The amount that is discharged versus the amount that is recycled is set to a ratio of 1/21 as is the case in Hattem.

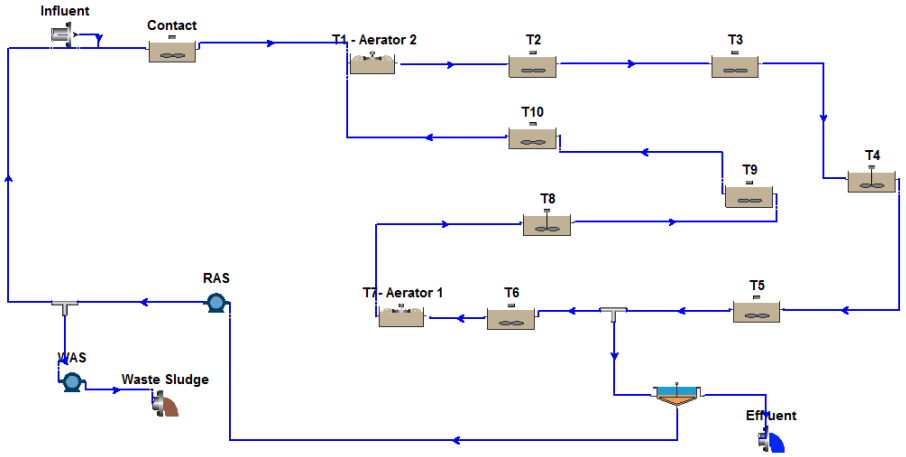

Figure 5.7: Lay-out of the constructed Biowin model of WWTP Hattem

The scenarios are plotted in the next sections. In the plots, some important locations are indicated by vertical lines. The first location is the influent entering the wastewater treatment plant. The magenta 'CT' line then indicates the beginning of the anaerobic contact tank. The green 'In' line indicates the location where the mixed liquor enters the oxidation ditch. At the same location, a red line indicates 'A2', the second aerator. The blue line is the location where the effluent exits the oxidation ditch. The red 'A1' afterwards represents aerator 1. Note that the oxidation ditch recirculates, and that after location 22, the water is recirculated to the location where the green 'In' line indicates the inlet of the oxidation ditch, as can also be seen in Figure 5.7. The results were plotted over an x-axis from 1:22 to obtain a scale comparable to the plotted results of the measurement campaign.

5.2.3 Base case

The base case was modelled as explained before. The results from the simulation can be seen in detail in Appendix I, Table I.10 and Table I.1. In Figure 5.8 some variables are plotted.

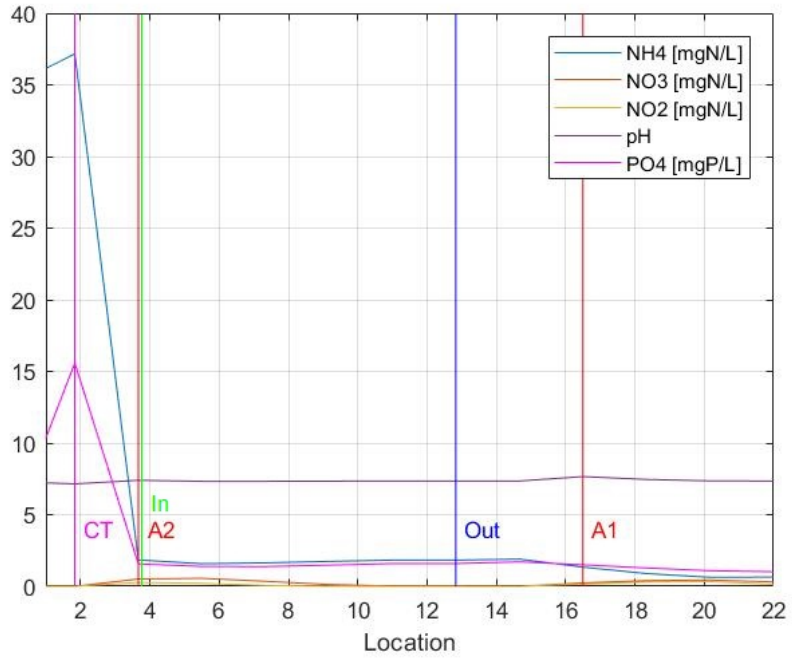

Figure 5.8: Simulation results: Base Case (DO A1:7 - A2:2.7)

Comparing the BioWin results with the obtained results from the measurements, similar trends can be seen. It should be kept in mind, that the exact values from the results from BioWin and the measurement campaign should not be compared, as the influent was different. However, the trend of the values can be compared.

Both results show a fairly constant pH. Although looking at the pH results from BioWin, a small increase in pH can be seen when subjected to aeration, see Table I.1. This was also found in literature, subsection 2.3.1. Unfortunately, it was not possible to recognize other important nutrient removal points in the pH profile, as was found in literature. The results from the measurement campaign and the BioWin results both show an increase in NH_4^+ and PO_4^{3-} concentration in the anaerobic tank. When entering the oxidation ditch the NH_4^+ and PO_4^{3-} concentrations decrease, partly due to the mixing with the mixed liquor present in the oxidation ditch, partly due to aeration. The nitrification after aeration can also be recognized by an increase in nitrate and nitrite and the decrease in nitrate and nitrite shows the denitrification process.

5.2.4 Scenarios

A few scenarios were modelled to check the impact of certain measures. The results are shown and discussed in the following sections.

Increased temperature

The used data was measured during winter with a water temperature of about 11 degrees Celsius. It is known that temperature affects the activated sludge processes and therefore a similar simulation was executed at a higher wastewater temperature. In this simulation, the temperature was increased to 20 degrees Celsius. Due to the higher temperature, less aeration was needed for similar removal results. Therefore, the aeration was decreased in both aerators for the summer simulation. The DO setpoints of the aerators were decreased from 7 mg/L to 4 mg/L and from 3 mg/L to 1.5 mg/L for aerator 1 and aerator 2, respectively. Detailed results can be found in Appendix I, Table I.2. In Figure 5.9 some variables are plotted. This plot shows only the locations in the oxidation ditch, so the influent and anaerobic tank are not plotted. Even with the lowered DO setpoint of both aerators in summer, the removal values were better in summer, as can be seen by the lower ammonium and phosphate concentrations. The initial influent values of all variables were the same for both simulations as were all other conditions.

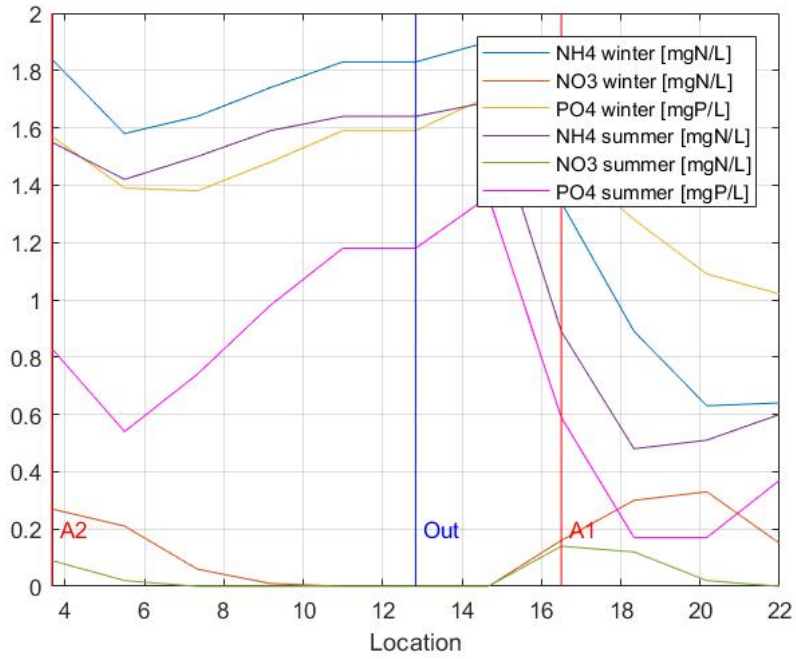

Figure 5.9: Simulation results: Winter (DO A1:7 - A2:3) vs. Summer (DO A1:4- A2:1.5)

Switching around the main aerator

In the next scenario simulated, the 'main'- and 'slave' aerator were switched. As explained in section 3.4, aerator 1 is set as the main aerator normally and aerator 2 jumps in when needed as the slave aerator. The disadvantage of having aerator 1 as a main aerator is that the influent entering the oxidation ditch, first passes by the withdrawal location of the oxidation ditch, before being subjected to the main aerator. Due to recirculation and when aerator 2 is in operation, aeration of the newly entered mixed liquor still occurs, but it could be beneficial to switch the main aerator and the slave aerator settings. The previous simulation with the increased temperature and decreased aeration was used, where only the DO setpoints were switched around. Detailed results of the simulation can be found in Appendix I, Table I.3 and Table I.2. In Figure 5.10 some results are plotted of both the original summer simulation and the switched aeration mode. Switching around the main aerator and the slave aerator was beneficial for the effluent concentrations of both PO_4^{3-} and NH_4^+. When A2 was set as the main aerator, both the PO_4^{3-}- and NH_4^+ concentrations decrease faster and show better removal. At the location where the wastewater is withdrawn from the oxidation ditch, the switched aerator simulation still shows better results. Only when the wastewater passes aerator 1, the values of the simulation where aerator 1 was the main aerator were slightly better, however this is only for a short period. The quality of the mixed liquor discharged from the oxidation ditch is crucial, therefore switching around the main and slave aerators would be beneficial. It should be noted that around location 8, no nitrate and oxygen was left in the mixed liquor and thus an anaerobic zone occurs, where P-release seems to ensure an increasing PO_4^{3-} concentration, giving less positive results for the effluent quality. It is interesting to look into different aeration modes to limit the increased PO_4^{3-} concentration before the outlet location.

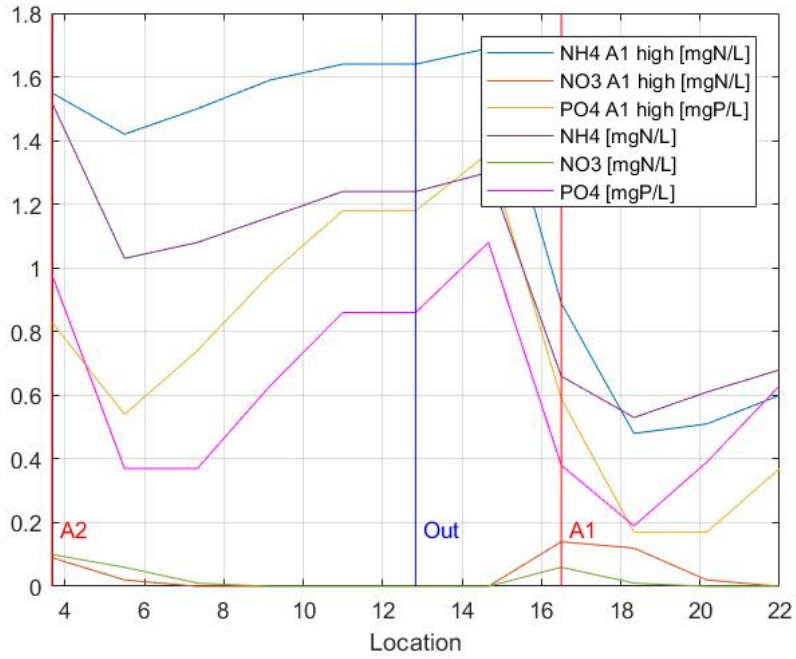

Figure 5.10: Simulation results: Aerator switch (DO A1:4 - A2:1.5) vs. (DO A1:1.5 - A2:4)

Different Aeration modes

Two scenarios were simulated using the switched aeration mode, as this seemed promising for the effluent quality from the previous simulations, however the DO setpoints of the aerators were altered to compare the N-removal and P-removal under increased aeration settings. For one simulation the DO setpoint was slightly increased with respect to the previous simulation, namely a DO of 2 mg/L and 5 mg/L for aerator 1 and aerator 2, respectively. The other scenario simulates a high aeration setting, with a DO of 3 mg/L and 7 mg/L for aerator 1 and aerator 2, respectively. Figure 5.11 shows the results of both simulations. Detailed results can be found in Appendix I, Table I.4 and Table I.5.

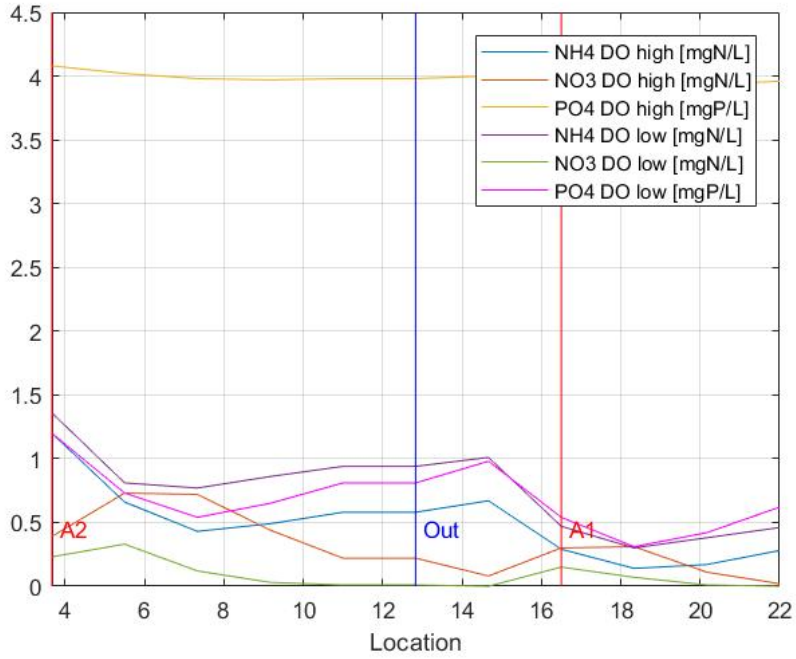

Figure 5.11: Simulation results: DO A1:3 - A2:7 vs. DO A1:2 - A2:5

N-removal still benefitted from the higher DO setpoint, but the P-removal was disadvantaged. This can

be seen in the resulting PO_4^{3-} concentration, as well as the PAO-concentration in mixed liquor, comparing Table I.4 and Table I.5 in Appendix I. As mentioned in the chapter 2, N-removal benefits of increased aeration, the down-side of increasing aeration is then mainly the increasing energy consumption. When dealing with BPR, this is not the case anymore, as an increasing aeration can also lead to a decreased removal efficiency. However the slightly increased DO setpoints of 2 and 5 with respect to the previous simulated scenario with a DO setpoint of 1.5 and 4, still gives beneficial removal results, as can be seen in the detailed results in Appendix I, comparing Table I.5 and Table I.3.

Extended Anaerobic Tank

Another scenario simulated was extending the anaerobic tank. As explained in chapter 2, PAOs have an advantageous position in an anaerobic environment towards other bacteria. Therefore, a sufficient anaerobic zone is desired, to make sure PAO selection is stimulated and PAO growth in the aerobic zone can be increased. This was tested by increasing the volume of the anaerobic tank from the existing 300 m^3 to 1000 m^3, where all other conditions were kept the same. The results are plotted in Figure 5.12. It is noticeable that the impact of the extended anaerobic time did not really affect the nitrification or denitrification, as the trends of the NH_4^+ and NO_3^- are practically similar. However, the biological phosphorus removal was improved. In Appendix I Table I.6 and Table I.7 detailed results of two simulations are shown. It can be seen that increasing the anaerobic tank and thus the HRT, benefits the PAOs. The PAO concentration, see Table I.6 and Table I.7, was increased and in the effluent less dissolved PO_4^{3-} was left.

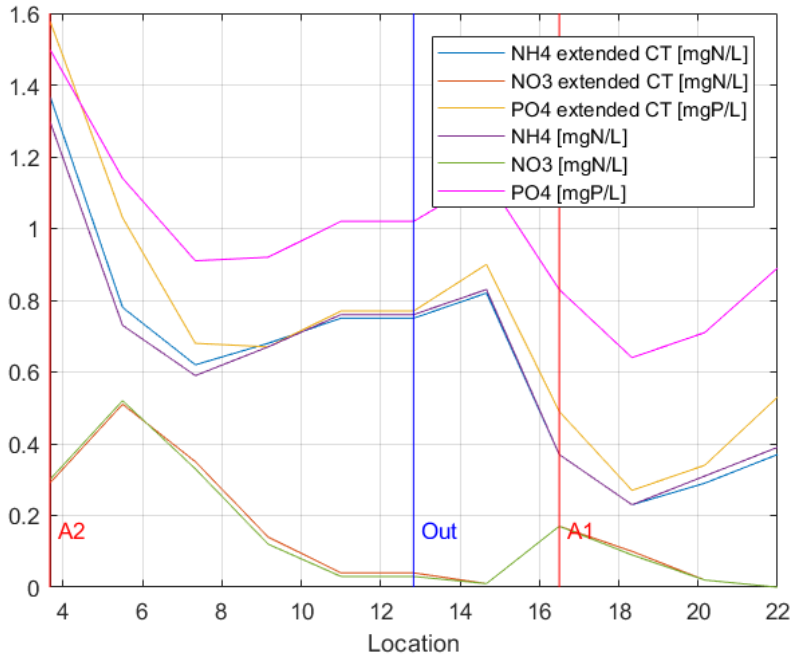

Figure 5.12: Simulation results: extended aeration tank vs. normal aeration tank

Different Aeration modes with extended anaerobic tank

The last scenario's compares different aeration modes with the extended anaerobic tank.

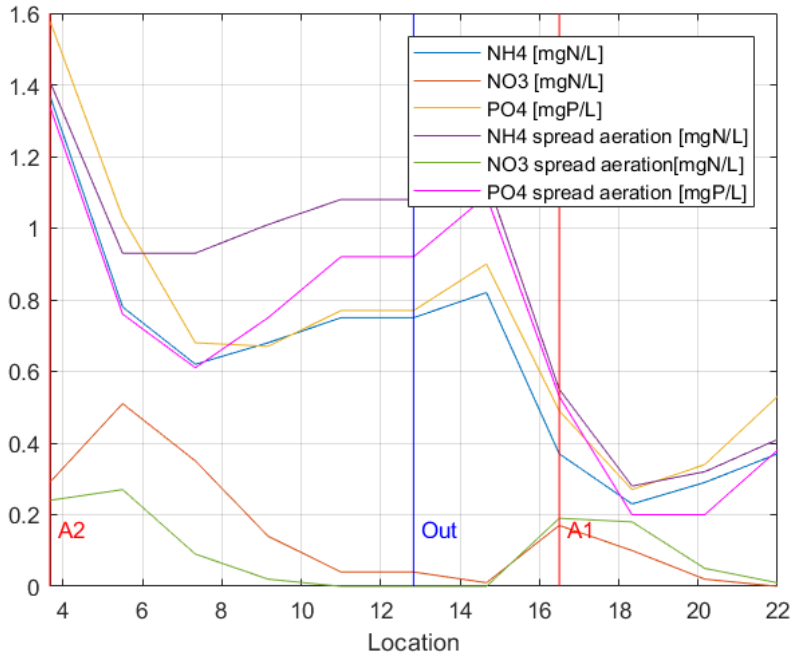

Figure 5.13: Simulation results: extended aeration tank (DO A1:2 - A2:6) & Extended aeration tank (DO A1:3 - A2:4)

In Figure 5.13, the results are plotted of the extended aeration tank scenario with two different aeration settings, one with DO setpoints of A1:2 mg/L and A2:6 mg/L and one with A1:3 mg/L and A2:4 mg/L. These settings were chosen, to compare the results of a more spread aeration over the two aerators compared to aeration where one aerator is substantially higher and operates as a 'main' aerator. In Appendix I, Table I.8 and Table I.6 detailed results can be found. From the results plotted in Figure 5.13, it can be concluded that the spread aeration mode was not beneficial for both the NH_4^+ and PO_4^{3-} concentrations in the effluent. For the spread aeration simulation, an anaerobic zone occurs from location 8 to 10, this means that P-release can occur, which can be seen in the increased PO_4^{3-} concentration at the same location. For the simulation with A1:2 and A2:6, the nitrate concentration was a bit higher and even though it was very little, the PO_4^{3-} concentration did not increase as much, probably due to less P-release.

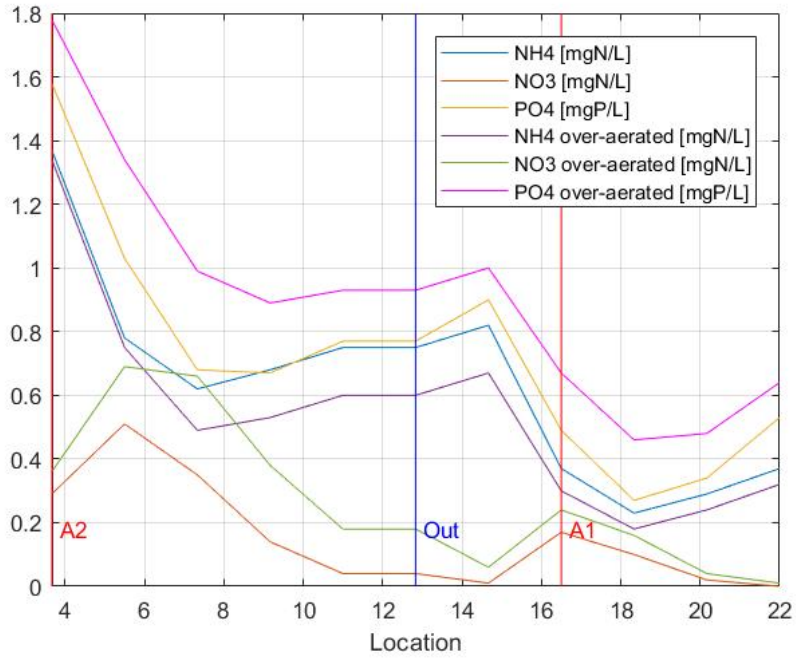

Figure 5.14: Simulation results: extended aeration tank (DO A1:2 - A2:6) & Extended aeration tank (DO A1:2 - A2:7)

In Figure 5.14 the results of the previous simulation with the DO setpoints A1:2 mg/L and A2:6 mg/L were compared with a simulation under the same conditions except for an increased A2 DO setpoint to 7 mg/L. The N-removal still benefits from the increased aeration, however the P-removal decreases, due to over-aeration of the PAOs. In Appendix I, Table I.9 and Table I.6 detailed results can be found. It can be seen from these results that indeed the PAO-concentration was decreased for the simulation with the higher DO setpoint.

5.2.5 Limitations Biowin

As the aeration system needed to be modeled, an aerated CSTR was modeled with a certain DO concentration. The DO concentrations or the aeration intensity at the moment of the used data from the waterboard was not known. As most data needed for the BioWin model was known, except for the aeration intensity, it was decided to solve the problem by iteration as it was the main unknown. This was done by iterating the DO concentration setpoint of the aerators. However, it must be kept in mind that this brings uncertainties to the simulation, as it cannot be stated as a fact that this represents the exact aeration intensity at the moment of the used data from the waterboard. Still, as the simulation results showed logical performance of the WWTP and the influences of different scenarios could be tested, it was considered sufficient for these simulations. For this simulation, also only one influent-effluent dataset was used, however it would be better to compare the same scenarios, using multiple influent/effluent data sets. The model is a representation of the WWTP of Hattem, but assumptions and simplifications had to be made to implement the treatment systems in the model, this could also alter the results. For example, it was chosen to model the oxidation ditch as a loop of 10 CSTRs, as seen in the benchmark of an oxidation ditch made by Abusam (2001). Also, the anaerobic tank in Hattem is a gutter, not a continuously stirred tank reactor. It might be more accurate to model the anaerobic ditch as a concatenation of CSTRs. Lastly, the second inlet has been neglected in these simulations. This was chosen as this inlet is only occasionally used and only little wastewater from a few houses arrives via this inlet. There is no data on this and it was assumed to be of little influence to the wastewater arriving the oxidation ditch via the primary inlet.

When comparing the results of BioWin to the results of the measurement campaign it should be kept in mind that other influent/ effluent data was used, and that for the BioWin case both aerators were turned on. Still some comparisons can be made for the trendlines of the concentrations and the removal behaviour of the WWTP, but direct values of concentrations could not be compared. The main purpose of the BioWin simulations was to test some scenarios with respect to operational or physical adjustments.

A downside of using BioWin was that the potassium could not be compared to Bio-P and that it is not possible to implement control strategies to test.

5.2.6 Summary BioWin results

An increased temperature, from 11 degrees Celsius to 20 degrees Celsius, benefited the biological phosphorus removal significantly, resulting in lower effluent phosphorus concentrations. The aeration intensity could be lowered at the higher temperature, still resulting in better removal compared to the base case. The DO setpoints of the aerators were decreased from 7 mg/L to 4 mg/L and from 3 mg/L to 1.5 mg/L for aerator 1 and aerator 2, respectively.

Switching around the main aerator and the slave aerator, resulted in improved effluent concentrations of phosphorus. When the aeration was slightly increased, namely to a DO concentration setpoint of 2 mg/L and 5 mg/L for aerator 1 and aerator 2, respectively, the N- and P-removal benefited. However, increasing the aeration further to 3 mg/L and 7 mg/L for aerator 1 and aerator 2, respectively, lead to a deteriorated phosphorus removal.

Extending the anaerobic tank from 300 m^3 to 1000m^3, increased the PAO concentration and improved the biological phosphorus removal.

Lastly, it could be concluded from the results that a more equally spread aeration mode, where both aerators were operating at similar DO setpoints, was disadvantageous compared to a clear main aerator and slave aerator setting. The spread aeration lead to an anaerobic zone, resulting in P-release.

5.3 Matlab/ Simulink

As it is not straightforward to implement and test control strategies in BioWin a suggestion is made for future research using a benchmark of an oxidation ditch in Matlab and Simulink, Abusam (2001). In this benchmark control strategies can be implemented, however biological phosphorus removal is not incorporated in this benchmark. A step-wise approach to incorporate phosphorus removal is presented in the Appendix J. As it is a set-up for future research, it is not incorporated in this chapter.

6 | Conclusions

From the literature study, the results of the measurement campaign and the simulations, the following can be concluded:

- The variables that seemed promising in literature for monitoring and controlling biological phosphorus removal were limited to pH, ORP, potassium, conductivity, DO and nitrate.
- From the obtained results of the measurements, trendlines of the variables over the length of the oxidation ditch could be achieved. However, none of these variables were suitable to monitor biological phosphorus removal, although some variables could contribute to a control system in a way:
  - The pH-profile throughout the oxidation ditch was rather constant and the profile seen in literature was not recognised.
  - The ORP measurements gave unreliable results when the direct and indirect measurements were compared. The ORP sensors showed a slow response.
  - The potassium concentration did not show the relationship that was expected from stoichiometry. The obtained $\frac{\Delta K}{\Delta P}$ values varied from negative values to positive values, instead of the expected $\frac{\Delta K}{\Delta P} = \frac{0.33}{1}$.
  - Conductivity had no clear relation with biological phosphorus removal based on the results of the measurement campaign.
  - DO is an important control variable for the process, since the main manipulative factor is the aeration intensity. However, it was not found to be a relevant monitoring variable on itself for a cheap alternative sensor for biological phosphorus removal in an oxidation ditch.
  - Nitrate measurements can contribute to a control system to inhibit P-release before the withdrawal location of the mixed liquor from the oxidation ditch by ensuring an anoxic zone. However, it cannot fully monitor the biological phosphorus removal on its own.
- From the BioWin results the following can be concluded:
  - Whilst increasing the DO setpoints of the aerators positively affected nitrogen removal, it could both positively and negatively affect phosphorus removal, as expected from literature. The distribution of the DO setpoints over the aerators influenced the nutrient removal processes. A more equally spread aeration mode was disadvantageous for the biological phosphorus removal, compared to a clear main aerator and slave aerator setting.
  - It is beneficial to use the aerator located before the withdrawal location of the mixed liquor from the oxidation ditch as the main aerator. Ammonium is transformed to nitrate due to the aeration. This ensures aerobic or anoxic zones before the withdrawal location, which is beneficial for the effluent quality as P-uptake can occur, whilst P-release is prohibited.
  - Increasing the anaerobic zone, by extending the anaerobic tank, would benefit the PAOs. As it is necessary that this zone is strictly anaerobic, the return of nitrate via activated sludge should be prevented.

To conclude, no alternative variables were found suitable to monitor biological phosphorus removal in an oxidation ditch. A control strategy using simple sensors to optimise biological phosphorus removal in an oxidation ditch was not obtained. As a control system was not obtained from this research, it is not known how the nitrogen removal efficiency would respond to bio-P driven control in an oxidation ditch. Although some types of control were examined in literature, no conclusion could be made on what type of control would be suitable for the control of biological phosphorus and nitrogen removal.

7 | Recommendations

7.1 Future research

- As mentioned in this report, a start was made in Appendix K for a benchmark of an oxidation ditch incorporating biological phosphorus removal. The implementation of biological phosphorus removal into the benchmark is recommended as a follow-up research. As explained in chapter 2, a benchmark can help to investigate the complex process of biological phosphorus removal and to find a control strategy. This follow-up research would consist of implementing ASM2d in C^{++} code in the C-MEX files of the S-functions, as explained in detail in Appendix K, and to then calibrate and validate the benchmark. This future research requires familiarity with C^{++} coding, Matlab and Simulink.
- To clarify if there is indeed a bypass between aerator 1 and aerator 2 at WWTP Hattem, as mentioned in subsection 5.1.2, this should be tested at the WWTP using a dye or other tracer. The WWTP used to have their influent inlet location at aerator 2 and this inlet location was later diverted to the location of aerator 1. Due to that construction, some influent might still flow towards the first aerator. This could explain the increasing ammonium concentration seen in variant 1 of Figure 5.2 and the decreasing ammonium concentration seen in variant 2 Figure 5.2.
- The simulated scenarios should be tested in BioWin using more influent/effluent datasets to increase the reliability of the results.
- Simulating more aeration scenarios in BioWin can provide more information on the multiple effects of altering the aeration on biological phosphorus removal:
  - Over-aeration of PAOs.
  - The ideal distribution of the aeration over the two aerators. It could be concluded from the results that a spread aeration mode was disadvantageous for the removal results compared to the settings were a 'main' and 'slave' aerator was appointed.
  - The influence of aeration settings on the nitrate level before the withdrawal location of the oxidation. It would be ideal to ensure nitrate in the mixed liquor before the withdrawal location of the oxidation ditch, to prevent P-release.
- The steady state simulations executed in this research should be complemented with dynamic simulations, to investigate the response of the WWTP under the dynamic conditions.

7.2 General advice for the WWTP in Hattem

- It is advised to change the main aerator in Hattem to aerator 2 instead of aerator 1 (at location 13). Changing the main and slave aerator settings in Hattem ensures that the activated sludge entering the oxidation ditch is being subjected to aeration before being withdrawn from the oxidation ditch, which is currently not the case.
- It is advised for Hattem to improve their screening of incoming influent. There is currently a lot of coarse material, such as chucks of toilet paper, sanitary pads, in the oxidation ditch. Improving the removal of coarse material can enhance the performance and the measurability of the oxidation ditch.

References

Abusam, A. (2001). Development of a benchmarking methodology for evaluating oxidation ditch control strategies. *PhD Thesis, Wageningen University*.

Alex, J., Benedetti, L., Copp, J., Gernaey, K., Jeppsson, U., Nopens, I., ... Vanrolleghem, P. (2008). *Benchmark simulation model no. 1 (bsm1)* (Vol. TEIE-7229; Tech. Rep.). Lund University.

Åmand, L., & Carlsson, B. (2012). Energy efficient ammonium feedback control. In *New developments in it & water, november 4-6, 2012, amsterdam, the netherlands.*

Amand, L., Olsson, G., & Carlsson, B. (2013). Aeration control – a review. *Water Science and Technology*, *67*(11), 2374–2398. Retrieved from `http://wst.iwaponline.com/content/67/11/2374` doi: 10.2166/wst.2013.139

Belchior, C. A. C., Araújo, R. A. M., & Landeck, J. A. C. (2012). Dissolved oxygen control of the activated sludge wastewater treatment process using stable adaptive fuzzy control. *Computers & Chemical Engineering*, *37*, 152–162.

Benhalla, A., Houssou, M., & Charif, M. (2010). Linearization of the full activated sludge model no 1 for interaction analysis. *Bioprocess and Biosystems Engineering*, *33*(6), 759–771. Retrieved from `https://doi.org/10.1007/s00449-009-0404-z` doi: 10.1007/s00449-009-0404-z

Bost, V. (2018). *Internship report: Setting up a measurement campaign to determine the trend of relevant variables with respect to biological phosphorus removal throughout the oxidation ditch in the wastewater treatment plant in hattem* (Tech. Rep.). Delft University of Technology.

Brdjanovic, D., Hooijmans, C., van Loosdrecht, M., Alaerts, G., & Heijnen, J. (1996). The dynamic effects of potassium limitation on biological phosphorus removal. *Water Research*, *30*(10), 2323–2328. Retrieved from `https://doi.org/10.1016/0043-1354(96)00121-2` doi: 10.1016/0043-1354(96)00121-2

Brdjanovic, D., Logemann, S., van Loosdrecht, M. C. M., Hooijmans, C. M., Alaerts, G. J., & Heijnen, J. J. (1998). Influence of temperature on biological phosphorus removal: process and molecular ecological studies. *Water Research*, *32*(4), 1035–1048. Retrieved from `https://doi.org/10.1016/s0043-1354(97)00322-9` doi: 10.1016/s0043-1354(97)00322-9

Brdjanovic, D., Slamet, A., van Loosdrecht, M., Hooijmans, C., Alaerts, G., & Heijnen, J. (1998). Impact of excessive aeration on biological phosphours removal from wastewater. *Water Research*, *32*(1), 200–208. Retrieved from `https://doi.org/10.1016/s0043-1354(97)00183-8` doi: 10.1016/s0043-1354(97)00183-8

Chang, C. H., & Hao, O. J. (1996). Sequencing batch reactor system for nutrient removal: Orp and ph profiles. *Journal of Chemical Technology & Biotechnology: International Research in Process, Environmental AND Clean Technology*, *67*(1), 27–38.

Copp, J. (2002). The cost simulation benchmark—description and simulator manual [Computer software manual]. Office for Official Publications of the European Communities.

Crites, R., & Tschobanoglous, G. (1998). *Biological treatment and nutrient removal* (E. Munson, Ed.). WCB/McGraw-Hill.

de Koning, M., van Schagen, K., Agarwalla, B., Trolio, R., & Domurad, M. (n.d.). *Predictive control in wastewater treatment.*

den Engelse, R., Boschloo, J., Kerstens, C., de Korte, K., Meijer, T., Stamperius, P., & Dirkzwager, A. (1992). *Handboek stikstofverwijdering.* Stowa.

El-Din, A. G., & Smith, D. W. (2002, mar). A neural network model to predict the wastewater inflow incorporating rainfall events. *Water Research*, *36*(5), 1115–1126. Retrieved from `https://doi.org/10.1016/s0043-1354(01)00287-1` doi: 10.1016/s0043-1354(01)00287-1

Gernaey, K. V., & Jørgensen, S. B. (2004). Benchmarking combined biological phosphorus and nitrogen removal wastewater treatment processes. *Control Engineering Practice*, *12*(3), 357–373. Retrieved from `https://doi.org/10.1016/s0967-0661(03)00080-7` doi: 10.1016/s0967-0661(03)00080-7

Grbic, R., Sliskovic, D., & Kadlec, P. (2012). Adaptive soft sensor for online prediction based on moving window gaussian process regression. In *Machine learning and applications (icmla), 2012 11th international conference on* (Vol. 2, pp. 428–433).

Henze, M., Gujer, W., Mino, T., Matsuo, T., Wentzel, M. C., Marais, G. v. R., & Van Loosdrecht, M. C. (1999). Activated sludge model no. 2d, asm2d. *Water Science and Technology*, *39*(1), 165–182.

Henze, M., Gujer, W., Mino, T., & Van Loosdrecht, M. (2000). *Activated sludge models asm1, asm2, asm2d and asm3.* IWA publishing.

Janssen, P., Meinema, K., & van der Roest, H. (2002). *Biological phosphorus removal: manual for design and operation.* IWA.

Jeppsson, U. (1996). *Modelling aspects of wastewater treatment processes.* Lund institute of technology Sweden.

Jeppsson, U., Alex, J., Pons, M., Spanjers, H., & Vanrolleghem, P. (2002). Status and future trends of ica in wastewater treatment–a european perspective. *Water Science and Technology*, *45*(4-5), 485–494.

Kristiansen, R., Nguyen, H. T. T., Saunders, A. M., Nielsen, J. L., Wimmer, R., Le, V. Q., ... others (2013). A metabolic model for members of the genus tetrasphaera involved in enhanced biological phosphorus removal. *The ISME journal*, *7*(3), 543.

Luccarini, L., Porrà, E., Spagni, A., Ratini, P., Grilli, S., Longhi, S., & Bortone, G. (2002). Soft sensors for control of nitrogen and phosphorus removal from wastewaters by neural networks. *Water Science and Technology*, *45*(4-5), 101–107. Retrieved from `http://wst.iwaponline.com/content/45/4-5/101`

Machnicka, A., Suschka, J., & Grübel, K. (2004). The importance of potassium and magnesium ions in biolgoical phosphorus removal from wastewater. In *Polish-swedish seminar, integration and optimization of urban sanitation systems* (p. 6-8).

Maurer, M., & Gujer, W. (1995). Monitoring of microbial phosphorus release in batch experiments using electric conductivity. *Water Research*, *29*(11), 2613 - 2617. Retrieved from `http://www.sciencedirect.com/science/article/pii/004313549500146C` doi: https://doi.org/10.1016/0043-1354(95)00146-C

Meijer, S. (2004). Theoretical and practical aspects of modelling activated sludge processes. *Delft, The Netherlands: Delft University of Technology*.

Menniti, A., Rieger, L., Boltz, J. P., Johnson, B., Daigger, G., Habermacher, J., ... Morgenroth, E. (2012). Critical review on the degradability of endogenous decay products. *Proceedings of the Water Environment Federation*, *2012*(7), 7406–7408. Retrieved from `https://doi.org/10.2175/193864712811703711` doi: 10.2175/193864712811703711

Mino, T., Van Loosdrecht, M., & Heijnen, J. (1998). Microbiology and biochemistry of the enhanced biological phosphate removal process. *Water research*, *32*(11), 3193–3207.

Mulkerrins, D., Dobson, A., & Colleran, E. (2004). Parameters affecting biological phosphate removal from wastewaters. *Environment International*, *30*(2), 249 - 259. Retrieved from http://www.sciencedirect.com/science/article/pii/S0160412003001776 doi: https://doi.org/10.1016/S0160-4120(03)00177-6

Olsson, G., Nielsen, M., Yuan, Z., Lynggaard-Jensen, A., & Steyer, J.-P. (2005). *Instrumentation, control and automation in wastewater systems*. IWA publishing.

Randall, C. W., Barnard, J. L., & Stensel, H. D. (1998). *Design and retrofit of wastewater treatment plants for biological nutritient removal* (Vol. 5). CRC Press.

Rickard, L., & McClintock, S. (1992). Potassium and magnesium requirements for enhanced biological phosphorus removal from wastewater. *Water Science & Technology*, *26*(9-11), 2203-2206.

Rieger, L., Jones, R. M., Dold, P. L., & Bott, C. B. (2014). Ammonia-based feedforward and feedback aeration control in activated sludge processes. *Water Environment Research*, *86*(1), 63–73.

Rosén, C., Jeppsson, U., & Vanrolleghem, P. A. (2004). Towards a common benchmark for long-term process control and monitoring performance evaluation. *Water Science and Technology*, *50*(11), 41–49.

Rosso, D., Larson, L. E., & Stenstrom, M. K. (2008). Aeration of large-scale municipal wastewater treatment plants: state of the art. *Water Science and Technology*, *57*(7), 973–978. Retrieved from https://doi.org/10.2166/wst.2008.218 doi: 10.2166/wst.2008.218

RoyalHaskoningDHV. (2018). *Carrousel® 1000; robust, reliable, intelligent control, easy to operate.* https://www.royalhaskoningdhv.com/-/media/royalhaskoningdhvcorporate/files/global/markets/water/3servicesheet_carrousel_1000_en.pdf?la=en-gb. (Accessed: 2018-09-24)

Shehab, O., Deininger, R., Porta, F., & Wojewski, T. (1996). Optimizing phosphorus removal at the ann arbor wastewater treatment plant. *Water Science and Technology*, *34*(1-2), 493–499. Retrieved from http://wst.iwaponline.com/content/34/1-2/493

Smolders, G. J. F., van der Meij, J., van Loosdrecht, M. C. M., & Heijnen, J. J. (1994a). Model of the anaerobic metabolism of the biological phosphorus removal process: Stoichiometry and pH influence. *Biotechnology and Bioengineering*, *43*(6), 461–470. Retrieved from https://doi.org/10.1002/bit.260430605 doi: 10.1002/bit.260430605

Smolders, G. J. F., van der Meij, J., van Loosdrecht, M. C. M., & Heijnen, J. J. (1994b). Stoichiometric model of the aerobic metabolism of the biological phosphorus removal process. *Biotechnology and Bioengineering*, *44*(7), 837–848. Retrieved from https://doi.org/10.1002/bit.260440709 doi: 10.1002/bit.260440709

Solon, K., Flores-Alsina, X., Mbamba, C. K., Ikumi, D., Volcke, E., Vaneeckhaute, C., ... Jeppsson, U. (2017). Plant-wide modelling of phosphorus transformations in wastewater treatment systems: Impacts of control and operational strategies. *Water Research*, *113*, 97–110. Retrieved from https://doi.org/10.1016/j.watres.2017.02.007 doi: 10.1016/j.watres.2017.02.007

Sotomayor, O., Park, S., & Garcia, C. (2001). A simulation benchmark to evaluate the performance of advanced control techniques in biological wastewater treatment plants. *Brazilian Journal of Chemical Engineering*, *18*, 81 - 101. Retrieved from http://www.scielo.br/scielo.php?script=sci_arttext&pid=S0104-66322001000100008&nrm=iso

Spagni, A., Buday, J., Ratini, P., & Bortone, G. (2001). Experimental considerations on monitoring orp, ph, conductivity and dissolved oxygen in nitrogen and phosphorus biological removal processes. *Water Science and Technology*, *43*(11), 197–204.

Takacs, I. (1991). A dynamic model of the clarification-thickening process. *Water Research*, *25*(10), 1263–1271. Retrieved from https://doi.org/10.1016/0043-1354(91)90066-y doi: 10.1016/0043-1354(91)90066-y

Tanwar, P., Nandy, T., Ukey, P., & Manekar, P. (2008). Correlating on-line monitoring parameters, pH, DO and ORP with nutrient removal in an intermittent cyclic process bioreactor system. *Bioresource Technology*, *99*(16), 7630–7635. Retrieved from `https://doi.org/10.1016/j.biortech.2008.02.004` doi: 10.1016/j.biortech.2008.02.004

A | Schematic lay-out WWTP Hattem

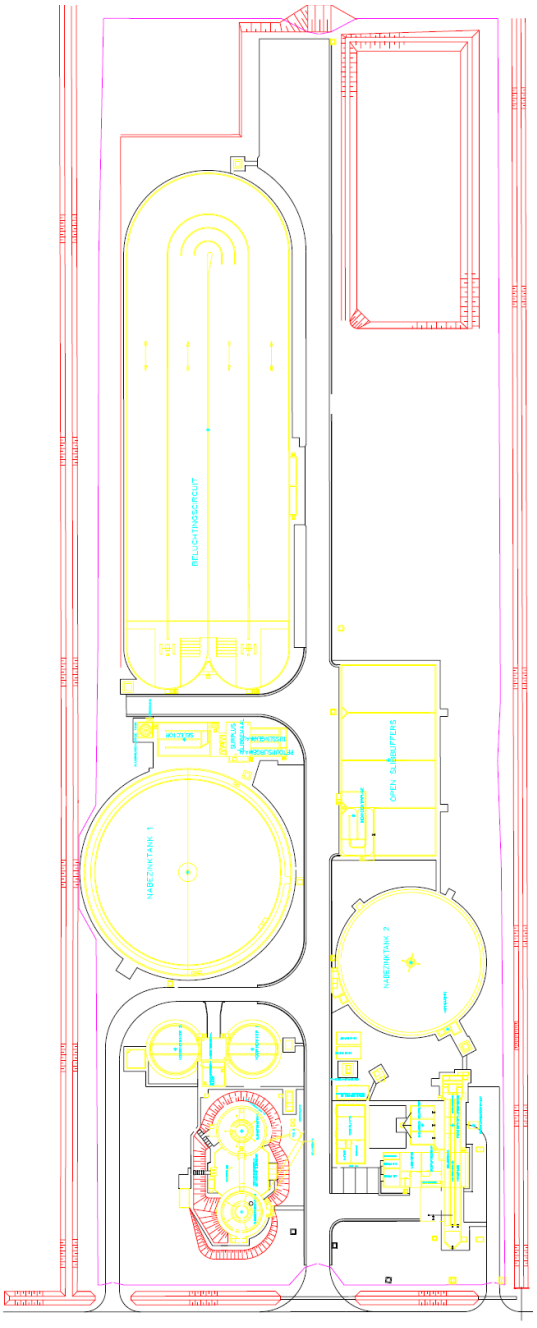

Figure A.1: Complete treatment scheme of WWTP Hattem

B | Data WWTP Hattem

Table B.1: Data WWTP Hattem

Flow and loading rates		
DWF	676	$[m^3/h]$
RWF	1500	$[m^3/h]$
BOD5	3663	$[kgBOD/day]$
NKj	489	$[kgNKj/day]$
Biological design parameters		
Biological volume	13,566	$[m^3]$
Sludge load	0.054	$[kgBOD/kgDS * day]$
Sludge concentration	4	$[g/L]$
Oxygen transfer capacity	312	$[kg/O_2 * h]$
Dimensions anaerobic tank		
Volume	300	$[m^3]$
Width	4	$[m]$
Depth	5	$[m]$
Dimensions oxidation ditch		
Volume	14,000	$[m^3]$
Width	8.5	$[m^3]$
Depth	3.75	$[m]$
Aeration capacity	150	$[kWh]$
Sedimentation tank		
Volume	3000	$[m^3]$
Surface load	1	$[m^3/m^2 * h]$
Sludge load	400	$[L/m^2 * h]$
Depth of the side	2	$[m]$
Slope	1:12	$[-]$

C | Measurement locations

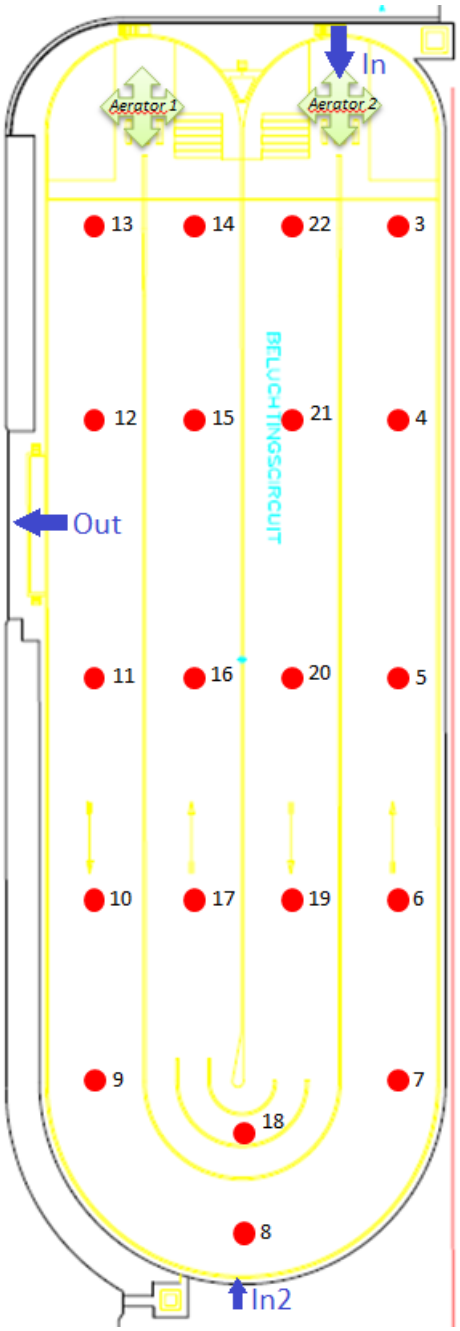

Figure C.1: Measurement locations and labeling oxidation ditch

D | Samples per locations - Aqualysis

Table D.1: Measured variable per location - water matrix

Location	Water matrix samples								
1	COD	Sum N	NH4	NO2	NO2+NO3	Ortho-P	Potassium	Magnesium	Calcium
2	COD	Sum N	NH4	NO2	NO2+NO3	Ortho-P	Potassium	Magnesium	Calcium
3	COD	Sum N	NH4	NO2	NO2+NO3	Ortho-P	Potassium	Magnesium	Calcium
4	-	-	-	-	-	-	-	-	-
5	COD	Sum N	NH4	NO2	NO2+NO3	Ortho-P	Potassium	Magnesium	Calcium
6	-	-	-	-	-	-	-	-	-
7	COD	Sum N	NH4	NO2	NO2+NO3	Ortho-P	Potassium	Magnesium	Calcium
8	-	-	-	-	-	-	-	-	-
9	COD	Sum N	NH4	NO2	NO2+NO3	Ortho-P	Potassium	Magnesium	Calcium
10	-	-	-	-	-	-	-	-	-
11	COD	Sum N	NH4	NO2	NO2+NO3	Ortho-P	Potassium	Magnesium	Calcium
12	COD	Sum N	NH4	NO2	NO2+NO3	Ortho-P	Potassium	Magnesium	Calcium
13	-	-	-	-	-	-	-	-	-
14	COD	Sum N	NH4	NO2	NO2+NO3	Ortho-P	Potassium	Magnesium	Calcium
15	-	-	-	-	-	-	-	-	-
16	-	-	-	-	-	-	-	-	-
17	COD	Sum N	NH4	NO2	NO2+NO3	Ortho-P	Potassium	Magnesium	Calcium
18	-	-	-	-	-	-	-	-	-
19	-	-	-	-	-	-	-	-	-
20	COD	Sum N	NH4	NO2	NO2+NO3	Ortho-P	Potassium	Magnesium	Calcium
21	-	-	-	-	-	-	-	-	-
22	COD	Sum N	NH4	NO2	NO2+NO3	Ortho-P	Potassium	Magnesium	Calcium

Table D.2: Measured variable per location - sludge matrix

Location	Sludge matrix samples						
1	Dry matter	Suspended solids	TKN	Total P	Potassium	Magnesium	Calcium
2	Dry matter	Suspended solids	TKN	Total P	Potassium	Magnesium	Calcium
3	Dry matter	Suspended solids	TKN	Total P	Potassium	Magnesium	Calcium
4	-	-	-	-	-	-	-
5	Dry matter	-	TKN	Total P	Potassium	Magnesium	Calcium
6	-	-	-	-	-	-	-
7	Dry matter	-	TKN	Total P	Potassium	Magnesium	Calcium
8	-	-	-	-	-	-	-
9	Dry matter	-	TKN	Total P	Potassium	Magnesium	Calcium
10	-	-	-	-	-	-	-
11	Dry matter	-	TKN	Total P	Potassium	Magnesium	Calcium
12	Dry matter	-	TKN	Total P	Potassium	Magnesium	Calcium
13	-	-	-	-	-	-	-
14	Dry matter	Suspended solids	TKN	Total P	Potassium	Magnesium	Calcium
15	-	-	-	-	-	-	-
16	-	-	-	-	-	-	-
17	Dry matter	Suspended solids	TKN	Total P	Potassium	Magnesium	Calcium
18	-	-	-	-	-	-	-
19	-	-	-	-	-	-	-
20	Dry matter	Suspended solids	TKN	Total P	Potassium	Magnesium	Calcium
21	-	-	-	-	-	-	-
22	Dry matter	-	TKN	Total P	Potassium	Magnesium	Calcium

E | Required equipment and materials

Personal Protective Equipment (PPE)

- Safety jacket
- Safety shoes
- Protective gloves
- Waterproof Overall

Sensors

- Multimeters: WTW Multi 3420 and Hanna HI9828
- Sensors:
  - pH : WTW, IDS SenTix pH electrode 940
  - ORP: WTW, IDS SenTix ORP-T 900
  - Conductivity: WTW, IDS TetraCon 325
  - Dissolved Oxygen: WTW, IDS FDO 925

Aqualysis equipment

- Syringe filters 0,45 μm
- Syringe
- Sample pots Aqualysis numbered:
- FGH001 (24x)
- FGH004 (24x)
- FGH011 (34x)
- FGH013 (24x)
- FGH014 (10x)
- FGH015 (24x)

Measuring equipment

- Tie wraps
- Weight
- Peristaltic pump
- Hose
- Telescopic pole 11[m]
- Extension reel

Additional necessities

- Centrifuge
- 2 x Bucket
- Toolbox
- Duct tape
- Table
- Funnel
- Ladle
- Booklet + Pen
- High pressure washer
- Tissues

Table E.1: Sample pots to fill at each locations - Version 2

	Location	FGH001	FGH004	FGH011	FGH013	FGH014	FGH015	Total
Water matrix	1	1	1	0	1	0	1	4
	2	1	1	0	1	0	1	4
	3	1	1	0	1	0	1	4
	5	1	1	0	1	0	1	4
	8	1	1	0	1	0	1	4
	11	1	1	0	1	0	1	4
	13	1	1	0	1	0	1	4
	14	1	1	0	1	0	1	4
	16	1	1	0	1	0	1	4
	18	1	1	0	1	0	1	4
	20	1	1	0	1	0	1	4
	22	1	1	0	1	0	1	4
Sludge matrix	1	0	0	2	0	1	0	3
	2	0	0	2	0	1	0	3
	3	0	0	1	0	0	0	1
	5	0	0	2	0	1	0	3
	8	0	0	1	0	0	0	1
	11	0	0	2	0	1	0	3
	13	0	0	1	0	0	0	1
	14	0	0	2	0	1	0	3
	16	0	0	1	0	0	0	1
	18	0	0	1	0	0	0	1
	20	0	0	1	0	0	0	1
	22	0	0	1	0	0	0	1
Total		12	12	17	12	5	12	70

F | Laboratory tests Aqualysis

Table F.1: Laboratory tests NEN specification

Variable	Method	NEN
		Water matrix
Sum N	M135	NEN 6646 + NEN 6961 for disclosure
NH4	M26	NEN 6646
COD	M44	NEN-ISO 15705
NO2	M137	NEN-EN-ISO 13395
NO2+NO3	M137	NEN-EN-ISO 13395
Ortho-P	M37	NEN-EN-ISO 15681-2
Magnesium	M29	NEN-EN-ISO 17294-2 + NEN 6961 & NEN-EN-ISO 15587-1 for disclosure
Calcium	M29	NEN-EN-ISO 17294-2 + NEN 6961 & NEN-EN-ISO 15587-1 for disclosure
Potassium	M29	NEN-EN-ISO 17294-2 + NEN 6961 & NEN-EN-ISO 15587-1 for disclosure
		Sludge Matrix
COD	M25	NEN 6633:2006
TKN	M136	NEN 6646 + NEN-EN 13341 for disclosure
Potassium	M28	NEN-EN-ISO 17294-2 + NEN 6950 for disclosure
Magnesium	M28	NEN-EN-ISO 17294-2 + NEN 6950 for disclosure
Calcium	M28	NEN-EN-ISO 17294-2 + NEN 6950 for disclosure
Nitrification capacity	M69	NEN-EN-ISO 9509
Phosphate release rate	M146	NEN-EN-ISO 15681-2
Total P	M140	NEN-EN-ISO 15681-2 + NEN-EN 14672 for disclosure
Suspended solids	M132	NEN-EN 872 en NEN 6499
Dry matter	M134	NEN-EN 15934

G | Measuring method

1. Preparation
   (a) The hose is attached to the telescopic pole
   (b) at one end of the hose a weight is attached, so that the hose stays at a certain depth. The other end is connected to the peristaltic pump
   (c) Extension reels are distributed all around the oxidation ditch, for power access at any location
   (d) All needed sample pots are labeled correctly, sorted and placed in order
   (e) Everything is put into place next to the oxidation ditch: gloves, computer, sample planning, syringes, filters, bucket, funnel, ladle, Multimeter, sensors, booklet and pen
2. Measurement: repeat for each location, until each location is measured
   (a) Place the hose at the right location, with the hose 1 [m] below surface
   (b) Turn on the pump, but do not catch up the sample in the bucket for a minute and a half (depending on the volume in the hose and pumping velocity)
   (c) Fill up a bucket with waste water from the measuring location
   (d) Place all sensors in the bucket and write down the results
   (e) Take samples from the bucket and fill all necessary sample pots Table E.1
   (f) For samples that need to be filtered:
      - Fill the measuring cups of the centrifuge with the sample and let it centrifuge
      - Fill a syringe with the centrifuged sample and put a filter on it
      - Fill the sample pots with filtered sample
   (g) Clean the bucket, sensors, centrifuge (with high pressure washer if convenient)

H | Results measurement campaign

Table H.1: Detailed measurement results: variant 1 - Sensor results

Location	Conductivity [μS/cm]	DO [mg/L]	pH	ORP [mV]	Temperature [degrees Celsius]
1	886	0.34	7.43	-80	8.4
2	880	0.04	7.4	-50	8.4
3 - In, A2	785	0.6	7.14	-29	9.4
5	788	3.5	7.12	-34	9.2
8 - In2	788	0.85	7.13	-32	9.1
11 - out	781	1.21	7.14	45	9.8
13	758	1.42	7.14	112	9.5
14 - A1	764	3.2	7.12	26	9.5
15	763	5.04	7.11	-37	9.8
16	769	4.45	7.1	45	10
17	769	0.22	7.11	12	9.8
18	771	4.36	7.12	-30	9.8
19	772	2.25	7.09	40	10.3
20	773	0.86	7.1	26	10.3
21	774	0.17	7.13	-25	9.3

Table H.2: Detailed measurement results: variant 2 - Sensor results

Location	Conductivity [μS/cm]	DO [mg/L]	pH	ORP [mV]	Temperature [degrees Celsius]
1	911	3.45	7.46	178	7.9
2	913	0.4	7.43	-98	7.4
3 - In, A2	792	2.32	7.21	-57	9.3
5	821	1.8	7.2	-70	10
8 - In2	830	1.88	7.19	-41	9.6
11 - Out	832	2.67	7.19	-28	10
13	833	6.3	7.19	-6	10.3
14 - A1	782	2.7	7.24	-184	8.1
16	820	3.65	7.20	-177	10
18	820	3.34	7.20	-88	10.3
20	819	4.92	7.21	60	10
22	785	0.55	7.19	-65	9.3

Table H.3: Detailed measurement results: variant 1 - Water matrix sample results

Location	COD mg/L	sum-N mg/L	NH4 mg/L	NO2 mg/L	NO2+NO3 mg/L	NO3 mg/L	Ortho-P mg/L	Potassium mg/L	Magnesium mg/L	Calcium mg/L	Sodium mg/L
1	34	15.5	13.4	0.31	0.52	0.22	3.8	53	5.1	48	70
2	36	16.4	14.7	<0.02	<0.05	<0.05	4.7	49	5.3	48	71
3 - In, A2	26	4.6	3.8	0.08	0.09	<0.05	2.2	47	4.8	50	70
5	25	4.7	3.9	0.03	<0.05	<0.05	2.4	46	4.8	49	69
8 - In2	24	4.8	4	<0.02	<0.05	<0.05	2.4	47	4.9	50	70
11 - Out	23	4.6	3.8	0.16	0.23	0.07	2.4	46	4.8	48	70
14 - A1	23	2.6	1.6	0.75	1.8	1.08	0.93	45	4.5	47	68
16	26	3.3	2.2	0.71	1.2	0.51	1	45	4.5	47	68
18	24	3.4	2.4	0.57	0.9	0.33	1	47	4.8	49	70
20	23	3.6	2.8	0.21	0.3	0.09	1.1	46	4.7	49	70
22	24	3.8	3.1	0.1	0.14	<0.05	1.1	47	4.8	49	70

Table H.4: Detailed measurement results: variant 2 - Water matrix sample results

Location	COD mg/L	sum-N mg/L	NH4 mg/L	NO2 mg/L	NO2+NO3 mg/L	NO3 mg/L	Ortho-P mg/L	Potassium mg/L	Magnesium mg/L	Calcium mg/L	Sodium mg/L
1	39	18.4	15.7	0.2	0.25	0.06	5	60	6	50	72
2	41	19.3	16.6	<0.02	<0.05	<0.05	6.1	57	6	49	73
3 - In, A2	26	5.2	3.8	0.02	<0.05	<0.05	3.4	53	5.3	48	71
5	26	8.3	7.2	0.18	0.32	0.14	4.5	55	5.7	50	75
8 - In2	25	8.3	7.3	0.14	0.2	0.06	4.3	53	5.6	50	72
11 - Out	27	8.4	7.3	0.02	<0.05	<0.05	4.4	53	5.6	49	72
13	26	8.6	7.4	<0.02	<0.05	<0.05	4.4	54	5.6	50	73
14 - A1	26	4.2	2.8	0.03	<0.05	<0.05	2.5	52	5.1	48	71
16	24	7.6	6.5	0.02	<0.05	<0.05	4.2	55	5.7	49	72
18	27	7.8	6.6	<0.02	<0.05	<0.05	4.4	53	5.5	47	71
20	25	7.9	6.8	<0.02	<0.05	<0.05	4.4	54	5.7	50	72
22	29	5.2	3.2	<0.02	<0.05	<0.05	3.1	54	5.4	50	26

Table H.5: Detailed measurement results: variant 1 - Sludge matrix sample results

Loc.	Dry mat. %	TSS g/L	FOS/TAC	VFA mg/L	TOC mg/L	tKN g/kgds	Total-P g/kg s	K+ mg/kgds	Mg2+ mg/kgds	Ca2+ mg/kgds	Na+ mg/kgds	Nitr. cap. mgN/g.ds.h	PO4 rel.rate mg/g.h
1	0.3	2.03	<0.01	<1	246	64	20	24	5.8	29	25		
2	0.3	2.17	<0.01	<1	243	59	19	23	5.5	27	26		
3 - In, A2	0.3					75	20	23	5.7	27	24		
5	0.3	2.52	<0.01	<1	187	59	20	22	5.6	27	22		
8 - In2	0.3	2.73				68	21	23	5.9	29	24	2	0.05
11 - Out	0.3	2.34	<0.01	<1	205	62	20	25	5.7	31	26		
14 - A1	0.3	2.38	<0.01	<1	178	64	20	22	5.9	27	23		
16	0.3					65	20	21	5.3	26	21		
18	0.3					61	20	22	5.6	28	22		
20	0.3					63	20	22	5.7	26	23		
22	0.3					58	20	22	5.6	28	23		

Table H.6: Detailed measurement results: variant 2 - Sludge matrix sample results

Location	Dry matter %	TSS g/L	FOS/TAC	VFA mg/L	TOC mg/L	tKN g/kg ds	Total-P g/kg ds	K+ mg/kg ds	Mg2+ mg/kg ds	Ca2+ mg/kg ds	Na+ mg/kg ds
1	0.3	2.53	<0.01	<1	258	65	21	25	5.8	28	22
2	0.3	2.47	<0.01	<1	261	66	21	25	5.8	27	24
3 - In, A2	0.2					66	20	29	6.2	32	29
5	0.3	2.71	<0.01	<1	214	72	21	24	5.8	27	22
8 - In2	0.3					68	21	23	5.7	27	22
11 - Out	0.3	2.77	<0.01	<1	211	65	22	25	6	28	25
13	0.3					67	21	26	6	29	25
14 - A1	0.3	2.66	<0.01	<1	202	68	20	23	5.6	27	22
16	0.3					65	21	23	5.7	28	22
18	0.3					74	21	24	5.8	25	23
20	0.3					66	21	24	5.9	29	23
22	0.3					64	20	24	5.7	27	22

Table H.7: Detailed measurement results: variant 1 - Relation results delta P - delta K

deltaP	delta K	delta K/ Delta P
0.9	-4	-4.4
-2.5	-2	0.8
0.2	-1	-5
0	1	-
0	-1	-
-1.5	-1	0.7
0.1	0	0
0	2	-
0.1	-1	-10
0	1	-

Table H.8: Detailed measurement results: variant 2 - Relation results delta P - delta K

deltaP	delta K	delta K/ Delta P
1.1	-3	-2.7
-2.7	-4	1.5
1.1	2	1.8
-0.2	-2	10
0.1	0	0
0	1	-
-1.9	-2	1.1
1.7	3	1.8
0.2	-2	-10
0	1	-
-1.3	0	0

Table H.9: Comparing ORP sensors of the type 'WTW, IDS SenTix ORP-T 900' to evaluate reliability and response rate in a laboratory

Medium	ORP sensor used [mV]	Similar type sensor #1 [mV]	Similar type sensor #2 [mV]
Tap water	235	224	222
Calibration liquid	304	299	304
pH4 buffer	422	420	421

I | BioWin

Table I.1: Detailed simulation results - Base Case

Elements	COD [mg/L]	TKN [mgN/L]	NH4[mgN/L]	NO2+NO3[mgN/L]	NO3 [mgN/L]	Soluble PO4-P [mgP/L]	Total P [mgP/L]	DO [mg/L]	TSS [mg/L]	PAO [mgCOD/L]	pH []
Influent	600	52.9	34.91	0	0	4.1	8.2	0	283.1	0.06	7.3
Contact	4406.7	266.59	37.17	0	0	15.58	128.59	0	3997.32	156.45	7.15
T1 - Aerator 2	4074.47	231.05	1.84	0.78	0.27	1.57	128.59	2.7	3901.39	164.66	7.4
T2	4072.43	230.8	1.58	0.77	0.21	1.39	128.59	0.35	3901.23	164.75	7.33
T3	4071.37	230.76	1.64	0.41	0.06	1.38	128.59	0.02	3900.88	164.75	7.33
T4	4070.81	230.76	1.74	0.14	0.01	1.48	128.59	0	3900.3	164.72	7.34
T5	4070.56	230.76	1.83	0.02	0	1.59	128.59	0	3899.86	164.7	7.35
Effluent	43.2	3.75	1.83	0.02	0	1.59	1.86	0	8.25	0.35	7.35
T6	4070.49	230.76	1.9	0	0	1.71	128.59	0	3899.35	164.66	7.35
T7- Aerator 1	4067.24	230.35	1.34	0.4	0.16	1.5	128.59	7	3898.21	164.77	7.66
T8	4064.9	230	0.89	0.7	0.3	1.28	128.59	3.39	3897.48	164.86	7.46
T9	4062.76	229.77	0.63	0.77	0.33	1.09	128.59	0.73	3896.88	164.94	7.36
T10	4061.46	229.71	0.64	0.46	0.15	1.02	128.59	0.07	3896.47	164.96	7.35
Waste Sludge	74132.99	4179.97	1.83	0.02	0	1.59	2333.35	0	71600.74	3023.83	7.35

Table I.2: Detailed simulation results - Increased Temperature

Elements	COD [mg/L]	TKN [mgN/L]	NH4[mgN/L]	NO2+NO3[mgN/L]	NO3 [mgN/L]	Soluble PO4-P [mgP/L]	Total P [mgP/L]	DO [mg/L]	TSS [mg/L]	PAO [mgCOD/L]	pH []
Influent	600	52.9	34.91	0	0	4.1	8.2	0	283.1	0.06	7.3
Contact	4455.25	268.83	37.51	0	0	23.71	135.96	0	4039.47	395.56	7.17
T1 - Aerator 2	4128.59	233.24	1.55	0.56	0.09	0.83	135.96	1.5	3960.77	416.51	7.41
T2	4126.93	233.07	1.42	0.32	0.02	0.54	135.96	0.08	3960.91	416.71	7.37
T3	4126.35	233.06	1.5	0.05	0	0.74	135.96	0	3960.22	416.69	7.37
T4	4126.2	233.06	1.59	0	0	0.98	135.96	0	3959.46	416.61	7.38
T5	4126.13	233.06	1.64	0	0	1.18	135.96	0	3958.72	416.5	7.39
Effluent	47.33	3.7	1.64	0	0	1.18	1.47	0	8.37	0.88	7.39
T6	4126.06	233.06	1.69	0	0	1.36	135.96	0	3957.99	416.4	7.39
T7- Aerator 1	4121.44	232.47	0.89	0.55	0.14	0.59	135.96	4	3957.89	416.82	7.57
T8	4118.66	232.16	0.48	0.63	0.12	0.17	135.96	0.57	3957.56	417.13	7.39
T9	4117.4	232.12	0.51	0.25	0.02	0.17	135.96	0.03	3956.91	417.18	7.38
T10	4116.93	232.12	0.6	0.04	0	0.37	135.96	0	3956.14	417.12	7.39
Waste Sludge	75083.48	4223.12	1.64	0	0	1.18	2475.65	0	72681.35	7646.95	7.39

Table I.3: Detailed simulation results - Increased Temperature, aerator switch

Elements	COD [mg/L]	TKN [mgN/L]	NH4[mgN/L]	NO2+NO3[mgN/L]	NO3 [mgN/L]	Soluble PO4-P [mgP/L]	Total P [mgP/L]	DO [mg/L]	TSS [mg/L]	PAO [mgCOD/L]	pH []
Influent	600	52.9	34.91	0	0	4.1	8.2	0	283.1	0.06	7.3
Contact	4449.06	268.48	37.5	0	0	24.67	141.8	0	4051.77	422.5	7.17
T1 - Aerator 2	4124.63	232.83	1.52	0.65	0.1	0.98	141.8	4	3975.39	444.64	7.56
T2	4121.94	232.42	1.03	0.8	0.06	0.37	141.8	0.43	3975.94	445	7.38
T3	4120.8	232.38	1.08	0.39	0.01	0.37	141.8	0.02	3975.34	445.01	7.38
T4	4120.21	232.38	1.16	0.09	0	0.63	141.8	0	3974.37	444.95	7.39
T5	4120.01	232.38	1.24	0.01	0	0.86	141.8	0	3973.61	444.87	7.4
Effluent	47.65	3.36	1.24	0.01	0	0.86	1.16	0	8.4	0.94	7.4
T6	4119.94	232.38	1.3	0	0	1.08	141.8	0	3972.83	444.76	7.4
T7- Aerator 1	4116.11	231.91	0.66	0.38	0.06	0.38	141.8	1.5	3972.62	445.18	7.44
T8	4114.52	231.78	0.53	0.19	0.01	0.19	141.8	0.1	3972.2	445.39	7.38
T9	4114.07	231.77	0.61	0.02	0	0.39	141.8	0	3971.51	445.36	7.38
T10	4113.98	231.77	0.68	0	0	0.63	141.8	0	3970.69	445.26	7.39
Waste Sludge	74965.32	4216.49	1.24	0.01	0	0.86	2588.46	0	72954.74	8167.74	7.4

Table I.4: Detailed simulation results - DO setpoints 7 and 3

Elements	COD [mg/L]	TKN [mgN/L]	NH4[mgN/L]	NO2+NO3[mgN/L]	NO3 [mgN/L]	Soluble PO4-P [mgP/L]	Total P [mgP/L]	DO [mg/L]	TSS [mg/L]	PAO [mgCOD/L]	pH []
Influent	600	52.9	34.91	0	0	4.1	8.2	0	283.1	0.06	7.3
Contact	4108.04	246.49	37.1	0	0	7.4	85.07	0	3673.06	42.08	7.08
T1 - Aerator 2	3760.05	209.14	1.2	0.62	0.39	4.08	85.07	7	3544.57	44.21	7.89
T2	3757.58	208.68	0.66	1.02	0.73	4.02	85.07	2.68	3543.88	44.24	7.55
T3	3755.62	208.45	0.43	1	0.72	3.98	85.07	0.37	3543.16	44.26	7.44
T4	3754.43	208.41	0.49	0.65	0.44	3.97	85.07	0.03	3542.74	44.26	7.43
T5	3753.62	208.41	0.58	0.35	0.22	3.98	85.07	0	3542.28	44.26	7.44
Effluent	39.8	2.43	0.58	0.35	0.22	3.98	4.15	0	7.49	0.09	7.44
T6	3753.06	208.41	0.67	0.13	0.08	4	85.07	0	3541.84	44.25	7.45
T7- Aerator 1	3750.6	208.12	0.29	0.38	0.3	3.97	85.07	3	3540.25	44.27	7.54
T8	3748.54	207.99	0.14	0.36	0.31	3.93	85.07	0.75	3539.09	44.28	7.43
T9	3747.34	207.94	0.17	0.14	0.11	3.93	85.07	0.09	3538.47	44.29	7.4
T10	3746.95	207.94	0.28	0.03	0.02	3.96	85.07	0.01	3538.15	44.29	7.41
Waste Sludge	68361.42	3791.73	0.58	0.35	0.22	3.98	1492.76	0	65035.7	812.52	7.44

Table I.5: Detailed simulation results - DO setpoints 5 and 2

Elements	COD [mg/L]	TKN [mgN/L]	NH4[mgN/L]	NO2+NO3[mgN/L]	NO3 [mgN/L]	Soluble PO4-P [mgP/L]	Total P [mgP/L]	DO [mg/L]	TSS [mg/L]	PAO [mgCOD/L]	pH []
Influent	600	52.9	34.91	0	0	4.1	8.2	0	283.1	0.06	7.3
Contact	4356.28	262.81	37.39	0	0	22.56	142.79	0	3994.68	306.19	7.16
T1 - Aerator 2	4025.67	226.61	1.36	0.63	0.23	1.2	142.79	5	3911.16	322.15	7.64
T2	4022.93	226.17	0.81	0.92	0.33	0.73	142.79	0.92	3911.36	322.39	7.41
T3	4021.32	226.07	0.77	0.54	0.12	0.54	142.79	0.05	3911.28	322.48	7.39
T4	4020.54	226.07	0.86	0.18	0.03	0.65	142.79	0	3910.55	322.43	7.4
T5	4020.2	226.07	0.94	0.03	0.01	0.81	142.79	0	3909.93	322.39	7.41
T6	4020.11	226.07	1.01	0	0	0.98	142.79	0	3909.26	322.32	7.41
T7- Aerator 1	4016.79	225.67	0.47	0.33	0.15	0.54	142.79	2	3908.5	322.56	7.47
T8	4014.89	225.53	0.3	0.19	0.07	0.31	142.79	0.21	3908.05	322.72	7.39
T9	4014.34	225.51	0.38	0.02	0.01	0.42	142.79	0.01	3907.52	322.72	7.39
T10	4014.23	225.51	0.46	0	0	0.62	142.79	0	3906.8	322.65	7.39
Effluent	45.28	2.98	0.94	0.03	0.01	0.81	1.11	0	8.27	0.68	7.41
Waste Sludge	73170.42	4106.97	0.94	0.03	0.01	0.81	2607.48	0	71785.62	5919.02	7.41

Table I.6: Detailed simulation results - Extended Anaerobic Tank (V=1000 m^3)

Elements	COD [mg/L]	TKN [mgN/L]	NH4[mgN/L]	NO2+NO3[mgN/L]	NO3 [mgN/L]	Soluble PO4-P [mgP/L]	Total P [mgP/L]	DO [mg/L]	TSS [mg/L]	PAO [mgCOD/L]	pH []
Influent	600	52.9	34.91	0	0	4.1	8.2	0	283.1	0.06	7.3
Contact	4253.18	256.31	38.44	0	0	34.52	143.47	0	3910.77	323.79	7.2
T1 - Aerator 2	3923.76	219.8	1.37	0.63	0.29	1.58	143.47	6	3842.38	341.47	7.75
T2	3921.23	219.32	0.78	1.02	0.51	1.03	143.47	1.75	3842.66	341.72	7.48
T3	3919.37	219.15	0.62	0.82	0.35	0.68	143.47	0.14	3842.88	341.88	7.41
T4	3918.29	219.13	0.68	0.41	0.14	0.67	143.47	0.01	3842.45	341.86	7.42
T5	3917.68	219.14	0.75	0.14	0.04	0.77	143.47	0	3841.78	341.8	7.43
Effluent	45.66	2.87	0.75	0.14	0.04	0.77	1.07	0	8.13	0.72	7.43
T6	3917.41	219.14	0.82	0.02	0.01	0.9	143.47	0	3841.2	341.75	7.43
T7- Aerator 1	3914.56	218.81	0.37	0.29	0.17	0.49	143.47	2	3840.56	341.96	7.49
T8	3912.75	218.68	0.23	0.19	0.1	0.27	143.47	0.26	3840.13	342.11	7.41
T9	3912.15	218.66	0.29	0.03	0.02	0.34	143.47	0.02	3839.67	342.12	7.4
T10	3912.03	218.66	0.37	0.01	0	0.53	143.47	0	3839	342.05	7.41
Waste Sludge	71277.62	3981.45	0.75	0.14	0.04	0.77	2620.79	0	70534.46	6275.42	7.43

Table I.7: Detailed simulation results - Same settings with current anaerobic tank (V=300 m^3)

Elements	COD [mg/L]	TKN [mgN/L]	NH4[mgN/L]	NO2+NO3[mgN/L]	NO3 [mgN/L]	Soluble PO4-P [mgP/L]	Total P [mgP/L]	DO [mg/L]	TSS [mg/L]	PAO [mgCOD/L]	pH []
Influent	600	52.9	34.91	0	0	4.1	8.2	0	283.1	0.06	7.3
Contact	4285	258.24	37.31	0	0	19.89	139.01	0	3938.71	234.75	7.15
T1 - Aerator 2	3950.02	221.71	1.3	0.63	0.3	1.5	139.01	6	3847.35	246.92	7.75
T2	3947.33	221.24	0.73	1	0.52	1.14	139.01	1.65	3847.26	247.09	7.46
T3	3945.46	221.08	0.59	0.75	0.33	0.91	139.01	0.13	3847.18	247.2	7.4
T4	3944.41	221.06	0.67	0.35	0.12	0.92	139.01	0.01	3846.7	247.18	7.41
T5	3943.84	221.06	0.76	0.1	0.03	1.02	139.01	0	3846.09	247.15	7.42
Effluent	43.85	2.76	0.76	0.1	0.03	1.02	1.31	0	8.13	0.52	7.42
T6	3943.63	221.07	0.83	0.01	0.01	1.14	139.01	0	3845.53	247.1	7.43
T7- Aerator 1	3940.69	220.73	0.37	0.29	0.17	0.83	139.01	2	3844.52	247.26	7.48
T8	3938.84	220.6	0.23	0.17	0.09	0.64	139.01	0.25	3843.99	247.37	7.4
T9	3938.29	220.57	0.31	0.02	0.02	0.71	139.01	0.02	3843.51	247.38	7.4
T10	3938.18	220.57	0.39	0	0	0.89	139.01	0	3842.85	247.33	7.4
Waste Sludge	71790.51	4018.75	0.76	0.1	0.03	1.02	2534.62	0	70613.44	4537.6	7.42

Table I.8: Detailed simulation results - Extended anaerobic tank, with staggered aeration

Elements	COD [mg/L]	TKN [mgN/L]	NH4[mgN/L]	NO2+NO3[mgN/L]	NO3 [mgN/L]	Soluble PO4-P [mgP/L]	Total P [mgP/L]	DO [mg/L]	TSS [mg/L]	PAO [mgCOD/L]	pH []
Influent	600	52.9	34.91	0	0	4.1	8.2	0	283.1	0.06	7.3
Contact	4285	258.24	37.31	0	0	19.89	139.01	0	3938.71	234.75	7.15
T1 - Aerator 2	3950.02	221.71	1.3	0.63	0.3	1.5	139.01	6	3847.35	246.92	7.75
T2	3947.33	221.24	0.73	1	0.52	1.14	139.01	1.65	3847.26	247.09	7.46
T3	3945.46	221.08	0.59	0.75	0.33	0.91	139.01	0.13	3847.18	247.2	7.4
T4	3944.41	221.06	0.67	0.35	0.12	0.92	139.01	0.01	3846.7	247.18	7.41
T5	3943.84	221.06	0.76	0.1	0.03	1.02	139.01	0	3846.09	247.15	7.42
Effluent	43.85	2.76	0.76	0.1	0.03	1.02	1.31	0	8.13	0.52	7.42
T6	3943.63	221.07	0.83	0.01	0.01	1.14	139.01	0	3845.53	247.1	7.43
T7- Aerator 1	3940.69	220.73	0.37	0.29	0.17	0.83	139.01	2	3844.52	247.26	7.48
T8	3938.84	220.6	0.23	0.17	0.09	0.64	139.01	0.25	3843.99	247.37	7.4
T9	3938.29	220.57	0.31	0.02	0.02	0.71	139.01	0.02	3843.51	247.38	7.4
T10	3938.18	220.57	0.39	0	0	0.89	139.01	0	3842.85	247.33	7.4
Waste Sludge	71790.51	4018.75	0.76	0.1	0.03	1.02	2534.62	0	70613.44	4537.6	7.42

Table I.9: Detailed simulation results - Extended anaerobic tank, over aerated

Elements	COD [mg/L]	TKN [mgN/L]	NH4[mgN/L]	NO2+NO3[mgN/L]	NO3 [mgN/L]	Soluble PO4-P [mgP/L]	Total P [mgP/L]	DO [mg/L]	TSS [mg/L]	PAO [mgCOD/L]	pH []
Influent	600	52.9	34.91	0	0	4.1	8.2	0	283.1	0.06	7.3
Contact	4182.08	251.68	38.39	0	0	33.87	140.61	0	3854.28	269.48	7.2
T1 - Aerator 2	3848.28	214.86	1.34	0.63	0.36	1.78	140.61	7	3781.63	284.13	7.91
T2	3845.89	214.37	0.75	1.06	0.69	1.34	140.61	2.68	3781.67	284.33	7.56
T3	3843.87	214.14	0.49	1.04	0.66	0.99	140.61	0.33	3781.76	284.48	7.44
T4	3842.63	214.1	0.53	0.65	0.38	0.89	140.61	0.02	3781.56	284.5	7.44
T5	3841.79	214.1	0.6	0.33	0.18	0.93	140.61	0	3781.01	284.46	7.45
Effluent	44.5	2.7	0.6	0.33	0.18	0.93	1.22	0	8	0.6	7.45
T6	3841.25	214.11	0.67	0.11	0.06	1	140.61	0	3780.43	284.42	7.46
T7- Aerator 1	3838.75	213.83	0.3	0.33	0.24	0.67	140.61	2	3779.69	284.57	7.51
T8	3836.97	213.72	0.18	0.23	0.16	0.46	140.61	0.31	3779.26	284.68	7.43
T9	3836.26	213.7	0.24	0.05	0.04	0.48	140.61	0.03	3778.87	284.69	7.42
T10	3836.09	213.69	0.32	0.01	0.01	0.64	140.61	0	3778.28	284.64	7.43
Waste Sludge	69901.81	3891.91	0.6	0.33	0.18	0.93	2565.5	0	69418.7	5222.6	7.45

Table I.10: Detailed simulation results - Base Case more detailed

Element name	Flow	Volatile suspended solids	Total suspended solids	Total COD	Filtered COD	Total N	Total Kjeldahl Nitrogen	Filtered TKN	Ammonia N	Nitrate N	Total P	Soluble PO4-P	Total Carbonaceous BOD	Filtered Carbonaceous BOD	Volume	Temperature
Clarifier	10264	5.74	8.25	43.2	34.66	3.77	3.75	3.27	1.83	0	1.86	1.59	2.2	0.39	3000	11
Contact	10854	2864.21	3997.32	4406.7	120.38	266.59	266.59	40.17	37.17	0	128.59	15.58	1071.32	56.92	300	11
Effluent	10264	5.74	8.25	43.2	34.66	3.77	3.75	3.27	1.83	0	1.86	1.59	2.2	0.39	0	11
Influent	10292	237.31	283.1	600	221.88	52.9	52.9	42.63	34.91	0	8.2	4.1	294.96	135.95	0	11
RAS	590	49865.22	71600.74	74132.99	34.66	4179.99	4179.97	3.27	1.83	0	2333.35	1.59	15754.29	0.39	0	11
spside	217080	2716	3899.86	4070.56	34.66	230.78	230.76	3.27	1.83	0	128.59	1.59	858.45	0.39	0	11
T1 - Aerator 2	227934	2717.5	3901.39	4074.47	36.14	231.84	231.05	3.57	1.84	0.27	128.59	1.57	861.7	1.94	1400	11
T10	217080	2710.59	3896.47	4061.46	34.54	230.17	229.71	2.27	0.64	0.15	128.59	1.02	853.41	0.75	1400	11
T2	227934	2716.75	3901.23	4072.43	35.44	231.57	230.8	3.29	1.58	0.21	128.59	1.39	860.31	1.37	1400	11
T3	227934	2716.36	3900.88	4071.37	35	231.17	230.76	3.26	1.64	0.06	128.59	1.38	859.43	0.92	1400	11
T4	227934	2716.08	3900.3	4070.81	34.84	230.9	230.76	3.27	1.74	0.01	128.59	1.48	858.84	0.64	1400	11
T5	227934	2716	3899.86	4070.56	34.66	230.78	230.76	3.27	1.83	0	128.59	1.59	858.45	0.39	1400	11
T6	217080	2715.9	3899.35	4070.49	34.67	230.76	230.76	3.28	1.9	0	128.59	1.71	858.22	0.31	1400	11
T7- Aerator 1	217080	2713.99	3898.21	4067.24	34.59	230.74	230.35	2.89	1.34	0.16	128.59	1.5	857.07	0.99	1400	11
T8	217080	2712.49	3897.48	4064.9	34.79	230.7	230	2.55	0.89	0.3	128.59	1.28	855.7	1.11	1400	11
T9	217080	2711.25	3896.88	4062.76	34.77	230.54	229.77	2.32	0.63	0.33	128.59	1.09	854.38	1.04	1400	11
WAS	28	49865.22	71600.74	74132.99	34.66	4179.99	4179.97	3.27	1.83	0	2333.35	1.59	15754.29	0.39	0	11
WAS splitter	562	49865.22	71600.74	74132.99	34.66	4179.99	4179.97	3.27	1.83	0	2333.35	1.59	15754.29	0.39	0	11
Waste Sludge	28	49865.22	71600.74	74132.99	34.66	4179.99	4179.97	3.27	1.83	0	2333.35	1.59	15754.29	0,39	0	11

J | Matlab files - Benchmark oxidation ditch

This appendix contains the two matlab files of the benchmark oxidation ditch by Abusam (2001). The files are explained in Appendix K together with the corresponding C^{++} files and Simulink model.

J.1 Main file - mhv.m

```
 global Time stab100 Pair Pcstr ICcstr Psettler ICsettler;
global IR;
tic

load stab100b;
Time=stab100b(:,1);
stab100b(:.1)=[];

%COST param.
v1=600; %volume
v2=600;
ya=0.24;% yield for autotrophic biomass g cell formed
yh=0.67; % yield for heterotrophic biomass g cell COD formed
fp=0.08;% fraction of biomass leading to particulate products
t ixb=0.08;% mass of nitrogen per mass of COD in biomass (gN (gCOD-1))
ixp=0.06; % mass of nitrogen per mass of COD in products from biomass (gN (gCOD-1))
muh=4.0;% max specific grotwth rate for heteretrophic biomass (d-1(
mua=0.5;% maxiumum spec. growth rate for autotrophic biomass (d-1)
ks=10;% half saturation coefficient for het. biomass (g COD /m3)
koh=0.2;% oxygen half-saturation coefficient for hetereotrophic biomass (g O2/m3)
kno=0.5; % nitrate half-saturation coefficient for denitrifying heterotrphic biomass (gNO3-N/m3)
bh=0.3; % decay coeff. for heter. biomass (d-1)
etag=0.8; % correction factor for muh under anoxic cond.
etah=0.8; % correction factor for hydrolysis under anoxic cond.
kh=3.0; % max. specific hydrolysis rate (g slowly biod. COD)
kx=0.1; % half-saturation coefficient for hydrolysis of slowsly biodegr. substrate
knh=1.0; % ammonia half-saturation coefficient for autotrophic biomass (g NH4-N/m3)
ba=0.05; % decay coeff for autotrophic biomass (d-1)
koa=0.4; % oxygen half-saturation coeff. for autotrohpic biomass (g O2 /m3)
ka=0.05; % ammonification rate (m3.COD(g.day-1))
sosat=8.0; % sat. conc. oxygen
kla1=0; % oxygen transfer rate (d-1)
kla2=240; % oxygen transfer rate (d-1)
%kla1=28.3*24;


IR=45; % the ditch internal recirculation rate


Pcstr=[v1 ya yh fp ixb ixp muh ks koh kno bh etag etah kh kx mua knh ba koa ka sosat kla1];%22;
```

```
Pair =[v2 ya yh fp ixb ixp muh ks koh kno bh etag etah kh kx mua knh ba koa ka sosat kla2];%22;

%icr: IC reactor (cstr);
icr1=15.2; icr2=0.70; icr3=77.3; icr4=40.9; icr5=1788.6; icr6=270.3; icr7=590.6;
icr8=0.005; icr9=14.96; icr10=2.57; icr11=0.6; icr12=2.82; icr13=2.31;
ICcstr=[icr1 icr2 icr3 icr4 icr5 icr6 icr8 icr9 icr10 icr11 icr12 icr13];%13;

% Initial conditions
a=1500; %surface area settler
zm=0.4; % layer depth settler (4m total / 10 layers)
vm=250; % max settling velocity
vv=474; % max Vesilind settling velocity
rh=0.000576; % hindered zone settling parameter
rp=0.00286; % flocculant zone settling parameter
fns=0.00228; % non-settleable fraction
xt=3000;
Psettler=[a zm vm vv rh rp fns xt];

%ics: IC settler;
ics1=3000; ics2=226.5; ics3=226.5; ics4=226.5; ics5=226.5;
ics6=226.5; ics7=42.8; ics8=18.7; ics9=11.8; ics10=8.6;
ICsettler=[ics1 ics2 ics3 ics4 ics5 ics6 ics7 ics8 ics9 ics10];

[t,x,y]=sim('hv2',Time);

toc
```

J.2 Influent variables file

```
 % stab100b
tt=[0:1:100]';
s1=30*ones(101,1); %Si g COD/m3
s2=69.5*ones(101,1); % Ss gCOD/m3
s3=51.20*ones(101,1); %Xi gCOD/m3
s4=202.32*ones(101,1); % Xs gCOD/m3
s5=28.17*ones(101,1); % Xh gCOD/m3
s6=zeros(101,1);% Xb,A
s7=zeros(101,1);% XP
s8=zeros(101,1);% So
s9=6.95*ones(101,1); %Sno
s10=31.56*ones(101,1); % Snh
s11=zeros(101,1); %Snd
s12=10.59*ones(101,1); % Xnd gN/3
s13=7*ones(101,1); %Salk gCOD/m3
q=18446*ones(101,1); % influent flow m3/d

stab100b=[tt s1 s2 s3 s4 s5 s6 s7 s8 s9 s10 s11 s12 s13 q];
save stab100b stab100b;
```

K | Benchmark for oxidation ditch using Matlab/ Simulink

K.0.1 Understanding the current Matlab, Simulink and C^{++} model

First of all the current model needed to be understood. The model is made with Matlab and Simulink, where the S-functions are written in C^{++}. Unfortunately the code is not explained and little comments are added to the code. This means that the code should be analyzed, to understand the origing and meaning of the variables, parameters and calculations in the code.

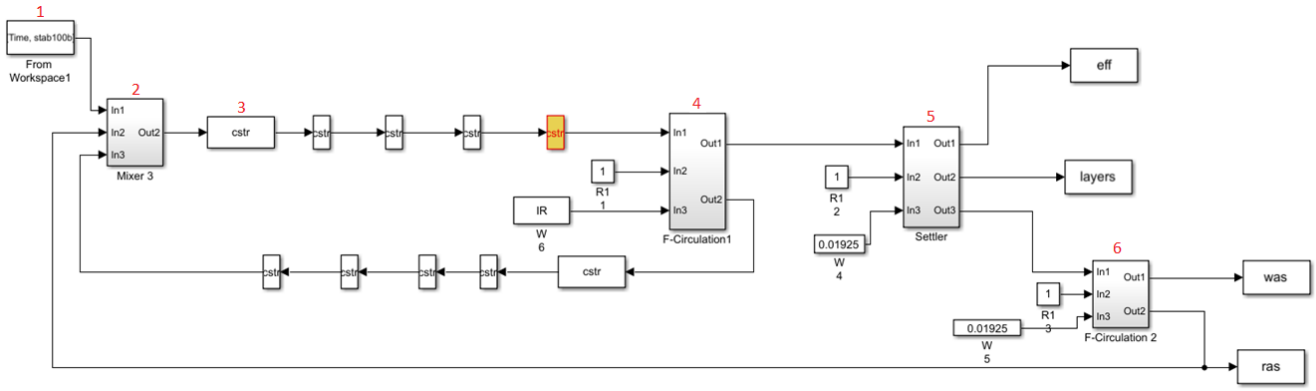

Figure K.1: Original Simulink model

The original layout of the Simulink model, see Figure K.1, will be explained here and the blocks will be elucidated with their corresponding scripts.

Main Matlab file Appendix J shows the main Matlab file, where the Simulink simulation is started and some variables are defined. The origin and meaning of the stated variables in the file were found to be the kinetic and stoichiometric parameter values defined for the simulation benchmark, see Table K.1 from (Copp, 2002). In the Matlab file comments have been added to clear this up, as can bee seen in Appendix J. In the main file also some initial conditions for the Reactor and Settler are given and the influent file is loaded. The stoichiometry and kinetics are based on the ASM1 model (Henze et al., 2000), see chapter 2 for more information about ASM1.

Table K.1: Stoichiometric and kinetic variables (Copp, 2002)

Stoichiometric variables			
Parameter Description	Symbol	Value	Units
Autotrophic yield	Y_A	0.24	$gX_{BA}COD$ formed $(gNutilised)^{-1}$
Heterotrophic yield	Y_H	0.67	$gX_{BH}COD$ formed $(gCODutilised)^{-1}$
Fraction of biomass to particulate products	f_p	0.08	$dimensionless$
Fraction nitrogen in biomass	i_{XB}	0.08	$gN(gCOD)^{-1}$ in biomass (X_{BA}&X_{BH})
Faction nitrogen in particulate products	i_{XP}	0.06	$gN(gCOD)^{-1}1$ in X_p
Kinetic variables			
Parameter Description	Symbol	Value	Units
Maximum heterotrophic growht rate	μ_{mH}	4.0	day^{-1}
Half-saturation (hetero. growth)	K_S	10.0	$gCODm^{-3}$
Half-saturation (hetero. oxygen)	K_{OH}	0.2	gO_2m^{-3}
Half-saturation (nitrate)	K_{NO}	0.5	$gNO_3 - Nm^{-3}$
Heterotrophic decay rate	b_H	0.3	day^{-1}
Anoxic growth rate correction factor	η_g	0.8	$dimensionless$
Anoxic hydrolysis rate correction factor	η_h	0.8	$dimensionless$
Maximum specific hydrolysis rate	K_h	3.0	$gX_s(gX_{BH}CODday) - 1$
Half-saturation (hydrolysis)	K_X	0.1	$gX_s(gX_{BH}COD)^{-1}$
Maximum autotrophic growth rate	μ_{mA}	0.5	$day - 1$
Half-sautration (auto. growth)	K_{NH}	1.0	$gNH_3 - Nm^{-3}$
Autotrophic decay rate	b_A	0.05	day^{-1}
Half-saturation (auto. oxygen)	K_{OA}	0.4	gO_2m^{-3}
Ammonification rate	k_a	0.05	$m3(gCODday)^{-1}$

Block 1 The first simulink block represents the influent. The influent variables represent the thirteen ASM1 variables: S_I, S_S, X_I, X_S, X_H, $X_{B,A}$, X_P, S_O, S_{NO}, S_{NH}, S_{ND}, X_{ND}, S_{ALK}. The 14th parameter represents the flow.

In Figure K.2 a part of the corresponding Matlab file can be seen, where these variables are defined. The origin of the values set for these variables were found in Alex et al. (2008). Here the file already has been extended with comments explaining the parameter origins. A mistake was detected in this file of the mode. S_{NO} is defined as 6,95 and S_{ND} as 0, whilst this should have been the other way around, as can be seen in Alex et al. (2008).

```
% stab100b
tt=[0:1:100]';
s1=30*ones(101,1); %Si g COD/m3
s2=69.5*ones(101,1); % Ss gCOD/m3
s3=51.20*ones(101,1); %Xi gCOD/m3
s4=202.32*ones(101,1); % Xs gCOD/m3
s5=28.17*ones(101,1); % Xh gCOD/m3
s6=zeros(101,1);% Xb,A
s7=zeros(101,1);% XP
s8=zeros(101,1);% So
s9=6.95*ones(101,1); %Sno
s10=31.56*ones(101,1); % Snh
s11=zeros(101,1); %Snd
s12=10.59*ones(101,1); % Xnd gN/3
s13=7*ones(101,1); %Salk gCOD/m3
q=18446*ones(101,1); % influent flow m3/d

stab100b=[tt s1 s2 s3 s4 s5 s6 s7 s8 s9 s10 s11 s12 s13 q];
save stab100b stab100b;
```

Figure K.2: Influent variables

Block 2 The second Simulink block receives the influent, return sludge and the recycled oxidation ditch water. In this block these are combined to one single effluent which enters the loop of CSTRs (the oxidation ditch). The S-function describing this block is written in C^{++}. In Figure K.3 a part of the S-function script can be seen. The input vector u(i) is a combined vector from the incoming streams, where u(0)-u(13) is the input vector coming from the influent, u(14)-u(27) the input vector from the oxidation ditch loop and u(28)-u(41) the input vector from the return sludge. All three input vectors consist of the thirteen ASM1 equations plus the flow rate. This means that u(0), u(14) and u(28) stand for the S_i value of the influent, oxidation ditch loop and return sludge, respectively. A mass balance is made with the flow calculating an output value for S_I of the mixing block, y(0).This is done for all the thirteen ASM1 variables making the output vector y(i). Lastly the output flow rate, y(13), is calculated, which is the summed flow of the three incoming streams u(13), u(27) and u(41). Comments were added in the code to clarify this, as can be seen in Figure K.3.

```
{
y[0]=(u(13)*u(0)+u(27)*u(14)+u(41)*u(28))/(u(13)+u(27)+u(41));  /*concentration of SI mixed */
y[1]=(u(13)*u(1)+u(27)*u(15)+u(41)*u(29))/(u(13)+u(27)+u(41)); /*concentration of Ss mixed */
y[2]=(u(13)*u(2)+u(27)*u(16)+u(41)*u(30))/(u(13)+u(27)+u(41)); /*concentration of Xi mixed */
y[3]=(u(13)*u(3)+u(27)*u(17)+u(41)*u(31))/(u(13)+u(27)+u(41)); /*concentration of Xs mixed */
y[4]=(u(13)*u(4)+u(27)*u(18)+u(41)*u(32))/(u(13)+u(27)+u(41)); /*concentration of Xbh mixed */
y[5]=(u(13)*u(5)+u(27)*u(19)+u(41)*u(33))/(u(13)+u(27)+u(41)); /*concentration of Xba mixed */
y[6]=(u(13)*u(6)+u(27)*u(20)+u(41)*u(34))/(u(13)+u(27)+u(41)); /*concentration of Xp mixed */
y[7]=(u(13)*u(7)+u(27)*u(21)+u(41)*u(35))/(u(13)+u(27)+u(41)); /*concentration of So mixed */
y[8]=(u(13)*u(8)+u(27)*u(22)+u(41)*u(36))/(u(13)+u(27)+u(41)); /*concentration of SNO mixed */
y[9]=(u(13)*u(9)+u(27)*u(23)+u(41)*u(37))/(u(13)+u(27)+u(41)); /*concentration of SNH mixed */
y[10]=(u(13)*u(10)+u(27)*u(24)+u(41)*u(38))/(u(13)+u(27)+u(41)); /*concentration of SND mixed */
y[11]=(u(13)*u(11)+u(27)*u(25)+u(41)*u(39))/(u(13)+u(27)+u(41)); /*concentration of XND mixed */
y[12]=(u(13)*u(12)+u(27)*u(26)+u(41)*u(40))/(u(13)+u(27)+u(41)); /*concentration of Salk mixed */
y[13]=(u(13)+u(27)+u(41)); /*flow of SI mixed */

/* u(13) = flow of water u(27) is flow of sludge u(41)= flow of recirculation in tank
 */
```

Figure K.3: S-funcition Block 2

Block 3 Block three represents the CSTR blocks. All CSTR blocks have the same code, only the input is altered between aerated or non-aerated CSTRs. In the S-function of the CSTR the ASM1 model is described. The part of the C^{++} code describing these ASM1 calculations can be seen in Figure K.4.

```
/* process rtes rho_j of all processes */
rho1=muh*(ss/(ks+ss))*(so/(koh+so))*xbh;
rho2=muh*(ss/(ks+ss))*(koh/(koh+so))*(sno/(kno+sno))*etag*xbh;
rho3=mua*(snh/(knh+snh))*(so/(koa+so))*xba;
rho4=bh*xbh;
rho5=ba*xba;
rho6=ka*snd*xbh;
rho7=kh*((xs/xbh)/(kx+(xs/xbh)))*((so/(koh+so))+(etah*(koh/(koh+so))*(sno/(kno+sno))))*xbh;
rho8=rho7*xnd/xs;

dx[0]=(u(13)*(u(0)-x[0])/v);
dx[1]=(u(13)*(u(1)-x[1])/v)+rho7-(rho1/yh)-(rho2/yh);
dx[2]=(u(13)*(u(2)-x[2])/v);
dx[3]=(u(13)*(u(3)-x[3])/v)+((1-fp)*rho4)+((1-fp)*rho5)-rho7;
dx[4]=(u(13)*(u(4)-x[4])/v)+rho1+rho2-rho4;
dx[5]=(u(13)*(u(5)-x[5])/v)+rho3-rho5;
dx[6]=(u(13)*(u(6)-x[6])/v)+(fp*rho4)+(fp*rho5);
if (so > 0)
dx[7]=(u(13)*(u(7)-x[7])/v)-((1-yh)*rho1/yh)-(rho3*(4.57-ya)/ya)+(kla*(sosat-x[7]));
else dx[7]=0;
dx[8]=(u(13)*(u(8)-x[8])/v)+(rho3/ya)-(((1-yh)*rho2)/(2.86*yh));
dx[9]=(u(13)*(u(9)-x[9])/v)-(ixb*rho1)-(ixb*rho2)-((ixb+(1/ya))*rho3)+rho6;
dx[10]=(u(13)*(u(10)-x[10])/v)+rho8-rho6;
dx[11]=(u(13)*(u(11)-x[11])/v)+((ixb-(fp*ixp))*rho4)-rho8+((ixb-(fp*ixp))*rho5);
dx[12]=(u(13)*(u(12)-x[12])/v)+(rho6/14)-((ixb*rho1)/14)+(rho2*((1-yh)/(14*2.86*yh)-(ixb/14)))-(rho3*((ixb/14)+(1/(7*ya))));
```

Figure K.4: S-function Block 3

Rho1 - rho8 describe the reaction rates 1-8 as can be found in the ASM1, see Figure K.5.

$$\rho = \begin{pmatrix} \mu_H \left(\frac{S_S}{K_S + S_S}\right)\left(\frac{S_O}{K_{OH} + S_O}\right) X_{BH} \\ \mu_H \eta_g \left(\frac{S_S}{K_S + S_S}\right)\left(\frac{K_{OH}}{K_{OH} + S_O}\right)\left(\frac{S_{NO}}{K_{NO} + S_{NO}}\right) X_{BH} \\ \mu_A \left(\frac{S_{NH}}{K_{NH} + S_{NH}}\right)\left(\frac{S_O}{K_{OA} + S_O}\right) X_{BA} \\ b_H X_{BH} \\ b_A X_{BA} \\ k_a S_{ND} X_{BH} \\ k_h \frac{X_S}{K_X X_{BH} + X_S}\left(\frac{S_O}{K_{OH} + S_O} + \eta_h \frac{K_{OH}}{K_{OH} + S_O}\frac{S_{NO}}{K_{NO} + S_{NO}}\right) X_{BH} \\ k_h \frac{X_{ND}}{K_X X_{BH} + X_S}\left(\frac{S_O}{K_{OH} + S_O} + \eta_h \frac{K_{OH}}{K_{OH} + S_O}\frac{S_{NO}}{K_{NO} + S_{NO}}\right) X_{BH} \end{pmatrix}$$

Figure K.5: Process rates rates ASM1

After that the mass balance equations are presented. The concentration is calculated using the mass balance equations. The differential equations have the set-up as explained before in chapter 2 in the section ASM1.

$$\frac{\mathrm{d}R\,(t)}{\mathrm{d}t} = r_i\,(t) + \frac{Q\,(t)}{V}\left(R_{in}\,(t) - R_t\,(t)\right) \tag{K.1}$$

Where:

$$r_i = \sum_j v_{i,j}\rho_{i,j} \tag{K.2}$$

Block 4 Block 4 in Simulink is the internal circulation block of the oxidation ditch. See Figure K.6 for the main part of S-function's C^{++} code. The input vector of the code is stated as u(0)-u(15) consists of the three inputs in the block. The first input u(0)-u(13) comes from the output vector of the CSTR, as explained previously this consists of the thirtheen ASM1 variables and the flow. The second input u(14) entering the block is the value for the sludge recycle rate, r. The third input u(15) accounts for the Internal Recirculation rate of the oxidation ditch, IR. With these values of the input vector u(0)-u(15), two output streams are generated. The output vector y(0)-y(27) covers these two streams, where the first stream y[0]-y[12] expresses the effluent out of the oxidation ditch and the second stream y[13]-y[27] expresses the water that continues in the oxidation ditch, the internal recirculated water. Both outputs consist of the 13 concentrations for the ASM1 variables plus the flow rate. As can be seen in the C^{++} code, see Figure K.6, the concentrations are kept same as the input concentrations, as these are not influenced. Only the flow rate y[13] and y[27] are calculated with the recirculation rates. The flow rates of the output combined equal the flow rate of the input.

```
y[0]=u(0);
y[1]=u(1);
y[2]=u(2);
y[3]=u(3);
y[4]=u(4);
y[5]=u(5);
y[6]=u(6);
y[7]=u(7);
y[8]=u(8);
y[9]=u(9);
y[10]=u(10);
y[11]=u(11);
y[12]=u(12);
y[13]=(1+u(14))*u(13)/(1+u(14)+u(15)); /* Qf */

y[14]=u(0);
y[15]=u(1);
y[16]=u(2);
y[17]=u(3);
y[18]=u(4);
y[19]=u(5);
y[20]=u(6);
y[21]=u(7);
y[22]=u(8);
y[23]=u(9);
y[24]=u(10);
y[25]=u(11);
y[26]=u(12);
y[27]=u(15)*u(13)/(1+u(14)+u(15)); /* Qir */
```

Figure K.6: S-function Block 4

Block 5 Block 5 simulates the settling tank. The C^{++} file describing this block uses the multi-layer dynamic model for the clarification/ thickening process presented by Takacs (1991) and explained in Sotomayor et al. (2001). The model divides the settler into ten layers and is based on solids flux concept and mass balance around each layer. The settling velocity used in the model is mathematically represented as:

$$v_{s,j} = v_0 e^{-r_h X_j^*} - v_0 e^{-r_p X_j^*} \tag{K.3}$$

$$0 \leq v_{s,j} \leq v_m \tag{K.4}$$

The first term, $v_0 e^{-r_h X_j^*}$, reflects the settling velocity of the large flocculating particles and the second term, $v_0 e^{-r_p X_j^*}$ is introduced as a correction factor to account for the smaller, slowly settling particles. v_m is the maximum settling velocity.

The settling velocity is then calculated for each layer with this as can be seen in Figure K.11. the maximum of the calculated settling velocity or 0 is taken, to prevent negative settling velocities. The calculated settling velocity is then used to calculate the settling flux. The flux, $J_{s,j}$, is calculated as shown in Figure K.8 and can be found back in the code at Figure K.12.

The flux is then used in the mass balance equations for the layers:

For layer 1 (bottom layer):

$$\frac{\mathrm{d}X_i}{\mathrm{d}t} = \frac{v_{dn}(x_i - x_{i-1})}{z_m} + \frac{\min(J_{s,i+1}, J_{s,i})}{z_m} \tag{K.5}$$

For layer 2-5:

$$\frac{\mathrm{d}X_i}{\mathrm{d}t} = \frac{v_{dn}(x_{i+1} - x_i)}{z_m} + \frac{\min(J_{s,i+1}, J_{s,i})}{z_m} - \frac{\min(J_{s,i+2}, J_{s,i=1})}{z_m} \tag{K.6}$$

For layer 6 (feed layer):

$$\frac{\mathrm{d}X_i}{\mathrm{d}t} = \frac{v_{up}(x_{i+1} - x_i)}{z_m} + \frac{(J_{c,i+1} - J_{c,i})}{z_m} \tag{K.7}$$

For layer 7-8-9:

$$\frac{\mathrm{d}X_i}{\mathrm{d}t} = \frac{v_{up}(x_{i+1} - x_i)}{z_m} + \frac{(J_{c,i+1} - J_{c,i})}{z_m} \tag{K.8}$$

For layer 10 (top layer):

$$\frac{\mathrm{d}X_{10}}{\mathrm{d}t} = \frac{v_{up}(x_8 - x_9)}{z_m} - \frac{(J_{c,10})}{z_m} \tag{K.9}$$

These equations can be found back in the code in Figure K.13.

The output vector y(0)-y(37) of the settling tank is composed out of three outputs. The first output y(0)-y(13) accounts for the effluent of the settling tank, where y(0)-y(12) covers the variables of the ASM1 model and y(13) is the flow of the effluent q_e. The soluble components stay the same as they are not influenced by the settleabiltiy, however the particulate components are adjusted with the calculations of the 10th (top) layer, as can be seen in the code Figure K.9. The second output y(14)-y(24) contains the results for calculation of each layer. The last output y(24)-y(37) is the underflow from the settling tank. This contains again the thirteen ASM1 variables y(24)-y(36) and the flow rate y(37), q_u. The soluble variables are unchanged and the particulate variables are adjusted with the results of the calculations for the bottom layer of the settling tank.

Table K.2: Parameter description

Symbol	Description	Units
f_{ns}	Non-settleable fraction	$-$
q_e	Effluent flow rate	m^3/day
q_u	Underflow flow rate	m^3/day
q_f	Feeding flow rate	m^3/day
v_{dn}	Downward velocity	m/day
v_{up}	Upward velocity	m/day
x_{min}	Minimum attainable suspended solids concentration	g/m^3
x_f	mixed liquor suspended solids concentration entering the settling tank	g/m^3
r	return sludge rate	$-$
w	waste sludge rate	$-$
z_m	height of each layer	m
v_{sj}	settling velocity in layer j	m/day
X_j^*	suspended solids concentration in layer j, subject to limiting condition X*j= Xj- Xmin	g/m^3
r_h	hindered zone settling parameter	m^3/gSS
r_p	flocculant zone settling parameter	m^3/gSS
v_o	maximum Vesilind settling velocity	m/day
v_m	maximum settling velocity	m/day

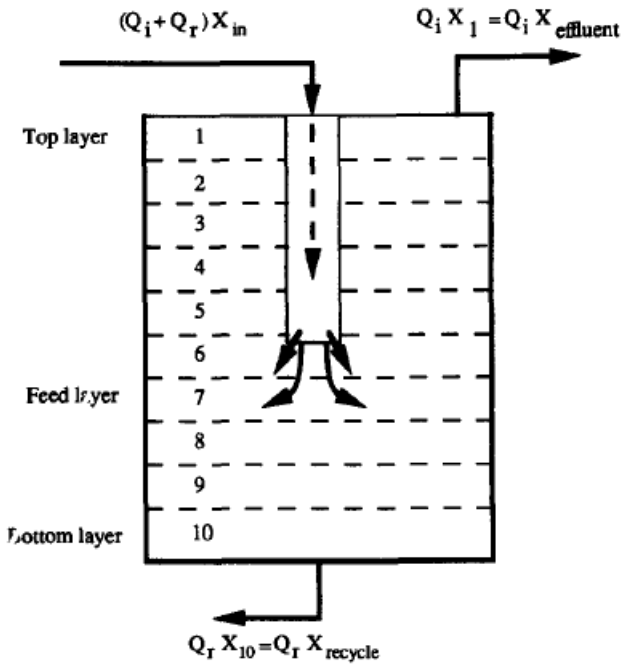

Figure K.7: Layered settler model

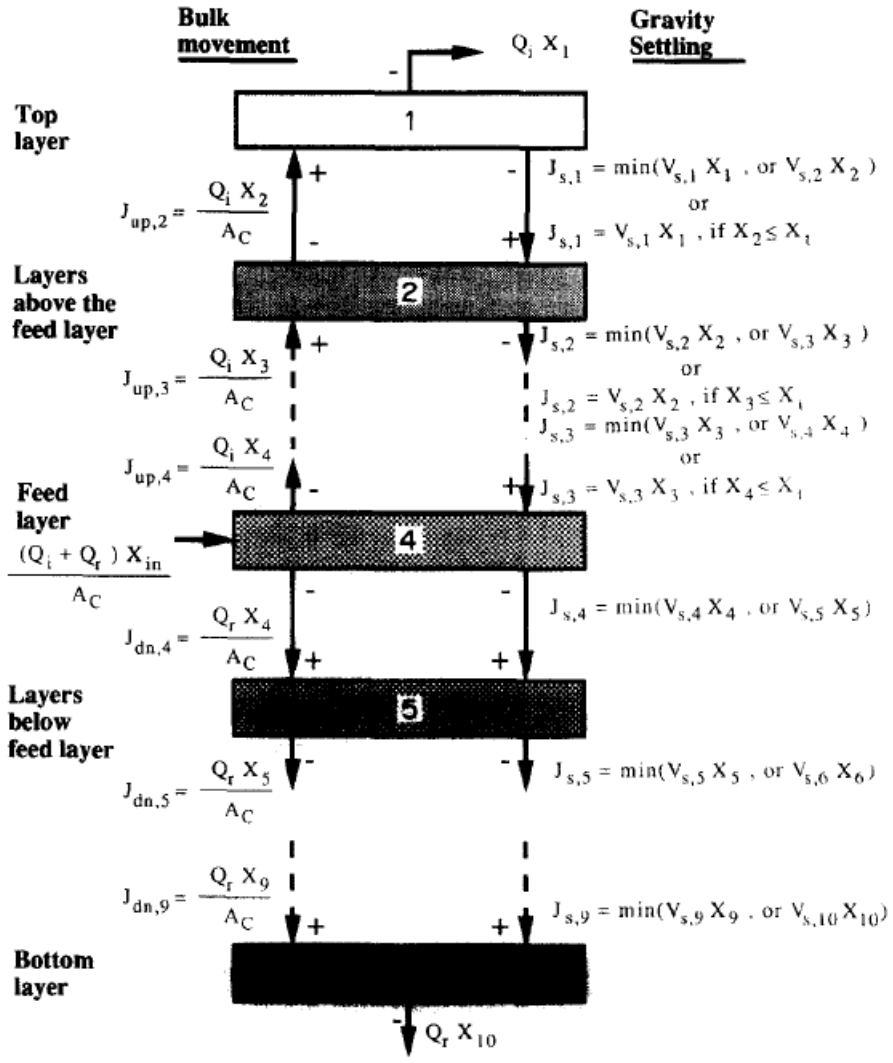

Figure K.8: Solids balance layered settler model with

```
r=u(14);
w=u(15);
qe=(u(13)*(1-w)/(1+r));
qu=u(13)*(r+w)/(1+r);
xf=0.75*(u(2)+u(3)+u(4)+u(5)+u(6)+u(11));

y[0]=u(0);
y[1]=u(1);
y[2]=x[9]*u(2)/xf;
y[3]=x[9]*u(3)/xf;
y[4]=x[9]*u(4)/xf;
y[5]=x[9]*u(5)/xf;
y[6]=x[9]*u(6)/xf;
y[7]=u(7);
y[8]=u(8);
y[9]=u(9);
y[10]=u(10);
y[11]=x[9]*u(11)/xf;
y[12]=u(12);
y[13]=qe;
```

Figure K.9: S-function Block 5

```
y[14]=x[9];
y[15]=x[8];
y[16]=x[7];
y[17]=x[6];
y[18]=x[5];
y[19]=x[4];
y[20]=x[3];
y[21]=x[2];
y[22]=x[1];
y[23]=x[0];

y[24]=u(0);
y[25]=u(1);
y[26]=x[0]*u(2)/xf;
y[27]=x[0]*u(3)/xf;
y[28]=x[0]*u(4)/xf;
y[29]=x[0]*u(5)/xf;
y[30]=x[0]*u(6)/xf;
y[31]=u(7);
y[32]=u(8);
y[33]=u(9);
y[34]=u(10);
y[35]=x[0]*u(11)/xf;
```

Figure K.10: S-function Block 5 - continued

```
r=u(14);
w=u(15);

qe=(u(13)*(1-w)/(1+r));
qu=u(13)*(r+w)/(1+r);
qf=u(13);
vdn=qu/a; vup=qe/a;
xf=0.75*(u(2)+u(3)+u(4)+u(5)+u(6)+u(11));
xmin=fns*xf;

vs1=max(0,min(vm,vv*(exp(-rh*(x[0]-xmin))-exp(-rp*(x[0]-xmin)))));
vs2=max(0,min(vm,vv*(exp(-rh*(x[1]-xmin))-exp(-rp*(x[1]-xmin)))));
vs3=max(0,min(vm,vv*(exp(-rh*(x[2]-xmin))-exp(-rp*(x[2]-xmin)))));
vs4=max(0,min(vm,vv*(exp(-rh*(x[3]-xmin))-exp(-rp*(x[3]-xmin)))));
vs5=max(0,min(vm,vv*(exp(-rh*(x[4]-xmin))-exp(-rp*(x[4]-xmin)))));
vs6=max(0,min(vm,vv*(exp(-rh*(x[5]-xmin))-exp(-rp*(x[5]-xmin)))));
vs7=max(0,min(vm,vv*(exp(-rh*(x[6]-xmin))-exp(-rp*(x[6]-xmin)))));
vs8=max(0,min(vm,vv*(exp(-rh*(x[7]-xmin))-exp(-rp*(x[7]-xmin)))));
vs9=max(0,min(vm,vv*(exp(-rh*(x[8]-xmin))-exp(-rp*(x[8]-xmin)))));
vs10=max(0,min(vm,vv*(exp(-rh*(x[9]-xmin))-exp(-rp*(x[9]-xmin)))));


js1=vs1*x[0];
js2=vs2*x[1];
js3=vs3*x[2];
js4=vs4*x[3];
js5=vs5*x[4];
js6=vs6*x[5];
```

Figure K.11: S-function Block 5 - continued

```
if (x[6]<=xt)
    jc7=vs7*x[6];
else
    jc7=min(vs7*x[6],vs6*x[5]);

if (x[7]<=xt)
    jc8=vs8*x[7];
else
    jc8=min(vs8*x[7],vs7*x[6]);

if (x[8]<=xt)
    jc9=vs9*x[8];
else
    jc9=min(vs9*x[8],vs8*x[7]);

if (x[9]<=xt)
    jc10=vs10*x[9];
else
    jc10=min(vs10*x[9],vs9*x[8]);
```

Figure K.12: S-function Block 5 - continued

```
dx[0]=(vdn*(x[1]-x[0])/zm)+(min(js2,js1)/zm);
dx[1]=(vdn*(x[2]-x[1])/zm)-(min(js2,js1)/zm)+(min(js3,js2)/zm);
dx[2]=(vdn*(x[3]-x[2])/zm)-(min(js3,js2)/zm)+(min(js4,js3)/zm);
dx[3]=(vdn*(x[4]-x[3])/zm)-(min(js4,js3)/zm)+(min(js5,js4)/zm);
dx[4]=(vdn*(x[5]-x[4])/zm)-(min(js5,js4)/zm)+(min(js6,js5)/zm);
dx[5]=(qf*xf/(zm*a))-((vdn+vup)*x[5]/zm)-(min(js6,js5)/zm)+(min(js6,jc7)/zm);
dx[6]=(vup*(x[5]-x[6])/zm)+((jc8-jc7)/zm);
dx[7]=(vup*(x[6]-x[7])/zm)+((jc9-jc8)/zm);
dx[8]=(vup*(x[7]-x[8])/zm)+((jc10-jc9)/zm);
dx[9]=(vup*(x[8]-x[9])/zm)-(jc10/zm);
```

Figure K.13: S-function Block 5 - continued

Block 6 The sixth block is modelled to divide the sludge stream into two separate streams, the waste activated sludge (WAS) stream and the Return activated sludge (RAS) stream. The coding in this C-MEX file can be seen in Figure K.14 and is similar to that in Block 4. The input vector consists again of three inputs together, where u(0)-u(13) comes from the first input, the sludge stream from the settler. The second input u(14) is the return sludge rate, r. The third input u(15) is the rate at which sludge is wasted, w. The two output vectors both have the concentrations of the ASM1 variables in them, y(0)-y(12) for the WAS-stream and y(14)-y(26) for the RAS-stream, and for both streams also the flow rate, y(13) and y(27) for the WAS- and RAS-stream respectively. The concentrations are equal to those of the input vector, as these are not influenced. The flow rate however is calculated using the return sludge rate and the sludge waste rate. The WAS flow rate and the RAS flow rate combined are equal to the incoming flow rate, logically as it is a flow-splitter.

```
y[0]=u(0);
y[1]=u(1);
y[2]=u(2);
y[3]=u(3);
y[4]=u(4);
y[5]=u(5);
y[6]=u(6);
y[7]=u(7);
y[8]=u(8);
y[9]=u(9);
y[10]=u(10);
y[11]=u(11);
y[12]=u(12);
y[13]=u(15)*u(13)/(u(14)+u(15)); /* Qw */

y[14]=u(0);
y[15]=u(1);
y[16]=u(2);
y[17]=u(3);
y[18]=u(4);
y[19]=u(5);
y[20]=u(6);
y[21]=u(7);
y[22]=u(8);
y[23]=u(9);
y[24]=u(10);
y[25]=u(11);
y[26]=u(12);
y[27]=u(14)*u(13)/(u(14)+u(15)); /* Qr */
```

Figure K.14: S-function Block 6

K.0.2 The implementation of biological phosphorus removal

To implement the phosphorus removal into the model, a few changes are necessary. First of all the Simulink model should be extended with an anaerobic tank. An anaerobic tank is essential for PAOs as explained in chapter 2. Then the return sludge is diverted to the anaerobic tank instead of the oxidation ditch, but the internal recycle of the oxidation ditch stays the same. The new Simulink layout can be seen in Figure K.15.

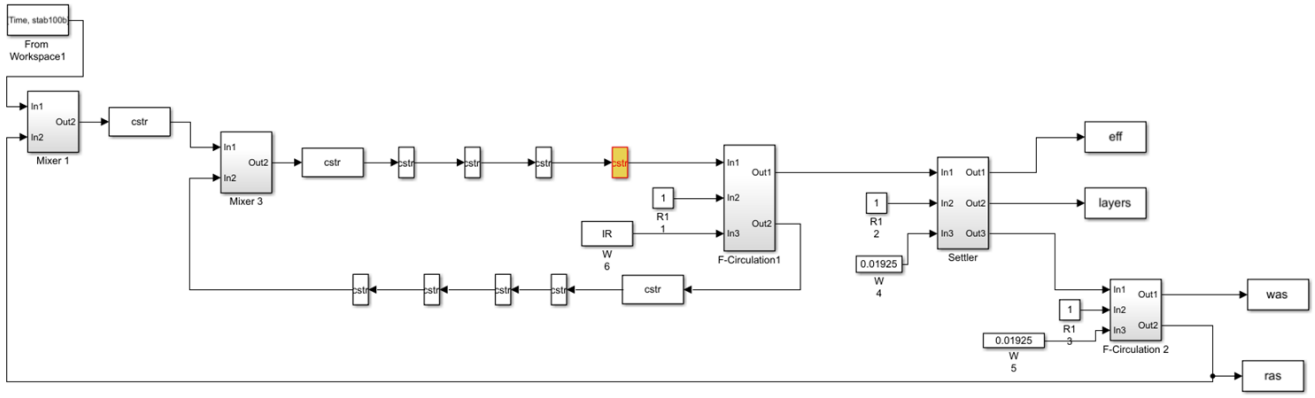

Figure K.15: New Simulink model incorporating anaerobic tank and diverted return sludge

Next all the files described need to be extended from ASM1 to ASM2d. This means that the thirteen ASM1 state variables that are calculated, should now be changed to the ASM2d variables. This has not been done yet, as it involves a lot of programming in C^{++}, which makes it unfeasible for this thesis. However the ASM2d matrix is given in Appendix L, the way the matrix works and can be used to obtain the differential equations is presentend inchapter 2 and the way the ASM is incorporated into the model is explained in this chapter.

L | ASM2d

Table L.1: ASM2d Matrix, part 1, Meijer (2004)

← Process			Component →	1 S_O gO_2/m^3	2 S_F $gCOD/m^3$	3 S_A $gCOD/m^3$	4 S_{NH} gN/m^3	5 S_{NO} gN/m^3	6 S_{N2} gN/m^3
1	r_h^O	Aerobic Hydrolysis	$gCOD_{XS}/d$		$1-f_{SI}$		$c_{N,1}$		
2	r_h^{NO}	Anoxic Hydrolysis	$gCOD_{XS}/d$		$1-f_{SI}$		$c_{N,1}$		
3	r_h^{AO}	Anaerobic Hydrolysis	$gCOD_{XS}/d$		$1-f_{SI}$		$c_{N,1}$		
Regular Heterotrophic Organisms X_H									
4	r_{SF}^O	Aerobic Growth on S_F	$gCOD_{XH}/d$	$-(1/Y_H-1)$	$-1/Y_H$		$c_{N,4}$		
5	r_{SA}^O	Aerobic Growth on S_A	$gCOD_{XH}/d$	$-(1/Y_H-1)$		$-1/Y_H$	$c_{N,5}$		
6	r_{SF}^{NO}	Anoxic Growth on S_F	$gCOD_{XH}/d$		$-1/Y_H$		$c_{N,6}$	$-\frac{(1/Y_H-1)}{2.86}$	$\frac{(1/Y_H-1)}{2.86}$
7	r_{SA}^{NO}	Anoxic Growth on S_A	$gCOD_{XH}/d$			$-1/Y_H$	$c_{N,7}$	$-\frac{(1/Y_H-1)}{2.86}$	$\frac{(1/Y_H-1)}{2.86}$
8	r_{fe}^{AN}	Fermentation	$gCOD_{SF}/d$		-1	1	$c_{N,8}$		
9	r_{HL}	Heterotrophic Lysis	$gCOD_{XH}/d$				$c_{N,9}$		
Phosphorus Accumulating Organisms X_{PAO}									
10	r_{SA}^{AN}	Anaerobic Storage of S_A	$gCOD_{SA}/d$			-1			
11	r_M^{AN}	Anaerobic Maintenance	gP/d						
12	r_{SA}^{NO}	Anoxic Storage of S_A	$gCOD_{SA}/d$			-1		$-\frac{(1-Y_{SA}^{NO})}{2.86}$	$\frac{(1-Y_{SA}^{NO})}{2.86}$
13	r_{PHA}^{NO}	Anoxic PHA Consumption	$gCOD_{PHA}/d$				$c_{N,13}$	$-\frac{(1-1/Y_{PHA}^{NO})}{2.86}$	$\frac{(1-1/Y_{PHA}^{NO})}{2.86}$
14	r_{PP}^{NO}	Anoxic Storage of poly-P	gP/d				$c_{N,14}$	$-\frac{(1/Y_{PP}^{NO})}{2.86}$	$\frac{(1/Y_{PP}^{NO})}{2.86}$
15	r_{GLY}^{NO}	Anoxic Glycogen Formation	$gCOD_{GLY}/d$				$c_{N,15}$	$-\frac{(1/Y_{GLY}^{NO}-1)}{2.86}$	$\frac{(1/Y_{GLY}^{NO}-1)}{2.86}$
16	r_M^{NO}	Anoxic Maintenance	$gCOD_{PAO}/d$				$c_{N,16}$	$-1/2.86$	$1/2.86$
17	r_{PHA}^O	Aerobic PHA Consumption	$gCOD_{PHA}/d$	$1/Y_{PHA}^O-1$			$c_{N,17}$		
18	r_{PP}^O	Aerobic Storage of poly-P	gP/d	$-1/Y_{PP}^O$			$c_{N,18}$		
19	r_{GLY}^O	Aerobic Glycogen Formation	$gCOD_{GLY}/d$	$1-1/Y_{GLY}^O$			$c_{N,19}$		
20	r_M^O	Aerobic Maintenance	$gCOD_{PAO}/d$	-1			$c_{N,20}$		
Autotrophic Nitrifying Organisms X_A									
21	r_A^O	Autotrophic Growth	$gCOD_{XA}/d$	$1-4.57/Y_A$			$c_{N,21}$	$1/Y_A$	
22	r_{AL}	Autotrophic Lysis	$gCOD_{XA}/d$				$c_{N,22}$		

↓ Composition		Component →	1 S_O gO_2	2 S_F gCOD	3 S_A gCOD	4 S_{NH} gN	5 S_{NO} gN	6 S_{N2} gN
1	COD	gCOD	-1	1	1		-2.86	...
2	TOC/COD	gC/gCOD		...	0.4			
3	Nitrogen	gN		$i_{N,SF}$	$i_{N,SA}$	1	1	1
4	Phosphorus	gP		$i_{P,SF}$	$i_{P,SA}$			
5	Ionic charge	mole			-1/64	+1/14	-1/14	
6	TSS	g						

Table L.2: ASM2d Matrix, part 2, Meijer (2004)

7	8	9	10	11	12	13	14	15	16	17	18
S_{PO}	S_I	S_{HCO}	X_I	X_S	X_H	X_{PAO}	X_{PP}	X_{PHA}	X_{GLY}	X_A	X_{TSS}
gP/m^3	$gCOD/m^3$	$mole/m^3$	$gCOD/m^3$	$gCOD/m^3$	$gCOD/m^3$	$gCOD/m^3$	gP/m^3	$gCOD/m^3$	$gCOD/m^3$	$gCOD/m^3$	g/m^3
$c_{P,1}$	f_{SI}	$c_{e,1}$		-1							$c_{TSS,1}$
$c_{P,1}$	f_{SI}	$c_{e,1}$		-1							$c_{TSS,1}$
$c_{P,1}$	f_{SI}	$c_{e,1}$		-1							$c_{TSS,1}$
$c_{P,4}$		$c_{e,4}$			1						$c_{TSS,4}$
$c_{P,5}$		$c_{e,5}$			1						$c_{TSS,5}$
$c_{P,6}$		$c_{e,6}$			1						$c_{TSS,6}$
$c_{P,7}$		$c_{e,7}$			1						$c_{TSS,7}$
$c_{P,8}$		$c_{e,8}$									$c_{TSS,8}$
$c_{P,9}$		$c_{e,9}$	$f_{XI,H}$	$1- f_{XI,H}$	-1						$c_{TSS,9}$
Y_{PO}^{AN}		$c_{e,10}$					$-Y_{PO}^{AN}$	Y_{SA}^{AN}	$1-Y_{SA}^{AN}$		$c_{TSS,10}$
1		$c_{e,11}$					-1				$c_{TSS,11}$
Y_{PO}^{NO}		$c_{e,12}$					$-Y_{PO}^{NO}$	Y_{SA}^{NO}			$c_{TSS,12}$
$c_{P,13}$		$c_{e,13}$				$1/Y_{PHA}^{NO}$		-1			$c_{TSS,13}$
$c_{P,14}$		$c_{e,14}$				$-1/Y_{PP}^{NO}$	1				$c_{TSS,14}$
$c_{P,15}$		$c_{e,15}$				$-1/Y_{GLY}^{NO}$			1		$c_{TSS,15}$
$c_{P,16}$		$c_{e,16}$				-1					$c_{TSS,16}$
$c_{P,17}$		$c_{e,17}$				$1/Y_{PHA}^{O}$		-1			$c_{TSS,17}$
$c_{P,18}$		$c_{e,18}$				$-1/Y_{PP}^{O}$	1				$c_{TSS,18}$
$c_{P,19}$		$c_{e,19}$				$-1/Y_{GLY}^{O}$			1		$c_{TSS,19}$
$c_{P,20}$		$c_{e,20}$				-1					$c_{TSS,20}$
$c_{P,21}$		$c_{e,21}$								1	$c_{TSS,21}$
$c_{P,22}$		$c_{e,22}$	$f_{XI,A}$	$1- f_{XI,A}$						-1	$c_{TSS,22}$

7	8	9	10	11	12	13	14	15	16	17	18
S_{PO}	S_I	S_{HCO}	X_I	X_S	X_H	X_{PAO}	X_{PP}	X_{PHA}	X_{GLY}	X_A	X_{TSS}
gP	gCOD	mole	gCOD	gCOD	gCOD	gCOD	gP	gCOD	gCOD	gCOD	g
	1		1	1	1	1		1	1	1	
	...		...	...	...	0.334 (α)		0.334	0.375	...	
	$i_{N,SI}$		$i_{N,XI}$	$i_{N,XS}$	$i_{N,XH}$	$i_{N,BM}$				$i_{N,BM}$	
1	$i_{P,SI}$		$i_{P,XI}$	$i_{P,XS}$	$i_{P,XH}$	$i_{P,BM}$	1			$i_{P,BM}$	
-1.5/31		-1					-1/31				
			$i_{TSS,XI}$	$i_{TSS,XS}$	$i_{TSS,BM}$	$i_{TSS,BM}$	$i_{TSS,PP}$	$i_{TSS,PHA}$	$i_{TSS,GLY}$	$i_{TSS,BM}$	1

Table L.3: ASM2d Matrix, part 3, Meijer (2004)

S_{NH} (gN·m^{-3})	S_{PO} (gP·m^{-3})
$c_{N,1} = i_{N,XS} - i_{N,SI} \cdot f_{SI} - i_{N,SF} \cdot (1 - f_{SI})$	$c_{P,1} = i_{P,XS} - i_{P,SI} \cdot f_{SI,H} - i_{P,SF} \cdot (1 - f_{SI,H})$
$c_{N,4} = i_{N,SF} / Y_H - i_{N,BM}$	$c_{P,4} = i_{P,SF} / Y_H - i_{P,BM}$
$c_{N,5} = -i_{N,BM}$	$c_{P,5} = -i_{P,BM}$
$c_{N,6} = i_{N,SF} / Y_H - i_{N,BM}$	$c_{P,6} = i_{P,SF} / Y_H - i_{P,BM}$
$c_{N,7} = -i_{N,BM}$	$c_{P,7} = -i_{P,BM}$
$c_{N,8} = i_{N,SF}$	$c_{P,8} = i_{P,SF}$
$c_{N,9} = i_{N,BM} - i_{N,XI} \cdot f_{XI,H} - i_{N,XS} \cdot (1 - f_{XI,H})$	$c_{P,9} = i_{P,BM} - i_{P,XI} \cdot f_{XI,H} - i_{P,XS} \cdot (1 - f_{XI,H})$
$c_{N,10} = 0$	$c_{P,10} = Y_{PO}^{AN}$
$c_{N,11} = 0$	$c_{P,11} = 1$
$c_{N,12} = 0$	$c_{P,12} = Y_{PO}^{NO}$
$c_{N,13} = -i_{N,BM} / Y_{PHA}^{NO}$	$c_{P,13} = -i_{PBM} / Y_{PHA}^{NO}$
$c_{N,14} = i_{N,BM} / Y_{PP}^{NO}$	$c_{P,14} = i_{P,BM} / Y_{PP}^{NO} - 1$
$c_{N,15} = i_{N,BM} / Y_{GLY}^{NO}$	$c_{P,15} = i_{P,BM} / Y_{GLY}^{NO}$
$c_{N,16} = i_{N,BM}$	$c_{P,16} = i_{P,BM}$
$c_{N,17} = -i_{N,BM} / Y_{PHA}^{O}$	$c_{P,17} = -i_{P,BM} / Y_{PHA}^{O}$
$c_{N,18} = i_{N,BM} / Y_{PP}^{O}$	$c_{P,18} = i_{P,BM} / Y_{PP}^{O} - 1$
$c_{N,19} = i_{N,BM} / Y_{GLY}^{O}$	$c_{P,19} = i_{P,BM} / Y_{GLY}^{O}$
$c_{N,20} = i_{N,BM}$	$c_{P,20} = i_{P,BM}$
$c_{N,21} = -i_{N,BM} - 1/Y_A$	$c_{P,21} = -i_{P,BM}$
$c_{N,22} = i_{N,BM} - i_{N,XI} \cdot f_{XI,A} - i_{N,XS} \cdot (1 - f_{XI,A})$	$c_{P,22} = i_{P,BM} - i_{P,XI} \cdot f_{XI,A} - i_{P,XS} \cdot (1 - f_{XI,A})$

Table L.4: ASM2d Matrix, part 4, Meijer (2004)

S_{HCO} (mole·m^{-3})	X_{TSS} (g·m^{-3})
$c_{e,1} = c_{N,1}/14 - c_{P,1}\cdot(1.5/31)$	$c_{TSS,1} = -i_{TSS,XS}$
$c_{e,4} = c_{N,4}/14 - c_{P,4}\cdot(1.5/31)$	$c_{TSS,4} = i_{TSS,BM}$
$c_{e,5} = c_{N,5}/14 - c_{P,5}\cdot(1.5/31) + 1/(64\cdot Y_H)$	$c_{TSS,5} = i_{TSS,BM}$
$c_{e,6} = c_{N,6}/14 - c_{P,6}\cdot(1.5/31) + (1/Y_H - 1)/(14\cdot 2.86)$	$c_{TSS,6} = i_{TSS,BM}$
$c_{e,7} = c_{N,7}/14 - c_{P,7}\cdot(1.5/31) + (1/Y_H - 1)/(14\cdot 2.86) + 1/(64\cdot Y_H)$	$c_{TSS,7} = i_{TSS,BM}$
$c_{e,8} = c_{N,8}/14 - c_{P,8}\cdot(1.5/31) - 1/64$	$c_{TSS,8} = 0$
$c_{e,9} = c_{N,9}/14 - c_{P,9}\cdot(1.5/31)$	$c_{TSS,9} = i_{TSS,XI}\cdot f_{XI,H} + i_{TSS,XS}\cdot(1 - f_{XI,H}) - i_{TSS,BM}$
$c_{e,10} = -Y_{PO}^{AN}\cdot(1.5/31) + 1/64 + Y_{PO}^{AN}/31$	$c_{TSS,10} = i_{TSS,PP}\cdot(-Y_{PO}^{AN}) + i_{TSS,PHA}\cdot Y_{SA}^{AN} + i_{TSS,GLY}\cdot(1 - Y_{SA}^{AN})$
$c_{e,11} = -1.5/31 + 1/31$	$c_{TSS,11} = -i_{TSS,PP}$
$c_{e,12} = -Y_{PO}^{NO}\cdot(1.5/31) + 1/64 + Y_{PO}^{NO}/31 + \left(1 - Y_{SA}^{NO}\right)/(14\cdot 2.86)$	$c_{TSS,12} = i_{TSS,PP}\cdot(-Y_{PO}^{NO}) + i_{TSS,PHA}\cdot Y_{SA}^{NO}$
$c_{e,13} = c_{N,13}/14 - c_{P,13}\cdot(1.5/31) - (1/Y_{PHA}^{NO} - 1)/(14\cdot 2.86)$	$c_{TSS,13} = i_{TSS,BM}/Y_{PHA}^{NO} - i_{TSS,PHA}$
$c_{e,14} = c_{N,14}/14 - c_{P,14}\cdot(1.5/31) + 1/(14\cdot 2.86\cdot Y_{PP}^{NO}) - 1/31$	$c_{TSS,14} = -i_{TSS,BM}/Y_{PP}^{NO} + i_{TSS,PP}$
$c_{e,15} = c_{N,15}/14 - c_{P,15}\cdot(1.5/31) + (1/Y_{GLY}^{NO} - 1)/(14\cdot 2.86)$	$c_{TSS,15} = -i_{TSS,BM}/Y_{GLY}^{NO} + i_{TSS,GLY}$
$c_{e,16} = c_{N,16}/14 - c_{P,16}\cdot(1.5/31) + 1/(14\cdot 2.86)$	$c_{TSS,16} = -i_{TSS,BM}$
$c_{e,17} = c_{N,17}/14 - c_{P,17}\cdot(1.5/31)$	$c_{TSS,17} = i_{TSS,BM}/Y_{PHA}^{O} - i_{TSS,PHA}$
$c_{e,18} = c_{N,18}/14 - c_{P,18}\cdot(1.5/31) - 1/31$	$c_{TSS,18} = -i_{TSS,BM}/Y_{PP}^{O} + i_{TSS,PP}$
$c_{e,19} = c_{N,19}/14 - c_{P,19}\cdot(1.5/31)$	$c_{TSS,19} = -i_{TSS,BM}/Y_{GLY}^{O} + i_{TSS,GLY}$
$c_{e,20} = c_{N,20}/14 - c_{P,20}\cdot(1.5/31)$	$c_{TSS,20} = -i_{TSS,BM}$
$c_{e,21} = c_{N,21}/14 - c_{P,21}\cdot(1.5/31) - 1/(14\cdot Y_A)$	$c_{TSS,21} = -i_{TSS,BM}$
$c_{e,22} = c_{N,22}/14 - c_{P,22}\cdot(1.5/31)$	$c_{TSS,22} = i_{TSS,XI}\cdot f_{XI,A} + i_{TSS,XS}\cdot(1 - f_{XI,A}) - i_{TSS,BM}$

Process	Kinetic Rate Equation (r_T)	Switch function (on / off)
Hydrolysis of Particulate Substrate X_S		
1 Aerobic Hydrolysis ($gCOD_{XS} \cdot d^{-1}$)	$r_h^O = k_h \cdot \frac{X_S/(X_H + X_{PAO})}{K_X + X_S/(X_H + X_{PAO})} \cdot (X_H + X_{PAO})$	
2 Anoxic Hydrolysis ($gCOD_{XS} \cdot d^{-1}$)	$r_h^{NO} = \eta_{NO} \cdot k_h \cdot \frac{X_S/(X_H + X_{PAO})}{K_X + X_S/(X_H + X_{PAO})} \cdot \frac{S_{NO}}{K_{NO} + S_{NO}} \cdot (X_H + X_{PAO})$	$\frac{K_O}{K_O + S_O}$
3 Anaerobic Hydrolysis ($gCOD_{XS} \cdot d^{-1}$)	$r_h^{AN} = \eta_{fe} \cdot k_h \cdot \frac{X_S/(X_H + X_{PAO})}{K_X + X_S/(X_H + X_{PAO})} \cdot (X_H + X_{PAO})$	$\frac{K_O}{K_O + S_O} \cdot \frac{K_{NO}}{K_{NO} + S_{NO}}$
Heterotrophic Micro-Organisms X_H		
4 Aerobic Growth on S_F ($gCOD_{XH} \cdot d^{-1}$)	$r_{gF}^O = \mu_H \cdot \frac{S_F}{S_A + S_F} \cdot \frac{S_F}{K_F + S_F} \cdot \frac{S_O}{K_O + S_O} \cdot X_H$	$\frac{S_{NH}}{K_N + S_{NH}} \cdot \frac{S_{PO}}{K_P + S_{PO}} \cdot \frac{S_{HCO}}{K_{HCO} + S_{HCO}}$
5 Aerobic Growth on S_A ($gCOD_{XH} \cdot d^{-1}$)	$r_{gA}^O = \mu_H \cdot \frac{S_A}{S_A + S_F} \cdot \frac{S_A}{K_A + S_A} \cdot \frac{S_O}{K_O + S_O} \cdot X_H$	$\frac{S_{NH}}{K_N + S_{NH}} \cdot \frac{S_{PO}}{K_P + S_{PO}} \cdot \frac{S_{HCO}}{K_{HCO} + S_{HCO}}$
6 Anoxic Growth on S_F ($gCOD_{XH} \cdot d^{-1}$)	$r_{gF}^{NO} = \eta_{NO} \cdot \mu_H \cdot \frac{S_F}{S_A + S_F} \cdot \frac{S_F}{K_F + S_F} \cdot \frac{S_{NO}}{K_{NO} + S_{NO}} \cdot X_H$	$\frac{K_O}{K_O + S_O} \cdot \frac{S_{NH}}{K_N + S_{NH}} \cdot \frac{S_{PO}}{K_P + S_{PO}} \cdot \frac{S_{HCO}}{K_{HCO} + S_{HCO}}$
7 Anoxic Growth on S_A ($gCOD_{XH} \cdot d^{-1}$)	$r_{gA}^{NO} = \eta_{NO} \cdot \mu_H \cdot \frac{S_A}{S_A + S_F} \cdot \frac{S_A}{K_A + S_A} \cdot \frac{S_{NO}}{K_{NO} + S_{NO}} \cdot X_H$	$\frac{K_O}{K_O + S_O} \cdot \frac{S_{NH}}{K_N + S_{NH}} \cdot \frac{S_{PO}}{K_P + S_{PO}} \cdot \frac{S_{HCO}}{K_{HCO} + S_{HCO}}$
8 Fermentation of S_F ($gCOD_{SF} \cdot d^{-1}$)	$r_{fe}^{AN} = q_{fe} \cdot \frac{S_F}{K_{fe} + S_F} \cdot X_H$	$\frac{K_O}{K_O + S_O} \cdot \frac{K_{NO}}{K_{NO} + S_{NO}} \cdot \frac{S_{HCO}}{K_{HCO} + S_{HCO}}$
9 Heterotrophic Lysis ($gCOD_{XH} \cdot d^{-1}$)	$r_{HL} = b_H \cdot X_H$	

Table 7a. Kinetic rate equations.

Table L.6: ASM2d Matrix, part 6, Meijer (2004)

Process	Kinetic Rate Equation (r_P)	Switch function (on / off)
Phosphorus Accumulating Organisms X_{PAO}		
10 Anaerobic storage of S_A ($gCOD_{SA}\cdot d^{-1}$)	$r_{SA}^{AN} = q_{AC}^{AN} \cdot \frac{S_A}{K_A + S_A} \cdot X_{PAO}$	$\frac{K_O}{K_O+S_O} \cdot \frac{K_{NO}}{K_{NO}+S_{NO}} \cdot \frac{X_{GLY}}{K_{GLY}+X_{GLY}} \cdot \frac{X_{PP}}{K_{PP}+X_{PP}}$
11 Anaerobic Maintenance ($gP\cdot d^{-1}$)	$r_M^{AN} = m_{AN} \cdot X_{PAO}$	$\frac{K_O}{K_O+S_O} \cdot \frac{K_{NO}}{K_{NO}+S_{NO}} \cdot \frac{X_{PP}}{K_{PP}+X_{PP}}$
12 Anoxic storage of S_A ($gCOD_{SA}\cdot d^{-1}$)	$r_{SA}^{NO} = q_{AC}^{NO} \cdot \frac{S_A}{K_A + S_A} \cdot \frac{S_{NO}}{K_{NO}+S_{NO}} \cdot X_{PAO}$	$\frac{K_O}{K_O+S_O} \cdot \frac{X_{PP}}{K_{PP}+X_{PP}}$
13 Anoxic PHA consumption ($gCOD_{SHA}\cdot d^{-1}$)	$r_{PHA}^{NO} = \eta_{NO} \cdot k_{PHA} \cdot \frac{X_{PHA}/X_{PAO}}{K_{PHA}+X_{PHA}/X_{PAO}} \cdot \frac{S_{NO}}{K_{NO}+S_{NO}} \cdot X_{PAO}$	$\frac{K_O}{K_O+S_O} \cdot \frac{S_{NH}}{K_N+S_{NH}} \cdot \frac{S_O}{K_P+S_O} \cdot \frac{S_{HCO}}{K_{HCO}+S_{HCO}}$
14 Anoxic storage of PP ($gP\cdot d^{-1}$)	$r_{PP}^{NO} = \eta_{NO} \cdot k_{PP} \cdot \frac{X_{PAO}}{X_{PP}} \cdot \frac{S_{PO}}{K_{PO}+S_{PO}} \cdot \frac{S_{NO}}{g_{PP}\cdot K_{NO}+S_{NO}} \cdot X_{PAO}$	$\frac{K_O}{K_O+S_O} \cdot \frac{X_{PHA}}{K_{PHA}+X_{PHA}} \cdot \frac{f_{PP}^{max} - X_{PP}/X_{PAO}}{f_{PP}+(f_{PP}^{max} - X_{PP}/X_{PAO})}$
15 Anoxic Glycogen formation ($gCOD_{XGLY}\cdot d^{-1}$)	$r_{GLY}^{NO} = \eta_{NO} \cdot k_{GLY} \cdot \frac{X_{PHA}}{X_{GLY}} \cdot \frac{S_{NO}}{K_{NO}+S_{NO}} \cdot X_{PAO}$	$\frac{K_O}{K_O+S_O} \cdot \frac{X_{PHA}}{K_{PHA}+X_{PHA}} \cdot \frac{f_{GLY}^{max} - X_{GLY}/X_{PAO}}{K_{fGLY}+(f_{GLY}^{max} - X_{GLY}/X_{PAO})}$
16 Anoxic Maintenance ($gCOD_{SHO}\cdot d^{-1}$)	$r_M^{NO} = m_{NO} \cdot \frac{S_{NO}}{K_{NO}+S_{NO}} \cdot X_{PAO}$	$\frac{K_O}{K_O+S_O}$
17 Aerobic PHA consumption ($gCOD_{SHA}\cdot d^{-1}$)	$r_{PHA}^{O} = k_{PHA} \cdot \frac{X_{PHA}/X_{PAO}}{K_{PHA}+X_{PHA}/X_{PAO}} \cdot \frac{S_O}{K_O+S_O} \cdot X_{PAO}$	$\frac{S_{NH}}{K_N+S_{NH}} \cdot \frac{S_{PO}}{K_P+S_{PO}} \cdot \frac{S_{HCO}}{K_{HCO}+S_{HCO}}$
18 Aerobic storage of PP ($gP\cdot d^{-1}$)	$r_{PP}^{O} = k_{PP} \cdot \frac{X_{PAO}}{X_{PP}} \cdot \frac{S_{PO}}{K_{PO}+S_{PO}} \cdot \frac{S_O}{g_{PP}\cdot K_O+S_O} \cdot X_{PAO}$	$\frac{X_{PHA}}{K_{PHA}+X_{PHA}} \cdot \frac{f_{PP}^{max} - X_{PP}/X_{PAO}}{K_{gPP}+(f_{PP}^{max} - X_{PP}/X_{PAO})}$
19 Aerobic Glycogen formation ($gCOD_{XGLY}\cdot d^{-1}$)	$r_{GLY}^{O} = k_{GLY} \cdot \frac{X_{PHA}}{X_{GLY}} \cdot \frac{S_O}{K_O+S_O} \cdot X_{PAO}$	$\frac{X_{PHA}}{K_{PHA}+X_{PHA}} \cdot \frac{f_{GLY}^{max} - X_{GLY}/X_{PAO}}{K_{fGLY}+(f_{GLY}^{max} - X_{GLY}/X_{PAO})}$
20 Aerobic Maintenance ($gCOD_{SHO}\cdot d^{-1}$)	$r_M^{O} = m_O \cdot \frac{S_O}{K_O+S_O} \cdot X_{PAO}$	
Autotrophic Nitrifying Organisms X_A		
21 Autotrophic growth ($gCOD_{XA}\cdot d^{-1}$)	$r_A^{O} = \mu_A \cdot \frac{S_{NH}}{K_{NH}+S_{NH}} \cdot \frac{S_O}{K_O+S_O} \cdot X_A$	$\frac{K_{IO}}{K_I+S_{IO}}$
22 Autotrophic Lysis ($gCOD_{XA}\cdot d^{-1}$)	$r_{AL} = b_A \cdot X_A$	